Anonymous Referee #1

General comments:

- ***The significance as addressed by "Impact of topography on black carbon transport to the southern Tibetan Plateau during pre-monsoon season and its climatic implication" is backed here. Understanding the sources and transport of aerosols becomes a hot topic in regional environmental studies because of their serious influence on the environment, climate, and (more vitally, human health). This could be very interesting and important coming to the Tibetan Plateau, an elevated region with relative few human activities which seems to be isolated from the world, considering its role in global atmospheric circulations and water resources feeding billions of people. Simulating the transport is one of the most powerful approaches, but becomes very challenging to this region due to the complex topography. However, I concern about the quality in science as well as presentation, as explained below.***

We thank the reviewer for the detailed and constructive comments. They are very helpful for improving the quality of the manuscript.

In the revised manuscript, we added a few new figures in the supporting material to support some statements in the text and to address the review comments. The main text is revised substantially. Specifically, upon the comments provided by the reviewers, we realized that the comparison of the simulations at 20 km and 4 km resolutions may complicate the analysis and deviate the readers from the focus of this study about the impacts of topography. Although our results show that the difference between the simulations at two resolutions is largely contributed by the impacts of different topography, we agree that the resolution itself can introduce difference in simulated results in many aspects. Therefore, now the manuscript is revised to focus on the analysis of the difference between the two experiments at 4 km with different topography representations. Some discussions about the related work are added. A lot more details about the experiment design are added. Other text and figures have also been revised as the reviewer suggested.

- ***Of firstly questioned about the scientific quality is the application of nudging, which dumps the physics of model leading to energy unbalanced. As the authors intended to investigate the impact of topography, the experiments should then be precisely controlled as the difference comes from the representation of topography. Obviously, the nudging violates the control, bringing varying information from the forcing reanalysis data. This means that the difference between simulations may also be contributed by, in addition to resolutions, the reanalysis data via nudging.***

The nudging method was widely used for studying the regional and small-scale feature. We intend to have the large-scale circulation reasonably simulated and focus on the small-scale feature that could be significantly affected by the complex topography. Therefore, we applied the spectral nudging over the outer domain covering a relatively large region and above the PBL. For the inner domain, the nudging was not applied. Now, the manuscript is revised to focus on the analysis of the difference between two nested 4-km experiments over the inner domain, which should not be affected by the nudging. Now it is clarified in the revised manuscript as "The modeled u and v component wind, atmospheric temperature, and geopotential height over the outer domain are nudged towards the reanalysis data with a nudging timescale of 6 h following previous studies (e.g., Stauffer and Seaman, 1990; Seaman et al., 1995; Liu et al., 2012; Zhao et al., 2014; Karki et al., 2017; Hu et al., 2016, 2020). Spectral nudging method is applied to balance the performance of simulation at the large and small scales (Liu et al., 2012), and only to the layers above the planetary boundary layer (PBL) with nudging coefficients of 3×10^{-4} s^{-1}. A wave number of three is selected for both south-north and west-east directions. Please note that the choices of nudging coefficients and wave numbers for spectral nudging in this study are empirical. The purpose of nudging is to simulate reasonably large-scale feature so that small-scale impacts from the complex topography can be focused. Therefore, the modeling sensitivity to these choices is not tested in this study. The results show that the simulations with nudging method can reproduce the large-scale circulation at 700 hPa and higher over the outer domain compared to the reanalysis dataset with the spatial correlation coefficient of 0.96-0.98."

- ***Of second questioned is the conclusion from their results; it is unclear that if it is because of the more valleys resolved, though the 4-km simulation yields larger BC flux which is somehow associated with the valleys resolved by the 4-km resolution (NOTE: not the valleys resolved by 20-km). Fine resolution may result to more valleys, but these valleys meanwhile become small and irregular shaped. Moreover, complex terrain tends to yield weak near-surface wind speed due to the stronger orographic drag in both forms of gravity wave and turbulence.***

We agree that the complex topography could increase the surface roughness and reduce the near-surface wind speed. However, our simulations show evident increase of lower-level wind in some valleys resolved across the Himalayas with more complex topography. This is consistent with previous studies based on observations and numerical simulations that found the role of valley channel could increase the wind through the valley over the Himalayas region (e.g., Egger et al., 2000; Zängl et al., 2001; Carrera et al., 2009; Karki et al., 2017; Lin et al., 2018). Obviously, the enhancement function of channel overcomes its impact on surface roughness at some valleys. Now we clarify it in the revised manuscript as "The enhanced valley wind across the Himalayas has also been found by previous studies with observations and numerical simulations (Egger et al., 2000; Zängl et al., 2001; Carrera et al., 2009; Karki et al., 2017; Lin et al., 2018)."

In addition, now, we attribute the difference between the simulations with different topography to a few influential factors. The enhanced valley wind is one of them. The other primary two are resolved deeper channel and induced change of small-scale circulation. Now, the discussion is added in the revised manuscript as "One reason for the enhanced transport across the Himalayas with the original topography is the resolved deeper valleys that lead to the increased valley wind. The wind across the valleys can be significantly larger with the original topography than the smooth one (Fig. S4). The enhanced valley wind across the Himalayas has also been found by previous studies with observations and numerical simulations (Egger et al., 2000; Zängl et al., 2001; Carrera et al., 2009; Karki et al., 2017; Lin et al., 2018). The second impact of resolved complex topography on the BC transport is that more BC masses can be transported with the deeper valley channels (Fig. S5a, b). With deeper valley, the column of high-concentration BC is deeper. Even with similar wind velocity, the transport flux can be larger. The third impact is through changing the small-scale circulations around the Himalayas due to the increase of topography complexity of Himalayas. The simulation with original topography produces more near-surface winds following the direction towards the TP compared to the one with smooth topography (Fig. S6), which favors the BC transport across the Himalayas. Lastly, the simulated PBL heights from the two experiments are a little different (Fig. 9), which may also contribute partly to the different transport flux. The sensitivity of PBL height and structure to topography complexity that can result in different surface heat has been studied before (e.g., Wagner et al., 2014)."

- ***Of third questioned is that some regional modeling studies (not CHEM-focused) over this region were ignored by the authors, but these studies are close related to the concerned topic. These studies generally found that fine-resolution simulations yield weaker surface wind speed compared to coarse-resolution, which is opposite to this study. This deserves a further check or discussion.***

As we respond to your comment above, we agree that the complex topography could increase the surface roughness and reduce the near-surface wind speed. However, the increase of lower-level wind in some valleys resolved across the Himalayas is consistent with previous studies based on observations and numerical simulations (e.g., Egger et al., 2000; Zängl et al., 2001; Carrera et al., 2009; Karki et al., 2017; Lin et al., 2018). Now we clarify it in the revised manuscript as "The enhanced valley wind across the Himalayas has also been found by previous studies with observations and numerical simulations (Egger et al., 2000; Zängl et al., 2001; Carrera et al., 2009; Karki et al., 2017; Lin et al., 2018)."

In the revised manuscript, we also cite more related references focusing on the meteorological fields over the region and discuss about them, as "Previous studies also found the induced change of circulation and transport due to the complex topography at convection-permitting scales with the focus on the meteorological fields (e.g., Karki et al., 2017; Lin et al., 2018). However, most of them conducted the sub-10 km simulations over a much smaller region (e.g., 101×96 grids at 5 km in Karki et al., 2017, and 181×121 grids at 2 km in Lin et al., 2018) compared to this study (400×300 grids at 4 km). Karki et al. (2017) found that the complex topography resolving more valleys and mountain ridges yielded more realistic strong and narrower winds and also small-scale mountain-valley circulations over the Himalayas region compared to the smoother topography. Lin et al. (2018) analyzed the simulations over the region situated in the central Himalayas (87°E-89°E) with very complex terrain including several high mountains and low valleys, e.g., Mt. Everest, Mt. Kanchenjunga, and the Yadong Valley. Although Lin et al. (2018) simulated enhanced moisture flux along the valley, the overall moisture transported was lower with the complex topography (10 km resolution) compared to that with the smooth topography (30 km resolution). The difference between their study and this study could be due to several factors. First, Lin et al. (2018) focused on a relatively small region of Himalayas (87°E-89°E) compared to that in this study (75°E-92°E). The lower-lever transport flux simulated in this study also exhibits weaker wind with complex topography between 87°E and 89°E (Fig. 9 and 12), maybe due to several very high mountains such as Mt. Everest and Mt. Kanchenjunga over this area. Second, the spatial (horizontal and vertical) distributions between air pollutants and moisture are also different and may contribute partly to the different impacts of topography on the overall transport flux across the Himalayas."

- ***Of final questioned is the balance between their short-period simulations (focusing on a special case) and their climatic implication.***

Yes, we agree that the short-period simulation cannot be used to access the climate impact. That's why we didn't discuss much about climatic impact in the manuscript. Instead, we estimate the impacts on radiative forcing in the atmosphere and snow. This study focuses on raising the potential issue of using smooth topography on modeling BC transport and radiative forcing over the TP, and can be treated as the implication for future study about climatic impact with high-resolution simulations. As we acknowledged in the manuscript that long-term climatic impact deserves further investigation.

"Since this study only demonstrates the potential impacts for a relatively short period, a longer-term study should be conducted to examine the impacts of topography on aerosol climatic effect over the TP."

"These potential impacts of aerosols on regional hydro-climate around the TP and over Asia using high-resolution model that can resolve the complex topography of Himalayas and TP deserve further investigation."

- ***With regards to the presentation quality, there are too many stuffs (especially in sections of Introduction and Methodology) that are not directly related to the main topic presented but some vital information missing. The latter is fatal because it led to the lack of reasonability of their design of the model experiment. In particular, I would not to say that the authors presented Methodology correctly, which is expected to state how to deal with the question argued in the Introduction and why the approach(es) can be appropriate to resolve the question. To be more detailed, I found no text addressed why the authors chose WRF-CHEM, why did nudging, why selected those parametrization schemes, and how these approaches are related to their goal (to answer how the representation of topography impacts on simulation of BC transport).***

A lot more details about the experiment design are added into the Introduction and Methodology sections in the revised manuscript, particularly responding to the comments here about the reason to choose the model and parameterizations. For example,

"In order to examine the potential impacts of complex topography on pollutant transport across the Himalayas over the TP, this study conducts multiple experiments with the Weather Research and Forecasting Model coupled with chemistry (WRF-Chem, Grell et al., 2005; Skamarock et al., 2008). The WRF-Chem model is selected because it includes the interaction between meteorology and aerosol and is widely used for regional modeling of aerosol and its climatic impact (e.g., Cao et al., 2010; Zhao et al., 2010, 2011, 2012, 2014; Wu et al., 2013; Gao et al., 2014; Huang et al., 2015; Fan et al., 2015; Feng et al., 2016; Zhong et al., 2017; Sarangi et al., 2019; Liu et al., 2020). The model has also been used to investigate the aerosol transport and climatic impact over the Himalayas region (e.g., Feng et al., 2016; Cao et al., 2010; Sarangi et al., 2019). The model is suitable for simulations at hydrostatic and non-hydrostatic scales and thus can be used for investigating the impacts of resolution-dependent feature, such as topography, on modeling results. In particular, the meteorological part of the model (WRF) has been systematically evaluated and used to investigate the impacts of resolutions on simulations of moisture transport and climate over the Himalayas region (e.g., Shi et al., 2008; Karki et al., 2017; Lin et al., 2018). All of these previous studies with the model lay the foundation for this modeling study."

"The goal of this study is to investigate the impacts of different representations of topography on the transport of BC across the Himalayas. Therefore, besides this control experiment, one sensitivity experiment is also conducted with the same configuration as the control one except that the topography of the inner domain at 4 km resolution is prescribed to follow that at 20 km resolution similar as previous studies (e.g., Shi et al., 2008; Wu et al., 2012; Lin et al., 2018). More specifically, the sensitivity experiment applies a single value for each nested 5×5 grids over the inner domain as the corresponding grid of 20 km from the outer domain. The two experiments are referred to the simulations with original and smooth topography, respectively, hereafter."

"The difference of results from the two experiments over the inner domain is analyzed as the impacts of topography representations. Therefore, all the results shown below are from the simulations of the inner domain at 4 km resolution with different topography if not otherwise stated."

"The detailed configuration of WRF-Chem experiments is summarized in Table 1. Due to the lack of publicly available in-situ observations, this study does not tend to evaluate systematically the simulated meteorological fields over the Himalayas region. However, as shown in Table 1, the choice of physical parameterizations in this study follows that of one previous study (Karki et al., 2017) that evaluated systematically the WRF simulation for one entire year over the Himalayas region. Their results showed that the WRF simulation at convection-permitting scale could generally capture the essential features of meteorological fields such as precipitation, temperature, and wind over the Himalayas region. Therefore, the WRF-Chem simulations in this study are reliable to investigate the impacts of topography over the Himalayas region."

- ***Moreover, descriptions of some analyses were also missing: 1) how the flux was calculated? based on model levels or interpolated pressure levels? 2) If it is the latter, how the influence of interpolation was considered? 3) Have the u and v been rotated? 4) How was the difference between different resolutions (grid spacing) calculated? regrided? and how? 5) and so on.***

Now the analysis focuses on the two experiments at 4 km with different topography, therefore, the interpolation between the resolutions is not needed. A lot more details about the analysis method are added into the Methodology and Result sections in the revised manuscript, particularly responding to the comments here about the flux calculation. For example,

"The transport flux is calculated by projecting the wind field perpendicularly to the cross line and then multiplying the BC mass concentration along the cross line. More specifically, the transport flux are calculated as following:

$$\mathrm{TF} = C * (u * \sin\alpha + v * \sin\beta) \qquad (1)$$

Where α is the angle between east-west wind component and the cross line, β is the angle between south-north wind component and the cross line, and C is the BC mass concentration at the grid along the cross line. The flux is estimated at each model level. Positive values represent the transport towards the TP, while negative values represent the transport away from the TP."

"The total mass flux is calculated by integrating the right-hand term of equation (1) as following:

$$\mathrm{ITF} = \int_{z=z_{sfc}}^{z=z_{top}} \delta z * C * (u * \sin\alpha + v * \sin\beta) \qquad (2)$$

Where δz is the thickness of each vertical model level. Similarly, positive values represent the transport towards the TP, while negative values represent the transport away from the TP."

- ***The language may also required to be polished by a native speaker. The problem is not much with the grammar but the lack of logic in the context, which could be due to inappropriate usage of some words.***

Thanks for your suggestion. The language is polished in the revised manuscript.

Specific comments:

- ***Section 2.1.1: Most of the model description are not related to and cannot assist to resolve the main issue. However, specific description of some diagnosis used in the analyses were not presented.***

Thanks for your suggestion. Now this part of the manuscript is revised substantially.

- ***L199-200: Does the model use z vertical coordination as revealed by fig2?***

The WRF-Chem simulations conducted in this study used the terrain following coordinate (Skamarock et al., 2008). We showed an average vertical distribution of model layer thickness over a region selected within the simulation domain in Fig. 2. Now we clarify this in the revised manuscript as "The WRF-Chem simulations conducted in this study use the terrain following coordinate (Skamarock et al., 2008). To resolve the vertical structure of transport across the Himalayas, the simulations are configured with 54 vertical layers and denser layers near the surface. For example, averaged over a region (26°N-28°N, 76°E-80°E) near the southern Himalayas, there are about 17 layers below 2 km above the ground (Fig. 2)."

- ***L205-207: Why 'probability distribution'(actually not pdf but normalized histogram as presented by Fig S1) to reveal the difference in topography?***

This figure is used to demonstrate better the difference between two topography over the Himalayas mountainous region. The similar figure was also used in previous studies, for example, Rhoades et al. (2018).

- ***L208-209: Why the simulation period and analysis period?***

In fact, we included the reason in the introduction section as "The simulations are conducted for April 2016 in pre-monsoon season, because South Asia is seriously polluted during this period and the pollutants transported to the TP during the period may have significant impacts on Asian monsoon system (e.g., Lau et al., 2006a, b; Ding et al., 2009; Kuhlmann and Quaas, 2010; Qian et al., 2011, 2015). In addition, the observed concentration of BC at the observation station besides Mt. Everest shows an evident pollution episode from April 5th to 16th of 2016, deserving the investigation of the transport mechanisms."

Now, we clarify the sentences in the Methodology part of revised manuscript as "The simulations are conducted for March 29th-April 20 of 2016 for the reason as discussed in the introduction. The results of April 1th-20th are analyzed for the observed pollution episode to allow a few days spin-up for chemical initial condition."

- ***L210-211: ECMWF has many products of reanalysis data; which?***

We use the ERA-Interim product. Now it is clarified in the revised manuscript as "The meteorological initial and lateral boundary conditions are derived from the European Centre for Medium-Range Weather Forecasts (ECMWF) reanalysis data at 0.5°×0.66° horizontal resolution and 6 h temporal intervals (ERA-Interim dataset)."

- ***L212: Why u, v, T but not PHI?***

We selected these variables for nudging to make sure the large-scale feature can be simulated reasonably following previous studies (e.g., Liu et al., 2012; Zhao et al., 2014; Karki et al., 2017; Hu et al., 2016, 2020). We did nudge geopotential height as well during the simulations. We correct this in the revised manuscript.

- ***L213-214: Citation here refers to?***

The citations here refer to the details about describing the nudging method in the model and also some previous related studies. Now the sentence is revised as "The modeled u and v component wind, atmospheric temperature, and geopotential height over the outer domain are nudged towards the reanalysis data with a nudging timescale of 6 h following previous studies (e.g., Stauffer and Seaman, 1990; Seaman et al., 1995; Liu et al., 2012; Zhao et al., 2014; Karki et al., 2017; Hu et al., 2016, 2020)."

- ***L216: Identical wave number for both domains? If so, why?***

The choice of wave number is empirical. The purpose of this study is not to investigate the modeling sensitivity to this parameter. However, we checked that the simulated large-scale circulations at 700 hPa and above over the outer domain are consistent with the reanalysis dataset with the spatial coefficients of ~0.98. Now we add the clarification in the revised manuscript as "Please note that the choices of nudging coefficients and wave numbers for spectral nudging in this study are empirical. The purpose of nudging is to simulate reasonably large-scale feature so that small-scale impacts from the complex topography can be focused. Therefore, the modeling sensitivity to these choices is not tested in this study. The results show that the simulations with nudging method can reproduce the large-scale circulation at 700 hPa and higher over the outer domain compared to the reanalysis dataset with the spatial correlation coefficient of 0.96-0.98."

- ***L221-227: Simulation period is 2016 but the quasi-global simulation that provide chemical initial and boundary conditions is done before 2013, considering the reference cited herein?***

Chemical initial and boundary conditions are from the quasi-global simulation for the same period in 2016. Now, we clarify it in the revised manuscript as "The chemical initial and boundary conditions are provided by a quasi-global WRF-Chem simulation for the same time period to include long-range transported chemical species. The quasi-global WRF-Chem simulation is performed at 1°×1° horizontal resolution using a quasi-global channel configuration with 360×130 grid cells (180°W-180°E, 60°S-70°N). More details about the general configuration of quasi-global WRF-Chem simulation can be found in Zhao et al. (2013b) and Hu et al. (2016)."

- ***Section 2.1.2: A completed table of model configuration here could be better***

Thanks for the suggestion. Now, we add a table to summarize the model configuration in the revised manuscript.

- ***Section 2.1.3: Emissions data described seem older that 2016?***

For anthropogenic emissions, the latest inventory publicly available for South Asia is from the Hemispheric Transport of Air Pollution version-2 (HTAPv2) inventory for year 2010 (Janssens-Maenhout et al., 2015). It is quite common to use the latest anthropogenic emission inventory for modeling in a different year. Therefore, it is used in this study. The biomass burning emission is from the inventory for the simulation period of 2016. As we discussed in the manuscript, the biomass burning emission is the dominant source near the southern Himalayas in the simulation period. Now we clarify it in the revised manuscript as "Biomass burning emissions are obtained from the Fire Inventory from National Center for Atmospheric Research (FINN) with hourly temporal resolution and 1 km horizontal resolution (Wiedinmyer et al., 2011) for the simulation period, and are vertically distributed following the injection heights suggested by Dentener et al. (2006) from the Aerosol Comparison between Observations and Models (AeroCom) project."

- ***L247: Biomass burning emission not of anthropogenic?***

Yes, biomass burning emission is often treated differently from the anthropogenic fossil fuel emissions such as from transport, power plant, and industry. In WRF-Chem, we separate anthropogenic fossil fuel and biomass burning emissions as two sources.

- ***L262: 'nadir'?***

The scanning angle of MODIS is ±55°, the resolution of scanning facing directly below is 10km (nadir, i.e., 0°). When the scanning angle is deviated from 0°, the resolution will be distorted.

- ***L265: 'identical'?***

We tend to mean that all radiometers are the similar instruments. We revise it to "similar".

- ***L269: Why 'AOD at 600 nm', while MODIS AOD at 550 nm?***

The model estimates AOD at the wavelengths of 300 nm, 400 nm, 600 nm, and 999 nm to reduce the computational cost. Now, we use the Angström exponent to interpolate the AOD at 600 nm to 550 nm from the simulations and revise the figures. The difference is quite small.

- ***L273-277: BC measurement: when? how? uncertainty?***

The BC measurement is collected for April 4-20 of 2016 at the Qomolangma (Mt. Everest) Station for Atmospheric and Environmental Observation and Research (QOMS, 86.94°E, 28.36°N) located at the northern slope of Himalayas, about 4276 meters above sea level. The BC mass concentrations are measured with the widely-used instrument Aethalometer (AE-33) that can provide real-time BC mass concentration measurements. The calibration of air flow is routinely conducted to maintain the data quality. Now, more details about the measurement and its uncertainty are provided in the revised manuscript as "The third one is the measurement of surface BC mass concentration collected during the simulation period for April 4-20 of 2016 at the Qomolangma (Mt. Everest) Station for Atmospheric and Environmental Observation and Research, Chinese Academy of Sciences (QOMS, 86.94°E, 28.36°N) which is located at the northern slope of the Himalayas, about 4276 meters above sea level. The BC mass concentration is measured with the widely-used instrument Aethalometer (AE-33) that can provide real-time BC mass concentration measurements. The calibration of air flow is routinely conducted to maintain the data quality. The instrument estimates the BC mass concentration based on the optical method through measuring the reduction in light intensity induced by BC. The method assumes that the relationship between attenuation and BC surface loading is linear for low attenuation values. However, this relationship becomes nonlinear when the attenuation values are high due to a filter saturation effect, which may lead to underestimation of the high BC concentration. The detection limit of AE-33 instrument is 5 ng/m^3, and the uncertainty is estimated to be within 10% (e.g., Chen et al., 2018; Bansal et al., 2019; Kant et al., 2019). The dataset of BC mass concentration used in this study was reported by Chen et al., (2018), where more details about the measurements can be found."

- ***Section 3.1: The initial chemical condition and the emission at the two resolutions of the simulation should be presented so as to discuss simulated transport of BC; moreover, the difference of terrain height (similar to fig5c) could reveal something.***

The initial chemical conditions of simulations at different resolutions are interpolated from the same global dataset, so that they are similar. In addition, as we mentioned in the manuscript, the simulations are conducted for March 29th-April 20 of 2016 but only the results of April 1th-20th are analyzed to allow a few days spin-up to avoid the impacts from the chemical initial conditions. Therefore, we do not think the initial chemical condition matters. In addition, now the manuscript is revised to focus on the analysis of the difference between the two experiments at 4 km with different topography representations instead of between the simulations at two resolutions.

Upon your suggestion, the difference of the terrain height is added in Fig. 3 of the revised manuscript.

Although the analysis of revised manuscript does not focus on the simulations at two resolutions any more, we calculate the emissions over the two resolutions, and the amounts are conservative with the difference less than 0.1% in the inner domain across different resolutions.

- ***L302-304: Why? Because of convergence? Or just because of the direction towards the TP?***

Yes, it is just because that the direction is toward the TP. It has been discussed in previous studies using back-trajectory models (e.g., Dumka et al., 2010; Kang et al., 2015; Cong et al., 2015a).

- ***L317-318: Meaningless to compare column and surface BC (fig5 vs fig8)***

Fig. 8 is deleted following your suggestion.

- ***L321-322: Something represents local circulation thanks to the difference to that of upper-air?***

This sentence is deleted in the revised manuscript.

- ***L333-336: Reasonably? No, the transport is not related to the concentration change, but the divergence is.***

Yes, we agree that the concentration is not directly linked with transport flux, instead is determined by divergence. The text is revised substantially, and this part is deleted. But, now we add some discussions about the contribution from different model processes including transport to the change of BC concentrations over the TP based on the processing analysis method introduced in Du et al., (2020). The discussion is added as "All the analysis above focuses on investigating the BC transport flux across the Himalayas. Although the inflow can reflect the impact of transport on the BC mass over the TP to some extent, the change of BC mass concentration is eventually determined by the convergence of transport. Therefore, the contribution of each model process (transport, dry-deposition, emission, PBL mixing, and wet deposition) to the increase of BC column mass averaged over the TP (with elevation > 4 km) during this episode is analyzed for both simulations following the methodology introduced by Du et al. (2020). The results show that the two main processes affecting the BC column mass over the TP during the period are transport and dry deposition. The transport is the dominant process that increases the BC column mass over the TP, while the dry deposition reduces it. The contribution of transport to the increase of BC column mass over the TP during the episode from the simulation with the original topography is significantly larger than that with the smooth topography, which is consistent with the results shown by analyzing the transport flux across the Himalayas."

- ***Section 3.2: A) I would rather expect two separated parts of flux, height-crossline plot of BC concentration and wind speed, so that we can diagnose the difference is due to either overall more column BC or wind speed, or both of them.***

Upon your suggestion, the cross sections of BC mass concentration and wind speed are added as Fig. S5a and b in the supporting material. The discussion about the reasons for the difference resulted from the complex topography is also added in the revised manuscript as "One reason for the enhanced transport across the Himalayas with the original topography is the resolved deeper valleys that lead to the increased valley wind. The wind across the valleys can be significantly larger with the original topography than the smooth one (Fig. S4). The enhanced valley wind across the Himalayas has also been found by previous studies with observations and numerical simulations (Egger et al., 2000; Zängl et al., 2001; Carrera et al., 2009; Karki et al., 2017; Lin et al., 2018). The second impact of resolved complex topography on the BC transport is that more BC masses can be transported with the deeper valley channels (Fig. S5a, b). With deeper valleys, the column of high-concentration BC is deeper. Even with similar wind velocity, the transport flux can be larger. The third impact is through changing the small-scale circulations around the Himalayas due to the increase of topography complexity of Himalayas. The simulation with original topography produces more near-surface winds following the direction towards the TP compared to the one with smooth topography (Fig. S6), which favors the BC transport across the Himalayas. Lastly, the simulated PBL heights from the two experiments are a little different (Fig. 9), which may also contribute partly to the different transport flux. The sensitivity of PBL height and structure to topography complexity that can result in different surface heat has been studied before (e.g., Wagner et al., 2014)."

- ***B) I would also expect spatial pattern of column (or lower model levels) BC transport.***

Now we show the spatial distribution of lower-level wind (below 500 m above the ground) in Fig. S6 in the supporting material. The discussion about the difference between the two experiments is also added in the revised manuscript as shown in the response to the comment above.

- ***L346-347: A) Prevailing westerlies, but 'northward' or 'southward' accounted here?***

Thanks for your checking. Now we clarify it in the revised sentence as "Positive values represent the transport towards the TP, while negative values represent the transport away from the TP."

- ***B) Can it be sensitive to the cross-line defined? How will the result be move the crossline towards or backwards the TP? See fig11, lower daytime transport towards TP than nighttime at north to ~29.5 deg N.***

Thanks for your suggestion. We move the cross line towards and away from the TP by about 50 km and re-calculate the flux (Fig. R1, R2, R3, R4, R5, and R6). Although the topography and strength of flux change, the key information about the cross-Himalayas transport is still evident. The transport in daytime is also stronger than in the nighttime. The results are generally consistent with that shown in Fig. 10. Now, we add this clarification in the revised manuscript as "The sensitivity analysis by moving the cross line (cross-section of the analysis in Fig. 9, 12, 13) towards or away from the TP within a certain distance and re-calculating the flux indicates that the impacts of topography on the simulated results do not change significantly."

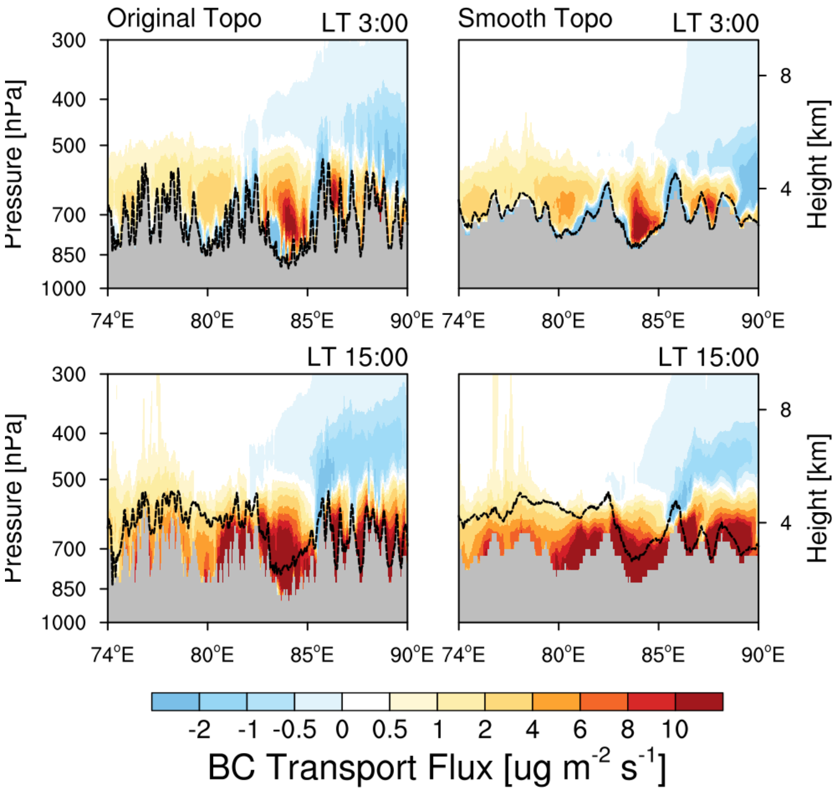

Figure R1. Longitude-height cross section of BC transport flux along the cross line about 50 km away from TP compared to the black dash line shown in Fig. 3 from the simulations at original and smooth topography at local time (LT) 03:00 and 15:00 averaged for April 1-20. The PBL height along the cross section is shown here as the black dash line.

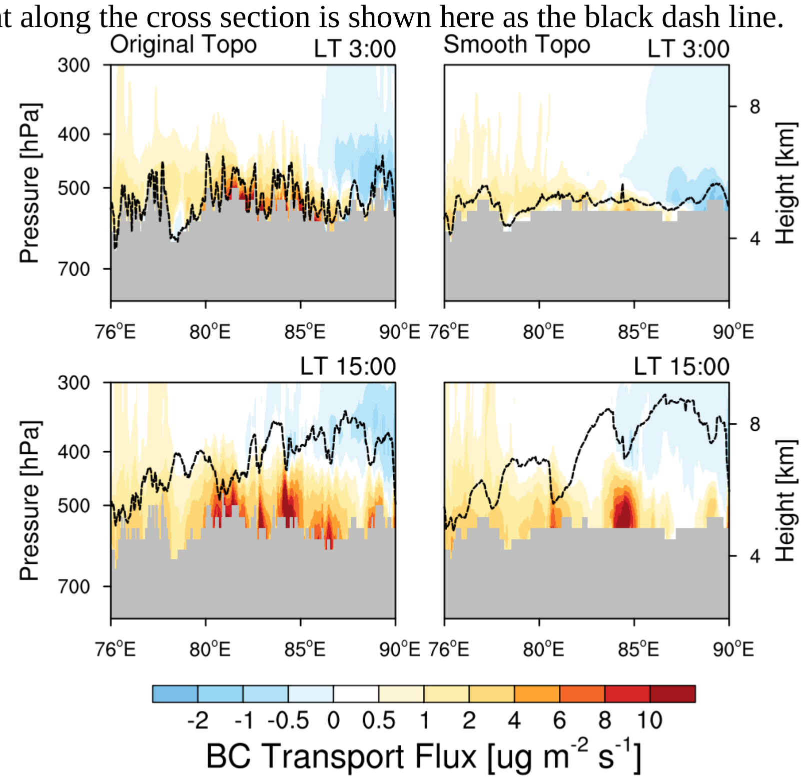

Figure R2. Longitude-height cross section of BC transport flux along the cross line about 50 km towards TP compared to the black dash line shown in Fig. 3 from the simulations at original and smooth topography at local time (LT) 03:00 and 15:00 averaged for April 1-20. The PBL height along the cross section is shown here as the black dash line.

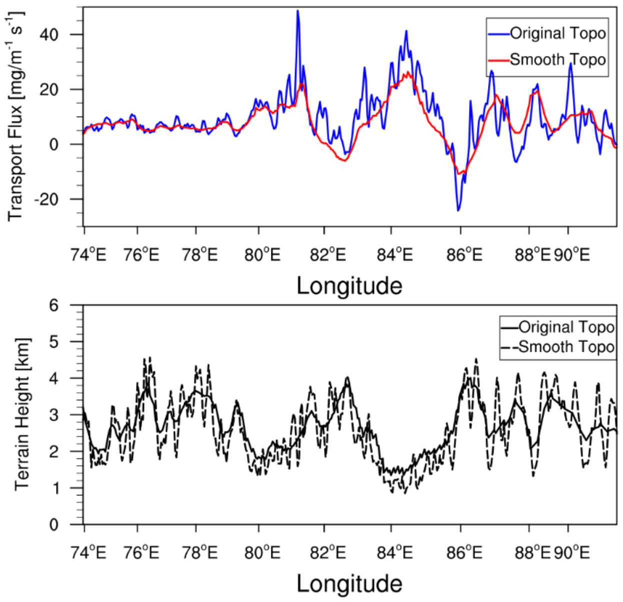

Figure R3. Longitudinal distribution of integrated BC mass flux along the cross section about 50 km away from TP compared to the black dash line shown in Fig. 3 from the simulations with original and smooth topography. The black lines represent the terrain heights with different topography.

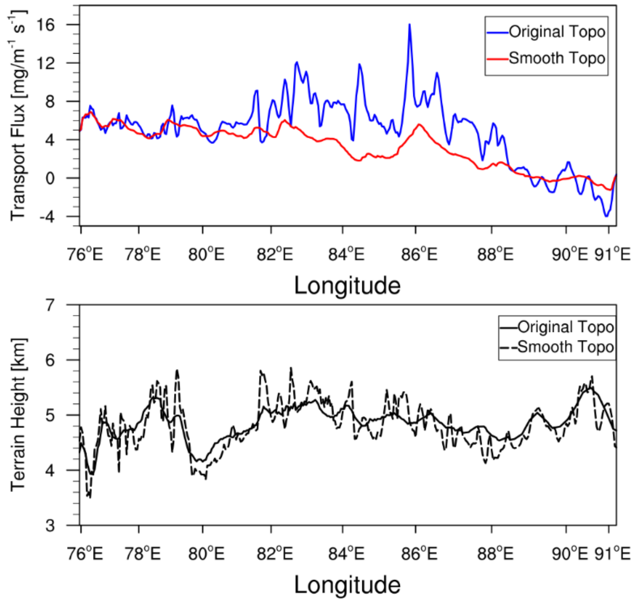

Figure R4. Longitudinal distribution of integrated BC mass flux along the cross section about 50 km towards TP compared to the black dash line shown in Fig. 3 from the simulations with original and smooth topography. The black lines represent the terrain heights with different topography.

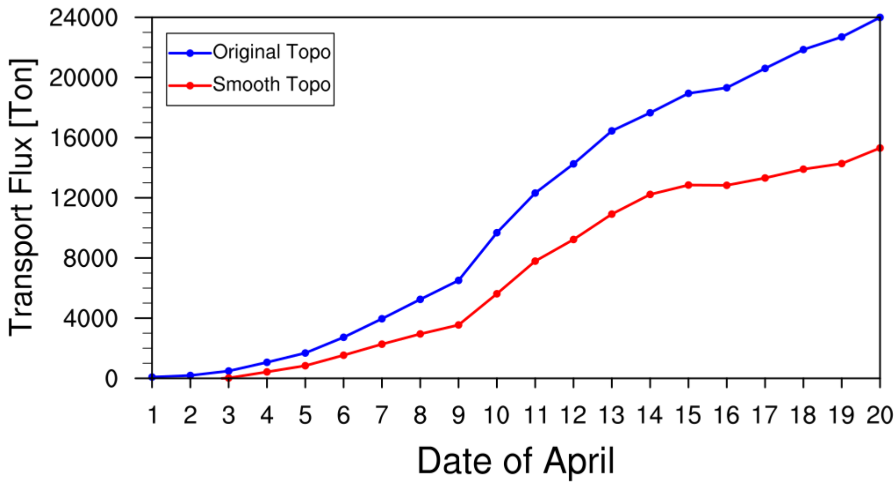

Figure R5. Accumulated integrated total transport flux of BC across the Himalayas along the cross section about 50 km away from the TP compared to the black dash line shown in Fig. 3 from the simulations at original and smooth topography during April 1-20, 2016.

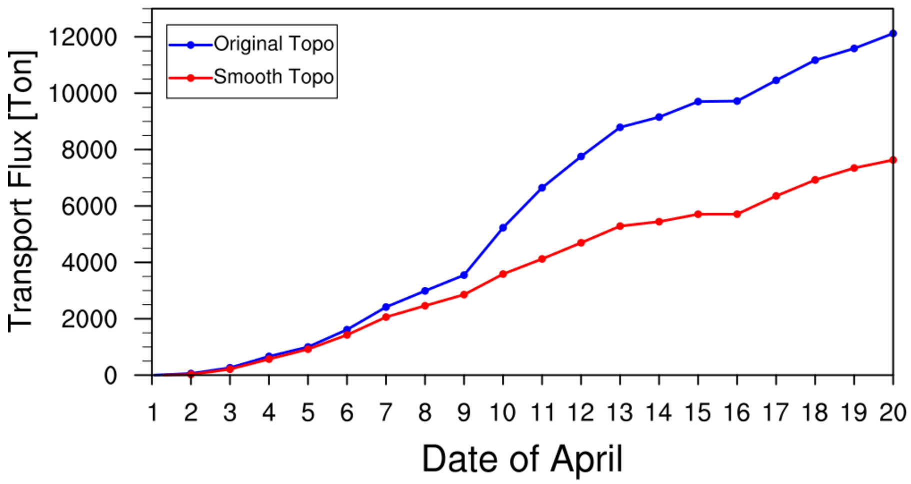

Figure R6. Accumulated integrated total transport flux of BC across the Himalayas along the cross section about 50 km towards the TP compared to the black dash line shown in Fig. 3 from the simulations at original and smooth topography during April 1-20, 2016.

- ***L353-357: Again, why diurnal cycle of local circulation while daily mean of large scale circulation?***

Sorry for the confusion. Here, we named "mean flux" as large-scale and "anomalies" as local-scale. Now, we remove these names and clarify the sentences in the revised manuscript as "If removing the mean flux during the simulation period, the transport flux anomalies show evident diurnal variation between the day and night (Fig. S3 in the supporting material). This suggests that on average, the large-scale westerly is one of the key mechanisms transporting BC across the Himalayas into the TP, while the circulation anomalies strengthen the prevailing import transport during the daytime and weakens the import during the night, particularly on the west of ~85°E."

- ***L359-360: It seems to be true to explain the diurnal cycle. But, 4-km simulation seems has shallower PBL compared to 20-km while larger BC transport than 20-km? Explanation?***

The sensitivity of simulated PBL height to model horizontal resolution has been found in previous studies. Now we add the discussion and references in the revised manuscript as "Lastly, the simulated PBL heights from the two experiments are a little different (Fig. 9), which may also contribute partly to the different transport flux. The sensitivity of PBL height and structure to topography complexity that can result in different surface heat has been studied before (e.g., Wagner et al., 2014)."

- ***L368-390: A) Two slices can serve as an example but cannot be used to draw a general conclusion; B) If BC transport can or not overcome ridges more depends on the height of the ridge and the vertical profile of BC concentration, as well as wind direction; as A), only two slices are insufficient to draw a general conclusion that BC transport can overcome ridges, and this conclusion is lack of a certain context (how high the ridges are).***

Yes, we agree that the two slices can only serve as examples to demonstrate the general picture. We did check more slices and the results are consistent. In fact, the conclusion of that transport can overcome mountain ridges are drawn from Fig. 9. Fig. 9 shows that although in the simulation with the original topography, the mountain ridges resolved weaken the crossing-Himalayas transport compared to the simulation with smooth topography, the overall positive values near the surface indicate that the transport can overcome most mountain ridges along the Himalayas. The transport fluxesflux near the surface from the simulation with the original topography become close-to-zero only at a few mountain ridges that are 6.5 km or higher. Now we add the discussion in the revised manuscript as
"The simulation with smooth topography produces overwhelming crossing-Himalayas transport towards the TP within the PBL, in particular during the daytime. Although, in the simulation with the original topography, the mountain ridges resolved weaken the crossing-Himalayas transport compared to the simulation with smooth topography, the overall positive values near the surface indicate that the transport can overcome most mountain ridges along the Himalayas. The transport fluxes near the surface from the simulation with the original topography become close-to-zero only at a few mountain ridges that are 6.5 km or higher."
"To better demonstrate the transport pathway across mountain ridges, one cross-section across the mountain ridge as shown as one black solid line in Fig. 3 is taken as one example. Figure 10 shows the latitude-height cross section of BC mass concentrations and transport flux across one mountain ridge from the simulations with the original and smooth topography at local time (LT) 03:00 and 15:00 averaged for April 1-20, 2016. Near the southern part of mountain, the elevated concentrations of BC mass accumulate and can mix up reaching as high as 5 km with the much stronger transport during the daytime It is obvious that the mountain ridge in the simulation with smooth topography is quite low. With the high mountain ridge resolved by the original topography, the simulated BC transport flux can still cross the mountain. Analysis of transport flux across a few more mountain ridges indicates similar results (not shown). The results above indicate that the transport of pollutants can cross a majority of mountain ridges of Himalayas, which is consistent with the observation-based estimate by Gong et al. (2019)

that also found pollutants could overcome the blocking effect of mountain ridges of Himalayas as a transport pathway. On the other hand, the resolved deeper valleys in the simulation with the original topography enhanced the transport flux compared to the simulation with the smooth topography. Similarly, Figure 11 shows one example of latitude-height cross section of BC mass concentrations and transport flux across one valley from the simulations with the original and smooth topography at local time (LT) 03:00 and 15:00 averaged for April 1-20, 2016. The transport is much stronger and deeper along the valley from the simulation with original topography than the one with smooth topography. Again, analysis of transport flux across a few more valleys does not show different results (not shown)."

- ***L391-392: Can the result shown in fig13 be sensitive to the location of the cross-line? It needs a check.***

Thanks for your suggestion. See our response to the comment above. We did the test and the key information about the cross-Himalayas transport is still evident, and the clarification is added in the revised manuscript.

- ***L410-421: It is unclear how the authors applied the 20-km resolution topography to the 4-km simulation. Does it mean that 5 by 5 grids at 4-km resolution have identical terrain height as the corresponding grid of 20-km resolution? If it is of this case (I guess it is), does it really represent a 20-km resolution topography? Thinking about the slope of neighbouring grids (0, 0, 0, 0, a huge value, 0, 0 ...)? ... NO, this check (if it is topographical impact) makes no sense.***

In the sensitivity experiment at 4 km resolution with smooth topography, we applied a single value for each nested 5×5 grids as the corresponding grid of 20 km. In this way, the simulation at 4 km will have almost identical topography as that at 20 km. It is quite common in the modeling community to check the impact of topography through conducting the sensitivity experiment through prescribing different topography during the simulation (e.g., Shi et al., 2008; Wu et al., 2012; Lin et al., 2018). Here, when we talk about topography impact, we mean the difference between the complex and smooth topography, i.e., the impact due to the difference between the topography at 20 km and 4 km resolutions.

We would argue that it is a valid way to investigate the impacts of different topography on modeling results. Now we add the clarification in the revised manuscript as "The goal of this study is to investigate the impacts of different representations of topography on the transport of BC across the Himalayas. Therefore, besides this control experiment, one sensitivity experiment is also conducted with the same configuration as the control one except that the topography of the inner domain at 4 km resolution is prescribed to follow that at 20 km resolution similar as previous studies (e.g., Shi et al., 2008; Wu et al., 2012; Lin et al., 2018). More specifically, the sensitivity experiment applies a single value for each nested 5×5 grids over the inner domain as the corresponding grid of 20 km over the outer domain. The two experiments are referred to the simulations with original and smooth topography, respectively, hereafter."

- ***L428: fig15: How about the region other than the TP, especially the south? (For fig5, 8, 16, 17, why the region other than the TP is masked? Without this part as well as boundary conditions, it is not able to check the mass balance, which is however fatal for understand transport)***

Since our focus is about the BC impacts over the TP, we decided to only show the values over the Himalayas and TP. Now we show the spatial distribution over the entire inner domain in Fig. 5, 15, and 16, although the Fig. 15 and Fig. 16 are similar to previous ones because there is no snow in the inner domain except the regions of Himalayas and TP.

- ***Section 3.3: The snow difference between different resolutions further indicates that not only topography play a role in the model experiments. For example, the adaptation of physical schemes to different resolution may also play a role.***

Yes, we agree that the resolution itself can introduce difference in simulated results in many aspects, and the comparison of the simulations at 20 km and 4 km resolutions may complicate the analysis and deviate the readers from the focus of this study about the impacts of topography. Therefore, now the manuscript is revised to focus on the analysis of the difference between the two experiments at 4 km with different topography representations. See our response to other comments as well.

Technical comments:

- ***L259: Abbreviation without the full name that it stands for. Here 'MODIS' as an example. Please recheck.***

Thanks for checking. Now the full names are provided for all abbreviations.

Anonymous Referee #2

General comments:

- ***This study uses WRF-Chem at two horizontal resolutions to investigate the impacts of topography on the transport and distribution of BC over the TP during the pre-monsoon season. A sensitivity test that the inner domain at 4 km resolution applies the 20 km-resolution topography is also conducted to confirm the importance of topography complexity. It is found that the prevailing up-flow across the Himalayas driven by the large-scale circulation is the dominant transport mechanism of South Asian BC into the TP in the simulations at both resolutions, and the simulation at the finer resolution (4 km) resolves more valleys and thus transport BC more efficiently. This is an interesting and important work in understanding BC contamination over the TP and its radiative impact. However, a number of caveats leave the conclusions unconvincing. The smooth 4 km sensitivity test has different results from the 20 km simulation, indicating the effects of other factors. It is necessary to discuss or quantify: 1) how wind field changes under different resolutions and whether/how much it is related to the representation of topography, 2) the impact of resolution on PBL and vertical mixing, 3) the influences of resolution on emissions, and 4) other possible parameters that could lead to the differences in BC transport over the TP. This paper still requires additional work.***

We thank the reviewer for the detailed and constructive comments. They are very helpful for improving the quality of the manuscript.

In the revised manuscript, the main text is revised substantially to make the conclusion more convincing. Specifically, upon the comments provided by the reviewers, we realized that the comparison of the simulations at 20 km and 4 km resolutions may complicate the analysis and deviate the readers from the focus of this study about the impacts of topography. Although our results show that the difference between the simulations at two resolutions is significantly contributed by the impacts of different topography, we agree that the resolution itself can introduce difference in simulated results in many aspects, such as wind circulation and PBL mixing. Therefore, now the manuscript is revised to focus on the analysis of the difference between the two experiments at 4 km with different topography representations. The emissions are checked to be conservative between the two resolutions. Some discussions about the related work are added. A lot more details about the experiment design are added. Other text and figures have also been revised as the reviewer suggested.

Major issues:

- ***1. This study only emphasizes the importance of topography, but according to the comparisons of the 20 km simulation and the smooth 4 km simulation in Figure 13, 15, 16, 17, and Figure S5, there could be other factors contributing to the differences in the transport of BC over the TP in the simulations at the two resolutions. The manuscript attempts to provide some interpretations, but many of them do not seem appropriate (e.g., L445-448). In particular, under the two resolutions, wind vectors show different patterns. A detailed examination on the interactions of modeling resolution, wind speed, and topography is required.***

Yes, we agree that the resolution itself can introduce difference in simulated results in many aspects, because the development of scale-aware physics, such as PBL and cloud physics, is still a challenging work in the modeling community. The comparison of the simulations at 20 km and 4 km resolutions may complicate the analysis and deviate the readers from the focus of this study about the impacts of topography. Although the impact of resolution on modeling the crossing-Himalayas transport is also interesting, it is beyond the scope of this study. Therefore, now the manuscript is revised to focus on the analysis of the difference between the two experiments at 4 km with different topography representations. The corresponding text is revised substantially in the revised manuscript.

- ***2. The study uses the MYNN planetary boundary layer scheme. This local PBL scheme may not be able to account for deeper vertical mixing. The study does not comment on the impact of cloud convection in vertical mixing, which could also contribute to the differences in BC transport flux. Does the simulation period include cloudy days? Does the study account for cloud layers, which normally serves as an extension of PBL?***

Yes, the MYNN PBL scheme does not include the non-local mixing term. However, both the local MY schemes (such as MYJ and MYNN) and non-local YSU scheme were used intensively. Especially, a recent study found that MYNN and YSU produced similar results in the tropical region (Hariprasad et al, 2014). Further, in India region, it showed that MYNN outperformed YSU regarding the boundary layer structure simulation (Gunwani and Mohan, 2017). In fact, one previous study (Karki et al., 2017) evaluated systematically the WRF simulation with the MYNN PBL scheme for one entire year over the Himalayas region. Their results showed that the WRF simulation at convection-permitting scale could generally capture the essential features of meteorological fields such as precipitation, temperature, and wind over the Himalayas region. Therefore, in our simulation, the MYNN scheme is selected as the PBL scheme.

Although the convective transport is accounted in this study, we did not discuss much about it because convection is not very active during the pre-monsoon season. Convective transport may play an important role during the monsoon season, and deserves further investigation. Now we acknowledge this in the discussion section of the revised manuscript as "In addition, the active convection during the monsoon season may also play an important role on pollutant transport across the Himalayas, which deserves further investigation."

- ***3. For emission, there are two main concerns: 1) The study uses a combined emission from two emission inventories for different years. Since emissions change dramatically in recent years, using different emissions over distinct regions could cause bias and also lead to inconsistency near the boundaries.***

For anthropogenic emissions, the latest inventory publicly available for South Asia is from the Hemispheric Transport of Air Pollution version-2 (HTAPv2) inventory for year 2010 (Janssens-Maenhout et al., 2015). It is quite common to use the latest anthropogenic emission inventory for modeling at a different year. Therefore, it is used for the inner domain and the regions of outer domain except East Asia in this study. Since this study does not focus on estimating the relative contributions from different regions to pollutants over the TP, we do not think this inconsistency will affect our results. In addition, as we discussed in the manuscript, the biomass burning emission is the dominant source near the southern Himalayas in the simulation period. The biomass burning emission is from the inventory for the simulation period of 2016. Now we clarify it in the revised manuscript as "Biomass burning emissions are obtained from the Fire Inventory from National Center for Atmospheric Research (FINN) with hourly temporal resolution and 1 km horizontal resolution (Wiedinmyer et al., 2011) for the simulation period, and are vertically distributed following the injection heights suggested by Dentener et al. (2006) from the Aerosol Comparison between Observations and Models (AeroCom) project."

- ***2) Are emissions conservative in the inner domain across different resolutions? This is crucial to understand the differences in BC transport at the two resolutions.***

The emissions for different resolutions are regrided from the same dataset. Although the analysis of revised manuscript does not focus on the simulations at two resolutions any more, we calculate the emissions at the two resolutions, and the amounts are conservative with the difference less than 0.1% in the inner domain across different resolutions.

- ***4. Figure 7: Although the magnitudes are similar, R values of the comparisons are actually quite low and there is no obvious improvement when using 4 km resolution. This indicates large uncertainties which could be due to model setup, such as emission and/or PBL scheme selection.***

We calculated the correlation coefficient between the simulations and the observations at the two sites. Although the values are similar between the two experiments at the NAM site (~0.2), but increase from 0.37 (smooth topography) to 0.53 (original topography) at the QOMS site. We agree that there may be other factors affecting the modeling results, including emission uncertainties. It deserves further investigation. As our response to the comment above, PBL mixing is important but the modeling biases are not necessary to be due to PBL scheme. We have selected the scheme commonly used over this region. Further investigation about the impact of PBL mixing on modeling pollutants over the TP may be interesting. Now, we add the discussion in the revised manuscript as "Although the correlation coefficient between the simulations and observation increases from 0.37 (smooth topography) to 0.53 (original topography) at the QOMS site, it is similar (~0.2) between the two simulations at the NAM site. The correlation coefficient is higher at the QOMS site near the source region than the NAM site farther away, which may indicate the model processes affecting the transport over the TP still need examination with more observations. The NAM site over the eastern TP may also be affected by other sources that are not counted in this study. The modeling of temporal variations of pollutants over the TP deserves further investigation with more observations."

- ***5. L480-483: The distribution of resolution-induced differences in BC forcing in snow do not follow that for snow water equivalent.***

Sorry for the confusion due to mixing up the effects of topography and resolution. As we respond to the comments above, now the manuscript is revised to focus on the analysis of the difference between the two experiments at 4 km with different topography representations.

- ***More information about SNICAR and how it represents snow processes are needed. The influences of fresh snow cover, BC caused snow melt runoff should all be investigated to understand BC forcing in snow.***

We agree that the snow processes are important for assessing the impacts of aerosols on snow. However, the purpose of this study is not to study the impacts of topography on aerosol climatic effects. As we respond to the comment of one reviewer, we agree that the short-period simulation cannot be used to access the climate impact. That's why we didn't discuss much about climatic impact in the manuscript. Instead, we estimate the impacts on radiative forcing in the atmosphere and snow for this short period. This study focuses on raising the potential issue of using smoothing topography on modeling BC transport and radiative forcing over the TP, and can be treated as the implication for future study about climatic impact with high-resolution simulations. We acknowledged in the revised manuscript as

"Since this study only demonstrates the potential impacts for a relatively short period, a longer-term study should be conducted to examine the impacts of topography on aerosol climatic effect over the TP."

And "These potential impacts of aerosols on regional hydro-climate around the TP and over Asia using high-resolution model that can resolve the complex topography of Himalayas and TP deserve further investigation."

Therefore, the details of modeling BC impacts on snow are not appropriate to be included in the manuscript. Instead, we refer the readers who are interested to find the details in our previous publication Zhao et al. (2014) as we clarified in the manuscript as "The radiative forcing of light absorbing aerosol in surface snow is estimated with the Snow, Ice, and Aerosol Radiative model (SNICAR) (Flanner and Zender, 2005) in the land surface scheme as introduced by Zhao et al. (2014). More details about the coupling between WRF-Chem and SNICAR models can be found in Zhao et al. (2014)."

Specific comments:

- ***L187-188: Please complete the sentence.***

Corrected.

- ***Figure 4: Why are averaged fire emissions calculated over the region between 26-29N instead the whole inner domain?***

The region selected is South Himalayas where the elevated pollutants can be transport to the TP efficiently. The average over the entire inner domain does not change the pattern. Now, we add the clarification in the revised manuscript as "The fossil fuel BC emissions over Nepal, the country nearby the southern Himalayas, are relatively low. Instead, biomass burning emissions of BC are extremely high in Nepal and Northwest India (South Himalayas, 26°N-29°N). Averaged over the South Himalayas of inner domain that may significantly affect the pollutant transport into the TP, the biomass burning emissions of BC are much higher than its anthropogenic fossil fuel emissions, particularly for the pollution episode (Fig. 4)."

- ***Additionally, the manuscript includes a lot of duplicate information, which need to be removed to make the writing more concise.***

Thanks for your suggestion. The language is polished in the revised manuscript.

Anonymous Referee #3

General Comments：

- ***Major issues, 1. This study only emphasizes the importance of topography, but didn't compare with different land use data. The manuscript attempts to provide some interpretations, but many of them do not seem appropriate. In particular, under the two resolutions, wind vectors show different patterns. A detailed examination on the interactions of modeling resolution, wind speed, and topography is required.***

We agree that there are many factors that may affect the cross-Himalayas transport. Topography and land use may be two of them. As we stated in the title, the focus of this study is about the impact of topography.

In addition, we agree that the resolution itself can introduce difference in simulated results in many aspects, because the development of scale-ware physics, such as PBL and cloud physics, is still a challenging work in the modeling community. The comparison of the simulations at 20 km and 4 km resolutions may complicate the analysis and deviate the readers from the focus of this study about the impacts of topography. Although the impact of resolution on modeling the crossing-Himalayas transport is also interesting, it is beyond the scope of this study. Therefore, now the manuscript is revised to focus on the analysis of the difference between the two experiments at 4 km with different topography representations.

- ***2. The study compare with only one station data and conclude that surface BC concentrations correlates highly with that of biomass burning emissions near the southern Himalayas, indicating the significant impacts of biomass burning on the pollutants over the TP. The authors need more station data comparisons with model simulation.***

We agree that it may be uncertain to analyze the source of pollutants based on one station data. However, the dataset we used is sampled at the Qomolangma Station (QOMS, 86.94°E, 28.36°N, 4276 m above sea level) near Mt. Everest. Given the remote location and very sparse local population, QOMS is an ideal place to monitor the atmospheric environment in the Himalayas. The dataset collected at this station has been used by previous studies (e.g., Cong et al., 2015a, b) to demonstrate the influence of biomass burning emissions from South Asia on North Himalayas. The in-situ observations over the study region are normally difficult to obtained, particularly the observations from multiple stations at the same time period. It is not uncommon to use one available site observation to compare with simulations and analyze the characteristics of pollutants over the region (e.g., Cao et al., 2010; Dumka et al., 2010). The comparison with this one station data is to show that the model captures the pollution episode. More observations, if available, will be used to further evaluate the model and investigate the transport mechanism in future.

The comparison between the observation site and the simulation results is to show that the simulation can accurately reproduce the concentration distribution on the plateau during this time period, and the sites where the black carbon data are available at the same time are particularly scarce over the TP.

Furthermore, one sensitivity experiment without biomass burning emission shows that the simulated BC concentration at QOMS will be significantly reduced without the peak, which further proves that the BC concentration over the northern Himalayas can be largely influenced by the pollution episode near the southern Himalayas. Now it is clarified in the manuscript as "One sensitivity experiment without biomass burning emissions shows that the simulated BC concentration at QOMS will be significantly reduced without the peak (not shown), which further proves that the BC concentration over the northern Himalayas can be largely influenced by the pollution episode near the southern Himalayas."

- ***3. The study didn't compare with meteorological variables like PBLH, wind etc. which play importance rule of BC transport.***

Yes, wind circulation is quite important. We applied the spectral nudging method to improve the simulated large-scale circulation that is important for pollutant transport. Now, we add the comparison of the simulated wind circulation with the reanalysis data at 700 hPa and above, and add the discussion in the revised manuscript as "The simulations with nudging method can reproduce the large-scale circulation at 700 hPa and higher over the outer domain compared to the reanalysis dataset with the spatial correlation coefficient of 0.96-0.98."

The publicly available in-situ measurements of wind and PBLH over the study region are scarce, particularly for Himalayas. It is difficult to evaluate the model performance at the small-scale. However, the configuration of WRF used in this study has also been used by previous study and was systematically evaluated over the Himalayas regions. The WRF simulated meteorology was proved with reasonable performance. We add the clarification in the revised manuscript as "The detailed configuration of WRF-Chem experiments is summarized in Table 1. Due to the lack of publicly available in-situ observations, this study does not tend to evaluate systematically the simulated meteorological fields over the Himalayas region. However, as shown in Table 1, the choice of physical parameterizations in this study follows that of one previous study (Karki et al., 2017) that evaluated systematically the WRF simulation for one entire year over the Himalayas region. Their results showed that the WRF simulation at convection-permitting scale could generally capture the essential features of meteorological fields such as precipitation, temperature, and wind over the Himalayas region. Therefore, the WRF-Chem simulations in this study are reliable to investigate the impacts of topography over the Himalayas region."

- ***4. The distribution of resolution-induced differences in BC forcing in snow do not follow that for snow water equivalent. More information about SNICAR and how it represents snow processes are needed. The influences of fresh snow cover, BC caused snow melt runoff should all be investigated to understand BC forcing in snow.***

As we respond to the comment above, we agree that the resolution itself can introduce difference in simulated results in many aspects. The comparison of the simulations at 20 km and 4 km resolutions may complicate the analysis and deviate the readers from the focus of this study about the impacts of topography. Now the manuscript is revised to focus on the analysis of the difference between the two experiments at 4 km with different topography representations. The topography-induced difference in BC forcing in snow follows that in snow water equivalent.

We also agree that the snow processes are important for assessing the impacts of aerosols on snow. However, the purpose of this study is not to study the impacts of topography on aerosol climatic effects. This study focuses on raising the potential issue of using smoothing topography on modeling BC transport and radiative forcing over the TP, and can be treated as the implication for future study about climatic impact with high-resolution simulations. We acknowledged in the revised manuscript as

"Since this study only demonstrates the potential impacts for a relatively short period, a longer-term study should be conducted to examine the impacts of topography on aerosol climatic effect over the TP."

And "These potential impacts of aerosols on regional hydro-climate around the TP and over Asia using high-resolution model that can resolve the complex topography of Himalayas and TP deserve further investigation."

Therefore, the details of modeling BC impacts on snow are not appropriate to be included in the manuscript. Instead, we refer the readers who are interested to find the details in our previous publication Zhao et al. (2014) as we clarified in the manuscript as "The radiative forcing of light absorbing aerosol in surface snow is estimated with the Snow, Ice, and Aerosol Radiative model (SNICAR) (Flanner and Zender, 2005) in the land surface scheme as introduced by Zhao et al. (2014). More details about the coupling between WRF-Chem and SNICAR models can be found in Zhao et al. (2014)."

Reference

Bansal, O., Singh, A., and Singh, D.: Characteristics of Black Carbon aerosols over Patiala Northwestern part of the IGP: Source apportionment using cluster and CWT analysis, Atmospheric Pollution Research, 10, 244–256, doi:10.1016/j.apr.2018.08.001, 2019.

Cao, J., Tie, X., Xu, B., Zhao, Z., Zhu, C., Li, G., and Liu, S.: Measuring and modeling black carbon (BC) contamination in the SE Tibetan Plateau, Journal of Atmospheric Chemistry, 67, 45-60, doi:10.1007/s10874-011-9202-5, 2010.

Carrera, M. L., Gyakum, J. R., and Lin, C. A.: Observational Study of Wind Channeling within the St. Lawrence River Valley, J. Appl. Meteor. Climatol., 48, 2341–2361, doi:10.1175/2009JAMC2061.1, 2009.

Chen, X., Kang, S., Cong, Z., Yang, J., and Ma, Y.: Concentration, temporal variation, and sources of black carbon in the Mt. Everest region retrieved by real-time observation and simulation, Atmos. Chem. Phys., 18, 12859–12875, doi:10.5194/acp-18-12859-2018, 2018.

Cong, Z., Kang, S., Kawamura, K., Liu, B., Wan, X., Wang, Z., Gao, S., and Fu, P.: Carbonaceous aerosols on the south edge of the Tibetan Plateau: concentrations, seasonality and sources, Atmos. Chem. Phys., 15, 1573–1584, doi:10.5194/acp-15-1573-2015, 2015a.

Cong, Z., Kawamura, K., Kang, S., and Fu, P.: Penetration of biomass-burning emissions from South Asia through the Himalayas: new insights from atmospheric organic acids, Scientific reports, 5, 9580, doi:10.1038/srep09580, 2015b.

Dentener, F., Kinne, S., Bond, T., Boucher, O., Cofala, J., Generoso, S., Ginoux, P., Gong, S., Hoelzemann, J. J., Ito, A., Marelli, L., Penner, J. E., Putaud, J. P., Textor, C., Schulz, M., van der Werf, G. R., and Wilson, J.: Emissions of primary aerosol and precursor gases in the years 2000 and 1750, prescribed data-sets for AeroCom, Atmos. Chem. Phys., 6, 4321–4344, doi:10.5194/acp-6-4321-2006, 2006.

Ding, Y., Sun, Y., Wang, Z., Zhu, Y., and Song, Y.: Inter-decadal variation of the summer precipitation in China and its association with decreasing Asian summer monsoon Part II: Possible causes, Int. J. Climatol., 29, 1926–1944, doi:10.1002/joc.1759, 2009.

Du, Q., Zhao, C., Zhang, M., Dong, X., Chen, Y., Liu, Z., Hu, Z., Zhang, Q., Li, Y., Yuan, R., and Miao, S.: Modelling diurnal variation of surface PM2.5 concentration over East China with WRF-Chem: Impacts from boundary layer mixing and anthropogenic emission, Atmos. Chem. Phys. Discuss., https://doi.org/10.5194/acp-2019-739, in review, 2020.

Dumka, U. C., Moorthy, K. K., Kumar, R., Hegde, P., Sagar, R., Pant, P., Singh, N., and Babu, S. S.: Characteristics of aerosol black carbon mass concentration over a high altitude location in the Central Himalayas from multi-year measurements, Atmospheric Research, 96, 510–521, doi:10.1016/j.atmosres.2009.12.010, 2010.

Egger, J., Bajracharya, S., Egger, U., Heinrich, R., Reuder, J., Shakya, P., Wendt, H., and Wirth, V.: Diurnal winds in the Himalayan Kali Gandaki Valley. Part I: Observations, Mon. Weather Rev., 128, 1106–1122, 2000.

Fan, J., Rosenfeld, D., Yang, Y., Zhao, C., Leung, L. R., and Li, Z.: Substantial contribution of anthropogenic air pollution to catastrophic floods in Southwest China, Geophys. Res. Lett., 42, 6066–6075, doi:10.1002/2015GL064479, 2015.

Feng, Y., Kotamarthi, V. R., Coulter, R., Zhao, C., and Cadeddu, M.: Radiative and thermodynamic responses to aerosol extinction profiles during the pre-monsoon month over South Asia, Atmos. Chem. Phys., 16, 247–264, doi:10.5194/acp-16-247-2016, 2016.

Flanner, M. G. and Zender, C. S.: Snowpack radiative heating: Influence on Tibetan Plateau climate, Geophys. Res. Lett., 32, L06501, doi:10.1029/2004GL022076, 2005.

Gao, Y., Zhao, C., Liu, X., Zhang, M., and Leung, L. R.: WRF-Chem simulations of aerosols and anthropogenic aerosol radiative forcing in East Asia, Atmospheric Environment, 92, 250–266, doi:10.1016/j.atmosenv.2014.04.038, 2014.

Gong, P., Wang, X., Pokhrel, B., Wang, H., Liu, X., Liu, X., and Wania, F.: Trans-Himalayan Transport of Organochlorine Compounds: Three-Year Observations and Model-Based Flux Estimation, Environ. Sci. Technol., 53, 6773–6783, doi:10.1021/acs.est.9b01223, 2019.

Grell, G. A., Peckham, S. E., Schmitz, R., McKeen, S. A., Frost, G., Skamarock, W. C., and Eder, B.: Fully coupled "online" chemistry within the WRF model, Atmospheric Environment, 39, 6957–6975, doi:10.1016/j.atmosenv.2005.04.027, 2005.

Gunwani, P. and Mohan, M.: Sensitivity of WRF model estimates to various PBL parameterizations in different climatic zones over India, Atmospheric Research, 194, 43–65, doi:10.1016/j.atmosres.2017.04.026, 2017.

Hariprasad, K.B.R.R., Srinivas, C. V., Singh, A.B., Vijaya Bhaskara Rao, S., Baskaran, R., and Venkatraman, B.: Numerical simulation and intercomparison of boundary layer structure with different PBL schemes in WRF using experimental observations at a tropical site, Atmospheric Research, 145-146, 27–44, doi:10.1016/j.atmosres.2014.03.023, 2014.

Hu, Z., Huang, J., Zhao, C., Jin, Q., Ma, Y., and Yang, B.: Modeling dust sources, transport, and radiative effects at different altitudes over the Tibetan Plateau, Atmos. Chem. Phys. Discuss., https://doi.org/10.5194/acp-2019-431, in press, 2020.

Hu, Z., Zhao, C., Huang, J., Leung, L. R., Qian, Y., Yu, H., Huang, L., and Kalashnikova, O.V.: Trans-pacific transport and evolution of aerosols: Evaluation of quasi global WRF-Chem simulation with multiple observations, Geosci. Model Dev. Discuss., 1–65, doi: 10.5194/gmd-2015-248, 2016.

Huang, X., Song, Y., Zhao, C., Cai, X., Zhang, H., and Zhu, T.: Direct Radiative Effect by Multicomponent Aerosol over China, J. Climate, 28, 3472–3495, doi:10.1175/JCLI-D-14-00365.1, 2015.

Janssens-Maenhout, G., Crippa, M., Guizzardi, D., Dentener, F., Muntean, M., Pouliot, G., Keating, T., Zhang, Q., Kurokawa, J., Wankmüller, R., van der Denier Gon, H., Kuenen, J. J. P., Klimont, Z., Frost, G., Darras, S., Koffi, B., and Li, M.: HTAP_v2.2: a mosaic of regional and global emission grid maps for 2008 and 2010 to study hemispheric transport of air pollution, Atmos. Chem. Phys., 15, 11411–11432, doi:10.5194/acp-15-11411-2015, 2015.

Kang, S.: Atmospheric Aerosol Elements over the Inland Tibetan Plateau: Concentration, Seasonality, and Transport, Aerosol Air Qual. Res., doi:10.4209/aaqr.2015.02.0307, 2015.

Kant, Y., Shaik, D. S., Mitra, D., Chandola, H. C., Babu, S. S., and Chauhan, P.: Black carbon aerosol quantification over north-west Himalayas: Seasonal heterogeneity, source apportionment and radiative forcing, Environmental pollution (Barking, Essex 1987), 113446, doi:10.1016/j.envpol.2019.113446, 2019.

Karki, R., ul Hasson, S., Gerlitz, L., Schickhoff, U., Scholten, T., and Böhner, J.: Quantifying the added value of convection-permitting climate simulations in complex terrain: a systematic evaluation of WRF over the Himalayas, Earth Syst. Dynam., 8, 507–528, doi:10.5194/esd-8-507-2017, 2017.

Kuhlmann, J. and Quaas, J.: How can aerosols affect the Asian summer monsoon? Assessment during three consecutive pre-monsoon seasons from CALIPSO satellite data, Atmos. Chem. Phys., 10, 4673–4688, doi:10.5194/acp-10-4673-2010, 2010.

Lau, K. M. and Kim, K. M.: Observational relationships between aerosol and Asian monsoon rainfall, and circulation, Geophys. Res. Lett., 33, D22101, doi: 10.1029/2006GL027546, 2006b.

Lau, K. M., Kim, M. K., and Kim, K. M.: Asian summer monsoon anomalies induced by aerosol direct forcing: the role of the Tibetan Plateau, Clim Dyn, 26, 855–864, doi: 10.1007/s00382-006-0114-z, 2006a.

Lin, C., Chen, D., Yang, K., and Ou, T.: Impact of model resolution on simulating the water vapor transport through the central Himalayas: implication for models' wet bias over the Tibetan Plateau, Clim Dyn, 51, 3195–3207, doi:10.1007/s00382-018-4074-x, 2018.

Liu, P., Tsimpidi, A. P., Hu, Y., Stone, B., Russell, A. G., and Nenes, A.: Differences between downscaling with spectral and grid nudging using WRF, Atmos. Chem. Phys., 12, 3601–3610, doi:10.5194/acp-12-3601-2012, 2012.

Liu, Z., Ming, Y., Zhao, C., Lau, N. C., Guo, J., Bollasina, M., and Yim, S. H. L.: Contribution of local and remote anthropogenic aerosols to a record-breaking torrential rainfall event in Guangdong Province, China, Atmos. Chem. Phys., 20, 223–241, doi:10.5194/acp-20-223-2020, 2020.

Qian, Y., Flanner, M. G., Leung, L. R., and Wang, W.: Sensitivity studies on the impacts of Tibetan Plateau snowpack pollution on the Asian hydrological cycle and monsoon climate, Atmos. Chem. Phys., 11, 1929–1948, doi:10.5194/acp-11-1929-2011, 2011.

Qian, Y., Yasunari, T. J., Doherty, S. J., Flanner, M. G., Lau, W. K. M., Ming, J., Wang, H., Wang, M., Warren, S. G., and Zhang, R.: Light-absorbing particles in snow and ice: Measurement and modeling of climatic and hydrological impact, Adv. Atmos. Sci., 32, 64–91, doi:10.1007/s00376-014-0010-0, 2015.

Rhoades, A. M., Ullrich, P. A., Zarzycki, C. M., Johansen, H., Margulis, S. A., Morrison, H., Xu, Z., and Collins, W. D.: Sensitivity of Mountain Hydroclimate Simulations in Variable-Resolution CESM to Microphysics and Horizontal Resolution, J. Adv. Model. Earth Syst., 10, 1357–1380, doi:10.1029/2018MS001326, 2018.

Sarangi, C., Qian, Y., Rittger, K., Bormann, K. J., Liu, Y., Wang, H., Lin, G., and Painter, T. H.: Impact of light-absorbing particles on snow albedo darkening and associated radiative forcing over high-mountain Asia: high-resolution WRF-Chem modeling and new satellite observations. Atmos. Chem. Phys., 19, 7105–7128, doi:10.5194/acp-19-7105-2019, 2019.

Seaman, N. L., Stauffer, D. R., and Lario-Gibbs, A. M.: A Multiscale Four-Dimensional Data Assimilation System Applied in the San Joaquin Valley during SARMAP. Part I: Modeling Design and Basic Performance Characteristics, J. Appl. Meteor., 34, 1739–1761, doi:10.1175/1520-0450(1995)034<1739:AMFDDA>2.0.CO;2, 1995.

Shi, X., Wang, Y., and Xu, X.: Effect of mesoscale topography over the Tibetan Plateau on summer precipitation in China: A regional model study, Geophys. Res. Lett., 35, 255, doi:10.1029/2008GL034740, 2008.

Skamarock, W. C., Klemp, J. B., Dudhia, J., Gill, D. O., Barker, D. M., Duda, M., Huang, X. Y., Wang, W., and Powers, J. G.: A Description of the Advanced Research WRF Version 3, NCAR Technical Note, NCAR/TN-468+STR, available at: http://wrf-model.org/wrfadmin/docs/arw v2.pdf, 2008.

Stauffer, D. R. and Seaman, N. L.: Use of Four-Dimensional Data Assimilation in a Limited-Area Mesoscale Model. Part I: Experiments with Synoptic-Scale Data, Mon. Wea. Rev., 118, 1250–1277, doi:10.1175/1520-0493(1990)118<1250:UOFDDA>2.0.CO;2, 1990.

Wagner, J. S., Gohm, A., and Rotach, M. W.: The Impact of Horizontal Model Grid Resolution on the Boundary Layer Structure over an Idealized Valley, Mon. Wea. Rev., 142, 3446–3465, doi:10.1175/MWR-D-14-00002.1, 2014.

Wiedinmyer, C., Akagi, S. K., Yokelson, R. J., Emmons, L. K., Al-Saadi, J. A., Orlando, J. J., and Soja, A. J.: The Fire INventory from NCAR (FINN): a high resolution global model to estimate the emissions from open burning, Geosci. Model Dev., 4, 625–641, doi:10.5194/gmd-4-625-2011, 2011.

Wu, G., Liu, Y., He, B., Bao, Q., Duan, A., and Jin, F.-F.: Thermal controls on the Asian summer monsoon, Scientific reports, 2, 404, doi:10.1038/srep00404, 2012.

Wu, L., Su, H., and Jiang, J. H.: Regional simulation of aerosol impacts on precipitation during the East Asian summer monsoon, J. Geophys. Res. Atmos., 118, 6454–6467, doi:10.1002/jgrd.50527, 2013.

Zängl, G., Egger, J., and Wirth, V.: Diurnal Winds in the Himalayan Kali Gandaki Valley. Part II: Modeling, Mon. Wea. Rev., 129, 1062–1080, doi:10.1175/1520-0493(2001)129<1062:DWITHK>2.0.CO;2, 2001.

Zhao, C., Chen, S., Leung, L. R., Qian, Y., Kok, J., Zaveri, R., and Huang, J.: Uncertainty in modeling dust mass balance and radiative forcing from size parameterization, Atmos. Chem. Phys., 13, 10733–10753, doi:doi:10.5194/acp-13-10733-2013, 2013b.

Zhao, C., Hu, Z., Qian, Y., Leung, L. R., Huang, J., Huang, M., Jin, J., Flanner, M., Zhang, R., Wang, H., Yan, H., Lu, Z., and Streets, D. G.: Simulating black carbon and dust and their radiative forcing in seasonal snow: a case study over North China with field campaign measurements, Atmos. Chem. Phys., 14, 11475–11491, doi:10.5194/acp-14-11475-2014, 2014.

Zhao, C., Liu, X., and Leung, L. R.: Impact of the Desert dust on the summer monsoon system over Southwestern North America, Atmos. Chem. Phys., 12, 3717–3731, doi:10.5194/acp-12-3717-2012, 2012.

Zhao, C., Liu, X., Leung, L. R., and Hagos, S.: Radiative impact of mineral dust on monsoon precipitation variability over West Africa, Atmos. Chem. Phys., 11, 1879–1893, doi:10.5194/acp-11-1879-2011, 2011.

Zhao, C., Liu, X., Leung, L. R., Johnson, B., McFarlane, S. A., Gustafson, W. I., Fast, J. D., and Easter, R.: The spatial distribution of mineral dust and its shortwave radiative forcing over North Africa: modeling sensitivities to dust emissions and aerosol size treatments, Atmos. Chem. Phys., 10, 8821–8838, doi:10.5194/acp-10-8821-2010, 2010.

Zhong, S., Qian, Y., Zhao, C., Leung, R., Wang, H., Yang, B., Fan, Ji., Yan, H., Yang, X., and Liu, D.: Urbanization-induced urban heat island and aerosol effects on climate extremes in the Yangtze River Delta region of China, Atmos. Chem. Phys., 17, 5439–5457, doi:10.5194/acp-17-5439-2017, 2017.

Impact of topography on black carbon transport to the southern Tibetan Plateau during pre-monsoon season and its climatic implication

[1]Meixin Zhang, [1]Chun Zhao*, [2,3]Zhiyuan Cong, [1]Qiuyan Du, [1]Mingyue Xu, [1]Yu Chen, [4]Ming Chen, [1]Rui Li, [1]Yunfei Fu, [1]Lei Zhong, [3,5]Shichang Kang, [6]Delong Zhao, [6]Yan Yang

[1]School of Earth and Space Sciences, University of Science and Technology of China, Hefei, China

[2]Key Laboratory of Tibetan Environment Changes and Land Surface Processes, Institute of Tibetan Plateau Research, Chinese Academy of Sciences (CAS), Beijing 100101, China

[3]CAS Center for Excellence in Tibetan Plateau Earth Sciences, Institute of Tibetan Plateau Research, CAS, Beijing 100101, China

[4]National Center for Atmospheric Research, Boulder, CO, USA

[5]State Key Laboratory of Cryosphere Science, Northwest Institute of Eco-Environment and Resources, CAS, Lanzhou 730000, China

[6]Beijing Weather Modification Office, Beijing 100101, China

Manuscript for submission to Atmos. Chem. Phys.

*Corresponding author: Chun Zhao (chunzhao@ustc.edu.cn)

Key points:

1. The ~~simulations show evident accumulation of aerosols near~~black carbon (BC) transport across the ~~southern~~ Himalayas ~~during~~can overcome a majority of mountain ridges, but the ~~pre-monsoon season.~~valley transport is much more efficient.

2. The ~~prevailing up-flow across the~~ complex topography results in stronger overall crossing-Himalayas ~~driven by the large~~transport primarily due to the enhanced valley wind, deeper valley channels, and induced small-scale favorable circulation ~~during the daytime is the dominant mechanism of South Asian BC transport to the TP~~.

3. The ~~BC transport across the Himalayas can overcome the mountain ridges, but the valley transport is much more efficient.~~

~~4. The simulation at 4 km resolution~~complex topography generates 50% higher transport flux of BC across the Himalayas and 30-~~40~~50% stronger BC radiative heating in the atmosphere up to 10 km over the ~~TP~~Tibetan Plateau (TP) than that ~~at 20 km resolution, primarily due to their different representations of~~with the smoother topography, which implies that global climate models with relatively coarse resolution may introduce significant negative biases in estimating BC radiative forcing over the TP due to smooth topography.

4. The different topography also leads to different distributions of snow cover and BC forcing in snow over the TP.

Abstract

Most of previous modeling studies about black carbon (BC) transport and impact over the Tibetan Plateau (TP) conducted simulations with horizontal resolutions coarser than 10 km that may not be able to resolve well the complex topography of the Himalayas. In this study, the two experiments covering entire Himalayas with the Weather Research and Forecasting Model coupled with chemistry (WRF-Chem) at ~~two~~the horizontal ~~resolutions (20 km and~~ resolution of 4 km but with two different topography datasets (4-km complex topography and 20-km smooth topography) are conducted for pre-monsoon season (April, 2016) to investigate the impacts of topography on modeling the transport and distribution of BC over the TP. ~~The simulations at both resolutions~~Both experiments show evident accumulation of aerosols near the southern Himalayas during the pre-monsoon season, consistent with the satellite retrievals. The observed episode of high surface BC ~~concentrations~~concentration at the station near the Mt. Everest due to heavy biomass burning near the ~~TP~~southern Himalayas is well captured by the simulations. The simulations ~~at both resolutions~~ indicate that the prevailing up-flow across the Himalayas driven by the large-scale circulation during the daytime is the dominant transport mechanism of South Asian BC into the TP, and is much stronger than that during the nighttime. ~~The valley wind can strengthen the prevailing up-flow transport. The simulations at coarse resolution (20 km) and fine resolution (4 km) show large differences in representing the distributions of topography of the Himalayas.~~ The simulation ~~at~~with 4 ~~-~~-km ~~resolution~~topography resolves more valleys and ~~thus produces much stronger transport fluxes, which indicates that although the transport of South Asian BC~~mountain ridges, and shows that the BC transport across the Himalayas can overcome ~~the~~a majority of mountain ridges~~,~~ but the valley transport is more efficient. The complex topography results in stronger overall crossing-Himalayas transport primarily due to the enhanced valley wind, deeper valley channels, and ~~cannot be ignored.~~induced small-scale favorable circulation. This results in 50% higher transport flux of BC across the Himalayas and 30-~~40~~50% stronger BC radiative heating in the atmosphere up to 10 km over the TP from the simulation ~~at~~with 4~~-~~-km complex topography than that ~~at~~with 20~~-~~-km ~~resolution~~smoother topography. The different topography also leads to different distributions of snow cover and BC forcing in snow. This study implies that global climate models generally with even coarser resolutions than 20 km and therefore relatively smoother topography may introduce significant negative biases in estimating light absorbing aerosol radiative forcing over the TP.

1. Introduction

The Tibetan Plateau (TP) is the highest plateau in the world with an average elevation over 4 km and an area of approximately 2.5 × 10^6 km^2, known as the world's third pole (Qiu, 2008), and its enormous dynamic and thermal effects have a huge impact on large-scale atmospheric circulation~~, such as Asian monsoon, and environmental changes~~ through the energy exchange with ~~free~~the atmosphere especially the troposphere, such as Asian monsoon (e.g., Ye and Wu, 1998; Duan and Wu, 2005; Wu et al., ~~2005~~2007, 2012~~, 2019~~; Boos and Kuang, 2013; Chen and Bordoni, 2014; He et al., 2019; Zhao et al., 2019). ~~The increase~~In addition, the glacial melting water of TP is one of the important sources of water resources of the Indus River, Ganges River, Yangtze River, and Yellow River in ~~aerosol concentration~~Asia (e.g., Singh and Bengtsson, 2004; Barnett et al., 2005; Immerzeel et al., 2010; Lutz et al., 2014). Previous studies found aerosols in the atmosphere over/around the TP ~~can~~could change the ~~circulation pattern over~~regional climate of Asia (e.g., Qian et al., 2011, 2015; Lau et al.,~~ 2016,~~ 2017, 2018). Model simulations showed that the absorptive aerosols changed the surface radiative flux over the TP by 5-25 W m^{-2} during the pre-monsoon season in April and May and led to the changes in summer monsoon circulations (Qian et al., 2011). Meanwhile, aerosol may affect the atmosphere by modulating the vertical structure of cloud and precipitation around the TP, and thus change the distribution of atmospheric latent heat around the TP, which is the main driving force of regional atmosphere ~~circulation (e.g., Li et al 2010, 2017, 2019). In addition, the TP is rich in glaciers and snow resources, the glacial melting water is one of the important sources of water resources of the Indus River, Ganges River, Yangtze River, and Yellow River in Asia (e.g., Singh and Bengtsson, 2004; Barnett et al., 2005; Immerzeel et al., 2010; Lutz et al., 2014). When absorbing aerosols adhere~~circulations (e.g., Li et al., 2010, 2017, 2019). Moreover, when absorbing aerosols settle on the snow-covered areas, they will blacken the surface of snow cover and glacier to a large extent (e.g., Hansen and Nazarenko~~.~~, 2004; Ramanathan and Carmichael, 2008; Lau et al., 2010, ~~2019~~2018; Lee ~~at~~et al., 2013; Zhang~~, Y. L.~~ et al., 2017, 2018)~~, and then~~ reduce the snow albedo so as to absorb more solar radiation and cause the consequences of accelerated melting (e.g., Ramanathan et al., 2007; Ming et al., 2009; Yasunari et al., 2010; Ji et al., 2015; Zhang et al., 2015). According to the Intergovernmental Panel on Climate Change Fifth Assessment Report (IPCC AR5~~,~~), the radiative forcing caused by the important component of absorbing aerosols, black carbon (BC), on the surface snow is 0.04 W m^{-2} (0.02-0.09 W m^{-2}) on global average, and the regional forcing (such as over the Arctic and the Himalayas) can be considerably large.

The TP is surrounded by ~~anthropogenic~~various sources of pollutants. Over the South of TP, previous studies have suggested that South Asia ~~are~~was the main ~~sources~~source of pollutants transported ~~over~~to the plateau (e.g., Cong et al., 2009, 2015a, b; Kopacz et al., 2011; Lu et al., 2012; Zhao et al., 2013; Wang et al., 2015; Zhang et al., 2015; Kang et al., 2015; Li et al., 2016; Chen et al., 2018; Kang et al., 2019). A huge blanket or layer of "haze" ~~generally~~ composes of light-absorbing carbonaceous aerosol particles that often erupts in the pre-monsoon season over South Asia and has a significant influence on the plateau (e.g., Prasad and Singh, 2007; Engling and Gelencser, 2010). ~~The strong~~Among them, biomass burning emission reaching the maximum in pre-monsoon season over South Asia ~~also leads to high loading~~is one of ~~absorbing aerosols over~~ the ~~southern TP~~dominant sources (e.g., Cong et al., 2015b). Many studies investigated the transport mechanisms of South Asian pollutants to the TP and found that the ~~pollutant transport~~pollutants transported across the Himalayas ~~was~~were mainly due to the combination of large-scale circulation and regional ~~winds~~wind (e.g., Hindman and Upadhyay, 2002; Cao et al., 2010; Dumka et al., 2010; Marinoni et al., 2010; Cong et al., 2015a; Kang et al., 2015; ~~Luthi~~Lüthi et al., 2015; Zhang et al., 2017). Cong et al. (2015a) conducted seven-day backward air-mass trajectories experiment and found strong ~~westerlies pass~~westerly passed through western Nepal, northwest India and Pakistan (i.e., southern Himalayas) in the pre-monsoon season. Dumka et al. (2010) and Kang et al. (2015) inferred from the trajectory analysis that long-distance transport from Africa and Europe may also affect the BC concentration of Himalayas in addition to the influence of regional pollution. ~~Zhang et al. (2017) suggested that the cut-off low pressure in the upper and middle layers of the troposphere can enhance the transport by the westerlies to the plateau based on a chemical transport model.~~

Although previous studies have confirmed the transport of pollutants across the Himalayas, the complex topography of Himalayas complicates transport mechanisms. On one hand, Cao et al. (2010) revealed that the Himalayas ~~acts~~acted as a huge barrier to the transport of a large amount of BC over the plateau based on model simulations. On the other hand, some studies found that the valleys across the Himalayas ~~serve~~served as channels for efficient transport of pollutants (e.g., Hindman and Upadhyay, 2002; Marinoni et al., 2010). Marinoni et al. (2010) analyzed the ~~wind field~~ observation of wind at ~~one site~~a station of the southern Himalayas and found that a distinct valley wind system with the ~~southerlies~~prominent southerly continuously transported pollutants to the plateau. Most of these studies used observations and back-trajectory models to demonstrate the transport pathways of pollutants to the TP, which cannot explicitly reveal the transport mechanisms underneath, in particular quantifying the impacts of complex topography.

A few of modeling studies investigated the pollutant transport mechanisms using 3-D chemical transport models (e.g., Kopacz et al., 2011; Liu et al., 2015; Zhang et al., 2017; Yang et al., 2018). However, most of them simulated transport processes at relatively coarse horizontal resolutions (e.g., 20-100 km), which cannot resolve well the complex topography of ~~the~~ Himalayas. It is noteworthy that studies about the aerosol climatic impact over the TP also used climate models at relatively coarse horizontal resolutions (e.g., Flanner and Zender, 2005; Menon et al., 2010; Kopacz et al., 2011; Qian et al., 2011, 2015; He et al., 2014; Zhang et al., 2015; Ji et al., 2016). So far, there is only one study that used a chemical transport model at a horizontal resolution of sub-10 km to investigate pollutant transport mechanisms over the eastern Himalayas (Cao et al., 2010). Furthermore, none of studies assessed quantitatively the impacts of topography on modeling the pollutant transport across the Himalayas and hence on estimating aerosol distribution and radiative forcing over the TP.

~~This study uses~~In order to examine the potential impacts of complex topography on pollutant transport across the Himalayas over the TP, this study conducts multiple experiments with the Weather Research and Forecasting Model coupled with chemistry (WRF-Chem, Grell et al., 2005; Skamarock et al., 2008~~) to investigate the impacts of topography on pollutant transport across the Himalayas. The experiments with two different horizontal resolutions (4 km versus 20 km) are conducted to illustrate the impacts on the transport mechanisms.~~). The WRF-Chem model is selected because it includes the interaction between meteorology and aerosol and is widely used for regional modeling of aerosol and its climatic impact (e.g., Cao et al., 2010; Zhao et al., 2010, 2011, 2012, 2014; Wu et al., 2013; Gao et al., 2014; Huang et al., 2015; Fan et al., 2015; Feng et al., 2016; Zhong et al., 2017; Sarangi et al., 2019; Liu et al., 2020). The model has also been used to investigate the aerosol transport and climatic impact over the Himalayas region (e.g., Feng et al., 2016; Cao et al., 2010; Sarangi et al., 2019). The model is suitable for simulations at hydrostatic and non-hydrostatic scales and thus can be used for investigating the impacts of resolution-dependent feature, such as topography, on modeling results. In particular, the meteorological part of the model (WRF) has been systematically evaluated and used to investigate the impacts of resolutions on simulations of moisture transport and climate over the Himalayas region (e.g., Shi et al., 2008; Karki et al., 2017; Lin et al., 2018). All of these previous studies with the model lay the foundation for this modeling study.

Two experiments with different topography representations are conducted to investigate the impacts of topography complexity on the pollutant transport across the Himalayas and the resulting radiative forcing over the TP. The simulations are conducted for April 2016 in pre-monsoon season, because South Asia is seriously polluted during this period and the pollutants transported to the TP during the period may have significant impacts on Asian monsoon system (e.g., Lau et al., 2006a, b; Ding et al., 2009; Kuhlmann and Quaas, 2010; Qian et al., 2011, 2015). In addition, the observed concentration of BC at the observation sitestation besides Mt. Everest showedshows an evident pollution episode from April 5^{th} to $15^{th}$$16^{th}$ of 2016, deserving the investigation of the transport mechanisms. This study particularly focuses on the impacts of different topographic representations in simulations at various horizontal resolutions on pollutant transport across the Himalayas and the resulting radiative forcing.

The rest of the paper is organized as follows. Section 2 describes briefly the WRF-Chem model, the physics parameterizations, and the model configuration for this study, followed by a description of data for evaluation. The series of numerical experiments at different resolutions are analyzed in Section 3. The findings are then summarized and discussed in Section 4.

2. Methodology

2.1 Model and experiments

2.1.1 WRF-Chem model

In this study, the version of WRF-Chem updated by University of Science and Technology of China (USTC version of WRF-Chem) is used. This USTC version of WRF-Chem includes some additional capabilities such as the diagnosis of radiative forcing of aerosol species, land surface coupled biogenic volatile organic compound (VOC) emission, aerosol-snow interaction compared with the publicallypublicly released version (Zhao et al., 2013a, b, 2014, 2016; Hu et al., 2019; Du et al., 2020). The MOSAIC (Model for Simulating Aerosol Interactions and Chemistry) aerosol model (MOSIAC) (Zaveri et al., 2008) and the Carbon Bond Mechanism-Z (CBM-Z (carbon bond mechanism) gas phase mechanisms (Zaveri and Peters, 1999) are selected. The MOSAIC aerosol scheme uses an approach of segmentation to represent aerosol size distribution with four or eight discrete size bins (Fast et al., 2006). The MOSAIC scheme classifies aerosols into multiple components including OM (organic matter), BC (black carbon), NO_3^- (nitrate), SO_4^{2-} (sulfate), NH_4^+ (ammonium), sea salt, mineral dust, and OIN (other inorganic). It consists of a range of physical and chemical processes such as nucleation, condensation, coagulation, aqueous phase chemistry, and water uptake by aerosol.

The parameterization of dry deposition of aerosol mass and number is according to the method of Binkowski and Shankar (1995), including particle diffusion and gravitational effects. Aerosol-cloud interactions were included in the model by Gustafson et al. (2007) for calculating the activation and re-suspension between dry aerosols and cloud droplets. The wet removal of grid-resolved stratiform clouds/precipitation includes two aspects, namely in-cloud removal (rainout) and below-cloud removal (washout) by Easter et al. (2004) and Chapman et al. (2009), respectively. Aerosol optical properties such as single scattering albedo (SSA) and scattering asymmetry and so on are calculated at each model grid through the function of wavelength. The shortwave (SW) and longwave (LW) refractive indices of aerosols use the Optical Properties of Aerosols and Clouds (OPAC) data set (Hess et al., 1998), with a detailed description of the computation of aerosol optical properties can be found in Barnard et al. (2010) and Zhao et al. (2013a). For both short wave and long wave radiation, aerosol radiation feedback combined with the Rapid Radiative Transfer Model (RRTMG) (Mlawer et al., 1997; Iacono et al., 2000) was implemented by Zhao et al (2011). For the ~~diagnose~~diagnosis of the optical properties and direct radiative forcing of various aerosol species in the atmosphere, ~~adopted~~ the method described by Zhao et al (2013a~~).~~) is adopted. The radiative forcing of light absorbing aerosol in surface snow is estimated with the Snow, Ice, and Aerosol Radiative model (SNICAR ~~model~~) (Flanner and Zender, 2005) in the land surface scheme as introduced by Zhao et al. (2014). More details about the coupling between the WRF-Chem and SNICAR models can be found in Zhao et al. (2014).

2.1.2 Numerical experiments

In this study, the WRF-Chem simulations are performed with two nested domains (one-way nesting), one outer domain at 20 km horizontal resolution with 350×250 grid cells (62°E -112°E, ~~0~~1°N -38°N) and one inner domain at 4 km horizontal resolution with 400×300 grid cells (75~~-91~~°E~~, 24~~ -92°E, 23°N -35°N) (~~Figure~~Fig. 1). The inner domain roughly covers the entire Himalayas. The WRF-Chem simulations conducted in this study use the terrain following coordinate (Skamarock et al., 2008). To resolve the vertical structure of transport across the Himalayas, the simulations are configured with 54 vertical layers and ~~roughly~~denser layers near the surface. For example, averaged over a region (26°N-28°N, 76°E-80°E) near the southern Himalayas, there are about 17 layers below 2 km above the ground (~~Figure~~Fig. 2). The goal of this study is to investigate the impacts of different representations of topography on the transport of BC across the Himalayas. Therefore, besides this control experiment, one sensitivity experiment is also conducted with the same configuration as the control one except that the topography of the inner domain at 4 km resolution is prescribed to follow that at 20 km resolution similar as previous studies (e.g., Shi et al., 2008; Wu et al., 2012; Lin et al., 2018). More specifically, the sensitivity experiment applies a single value for each nested 5×5 grids over the inner domain as the corresponding grid of 20 km over the outer domain. The two experiments are referred to the simulations with complex and smooth topography, respectively, hereafter. Fig.. Figure 3 shows the spatial distribution of terrain height fromover the outerinner domain at 20 with complex (4-km resolutiondataset) and the inter domain at 4 smooth (20-km over the Himalayas (75-91°E, 24-35°N).dataset) topography. It is evident that the terrain is much smoother atfrom the 20--km dataset than atfrom the 4 km resolutiondataset. The hillsidesmountain ridges and valleys can be resolved to some extent atin the 4--km resolutiondataset but mostly missed or underestimated at 20--km. The probability distributions of terrain height atfrom the 20--km and 4--km resolutionsdatasets (Fig. S1 in the supporting material) show that the difference between the two resolutionsdatasets is small for the terrain height lower than ~4.5 km but is significant for the terrain height above ~4 km. .5 km. The difference of results from the two experiments over the inner domain is analyzed as the impacts of topography representations. Therefore, all the results shown below are from the simulations of the inner domain at 4 km resolution with different topography if not otherwise stated.

The simulations are conducted for March 29th-April 20 of 2016. for the reason as discussed in the introduction. The results of April 5th1th-20th are analyzed for the observed pollution episode.

to allow a few days spin-up for chemical initial condition. The meteorological initial and lateral boundary conditions are derived from the European Centre for Medium-Range Weather Forecasts (ECMWF) reanalysis data at 0.5°×0.66° horizontal resolution and 6 h temporal intervals. (ERA-Interim dataset). The modeled u component and v component wind and, atmospheric temperature, and geopotential height over the outer domain are nudged towards the reanalysis data with a nudging timescale of 6 h (following previous studies (e.g., Stauffer and Seaman, 1990; Seaman et al., 1995; Liu et al., 20122012; Zhao et al., 2014; Karki et al., 2017; Hu et al., 2016, 2020). Spectral nudging method is applied to balance the performance of simulation at the large and small scales (Liu et al., 2012), and only to the layers above the PBLplanetary boundary layer (PBL) with nudging coefficients of 3×10^{-4} s^{-1}. A wave number of three is selected for both south-north and west-east directions. The MYNN planetary boundary layer scheme (Nakanishi and Niino, 2006), CLMPlease note that the choices of nudging coefficients and wave numbers for spectral nudging in this study are empirical. The purpose of nudging is to simulate reasonably large-scale feature so that small-scale impacts from the complex topography can be focused. Therefore, the modeling sensitivity to these choices is not tested in this study. The results show that the simulations with nudging method can reproduce the large-scale circulation at 700 hPa and higher over the outer domain compared to the reanalysis dataset with the spatial correlation coefficient of 0.96-0.98.

The Mellor-Yamada-Nakanishi-Niino (MYNN) planetary boundary layer scheme (Nakanishi and Niino, 2006), Community Land Model (CLM) land surface scheme (Oleson et al., 2010), Morrison 2-moment microphysics scheme (Morrison et al., 2009), Kain-Fritsch cumulus scheme (Kain, 2004), and Rapid Radiative Transfer Model (RRTMG) longwave and shortwave radiation schemes (Iacono et al., 2000) are used in this study. The chemical initial and boundary conditions are provided by a quasi-global WRF-Chem simulation for the same time period to include long-range transported chemical species ~~(Zhao et al., 2013b; Hu et al., 2016).~~. The quasi-global WRF-Chem simulation is performed at 1°×1° horizontal resolution using a quasi-global channel configuration with 360×130 grid cells (180°W-180°E, 60°S-70°N). ~~More details about the quasi-global WRF-Chem simulation can be found in Zhao et al. (2013b) and Hu et al. (2016).~~More details about the general configuration of quasi-global WRF-Chem simulation can be found in Zhao et al. (2013b) and Hu et al. (2016). The detailed configuration of WRF-Chem experiments is summarized in Table 1. Due to the lack of publicly available in-situ observations, this study does not tend to evaluate systematically the simulated meteorological fields over the Himalayas region. However, as shown in Table 1, the choice of physical parameterizations in this study follows that of one previous study (Karki et al., 2017) that evaluated systematically the WRF simulation for one entire year over the Himalayas region. Their results showed that the WRF simulation at convection-permitting scale could generally capture the essential features of meteorological fields such as precipitation, temperature, and wind over the Himalayas region. Therefore, the WRF-Chem simulations in this study are reliable to investigate the impacts of topography over the Himalayas region.

2.1.3 Emissions

Anthropogenic emissions for outer and inner simulation domains are obtained from the Hemispheric Transport of Air Pollution version-2 (HTAPv2) at 0.1°×0.1° horizontal resolution and a monthly temporal resolution for year 2010 (Janssens-Maenhout et al., 2015), except that emissions ~~over~~of East ~~and South~~ Asia ~~within the domains~~ are from the MIX Asian anthropogenic emission inventory at 0.1°×0.1° horizontal resolution for 2015 (Li et al., 2017).

Biomass burning emissions are obtained from the Fire Inventory from ~~NCAR~~National Center for Atmospheric Research (FINN) with hourly temporal resolution and 1 km horizontal resolution (Wiedinmyer et al., 2011~~),~~) for the simulation period, and are vertically distributed following the injection heights suggested by Dentener et al. (2006) from the Aerosol Comparison between Observations and Models (AeroCom) project. Sea-salt emission follows Zhao et al. (~~2013~~2013b), which includes correction of particles with radius less than 0.2 µm (Gong, 2003) and dependence of sea-salt emission on sea surface temperature (Jaeglé et al., 2011). The vertical dust fluxes are calculated with the ~~GOCART~~Georgia Tech/Goddard Global Ozone Chemistry Aerosol Radiation and Transport (GOCART) dust emission scheme (Ginoux et al., 2001), and the emitted dust particles are distributed into the MOSAIC aerosol size bins following a theoretical expression based on the physics of scale-invariant fragmentation of brittle materials derived by Kok (2011). More details about the dust emission scheme coupled with MOSAIC aerosol scheme in WRF-Chem can be found in Zhao et al. (2010, 2013b).

As shown in ~~Figure~~Fig. 1, anthropogenic fossil fuel emissions of BC are high over Northeast India. The fossil fuel BC emissions over Nepal, the country nearby the southern Himalayas, are relatively low. Instead, biomass burning emissions of BC are extremely high in Nepal and Northwest India (South Himalayas~~). On average~~, 26°N-29°N). Averaged over the South Himalayas of inner domain that may significantly affect the pollutant transport into the TP, the biomass burning ~~emission~~emissions of BC ~~is~~are much higher than its anthropogenic fossil fuel emissions, particularly for the pollution episode (Fig. 4). The anthropogenic BC ~~emission is~~emissions are set constant through April, while biomass burning ~~emission shows~~emissions show a strong fire event in April 5-16. During the event, the biomass burning BC ~~emission~~emissions can be close to a factor of 2 of the anthropogenic fossil fuel BC ~~emission~~emissions over South Himalayas.

2.2 Dataset

Three datasets are used to compare with the modeling results to ~~indicate~~demonstrate the pollutant episode and spatial distribution. One is from the Moderate Resolution Imaging Spectroradiometer (MODIS) instruments on Aqua and Terra satellites. The MODIS Aerosol Product monitors the ambient aerosol optical thickness over the oceans globally and over the continents. Daily Level 2 ~~aerosol optical depth~~Aerosol Optical Depth (AOD) at 550 nm products with the spatial resolution of 10 km×10 km (at nadir) from both Aqua and Terra are applied. When compared with the modeling results, the simulations are sampled at the satellite overpass time and location. The second one is from the Aerosol Robotic Network (AERONET)

(Holben et al., 1998) that has ~100 ~~identical~~similar globally distributed sun~~-~~ and sky~~-~~ scanning ground-based automated radiometers, which provide measurements of aerosol optical properties throughout the world (Dubovik and King, 2000; Dubovik et al., 2002). In this study, AERONET measured AOD at 675 nm and 440 nm from two sites over the TP, Qomolangma site (QOMS, 86.~~56~~94°E, 28.~~21~~36°N~~; ~~) and Namco site (NAM, 90.96°E, 30.77°N) are used to derive the AOD at ~~600~~550 nm (using the Angström exponent) for comparison with modeling results at 550 nm. All of the retrievals of AOD are at quality level 2, and the uncertainty of AOD measurements is about 0.01 (Holben et al., 2001). In this study, the available data in April 2016 are used to evaluate the modeling results during the same period. ~~The third one is the measurement of surface BC mass concentration collected at the comprehensive observation and research station (QOMS) of the Everest and the Environment of the Chinese Academy of Sciences located at the northern slope of Himalayas (28.21°N and 86.56°E), about 4276 meters above sea level (Chen et al., 2018).~~

The third one is the measurement of surface BC mass concentration collected during the simulation period for April 4-20 of 2016 at the Qomolangma (Mt. Everest) Station for Atmospheric and Environmental Observation and Research, Chinese Academy of Sciences (QOMS, 86.94°E, 28.36°N) which is located at the northern slope of the Himalayas, about 4276 meters above sea level. The BC mass concentration is measured with the widely-used instrument Aethalometer (AE-33) that can provide real-time BC mass concentration measurements. The calibration of air flow is routinely conducted to maintain the data quality. The instrument estimates the BC mass concentration based on the optical method through measuring the reduction in light intensity induced by BC. The method assumes that the relationship between attenuation and BC surface loading is linear for low attenuation values. However, this relationship becomes nonlinear when the attenuation values are high due to a filter saturation effect, which may lead to underestimation of the high BC concentration. The detection limit of AE-33 instrument is 5 ng/m^3, and the uncertainty is estimated to be within 10% (e.g., Chen et al., 2018; Bansal et al., 2019; Kant et al., 2019). The dataset of BC mass concentration used in this study was reported by Chen et al., (2018), where more details about the measurements can be found.

3. Results

3.1 Spatial distribution of BC around the TP

Figure 5 shows the spatial ~~distribution~~distributions of column integrated BC mass ~~over the area with the terrain height larger than 0.5 km~~ within the inner domain from the simulations at ~~20 km~~4 km resolution with complex and ~~4 km resolutions~~smooth topography averaged for April ~~5~~1-20, 2016~~. The~~, and the difference between the ~~simulations at~~ two ~~resolutions~~ is also shown. ~~The wind fields at 500 hPa are also shown. The~~For both experiments, the southern Himalayas is an apparent boundary line for the distribution of BC~~. There is~~ with a sharp gradient across the Himalayas. The high BC mass loading exists near the southern Himalayas reaching over ~~20~~10 mg/m^2, ~~while the value reduces significantly to less than 0.5 mg/m^2 over the TP. The high BC mass loading near the southern Himalayas~~ which is ~~primarily~~largely contributed by the biomass burning ~~emission~~emissions during the period (Fig. ~~4). The relatively large difference between the two simulations over the source region near the southern Himalayas is mainly due to the different spatial distributions of emissions at the different resolutions. Over the TP~~4), while the value reduces significantly to less than 0.4 mg/m^2 over the TP. In general, the column BC mass loading from the simulation ~~at 4 km~~with complex topography is higher ~~than that at 20 km resolution~~over the TP and lower over the region to the south of Himalayas compared with the smooth topography. Figure 6 displays the spatial distributions of AOD from the MODIS retrievals and the simulations at 4 km ~~and 20 km resolutions~~with two different topography averaged for April ~~5~~1-20, 2016. In general, ~~the~~both simulations reproduce the overall spatial distribution of AOD, with the large ~~value~~values near the southern Himalayas, consistent with the BC mass loading. The difference between the simulations and retrievals may be partly related to the uncertainties in emissions particularly for biomass burning ~~emission. Not only the strong emission near the southern Himalayas~~emissions. Other than intense emissions, the wind ~~circulations~~circulation around the TP may also play an important role in accumulating BC near the ~~slope of~~southern Himalayas. Because of the block of Himalayas, the wind circulation at 500 hPa is divided into two branches as westerly and northwesterly. Both of them are relatively dry airflows with little effect on pollutant removal~~. The westerlies~~, favor the accumulation of pollutants near the southern Himalayas, and ~~can~~ carry the pollutants to the TP (~~Vernekar~~e.g., Dumka et al., ~~2003; Ramanathan~~2010; Kang et al., ~~2008~~2015; Cong et al., 2015a). ~~The MODIS AOD retrievals over the TP are scarce.~~

The AOD retrieved at two AERONET sites over the TP are compared with the two simulations ~~at 4 km and 20 km resolutions~~ for April 1-20, 2016 (~~Figure~~Fig. 7). The AOD at the QOMS site near the northern Himalayas is higher than that at the NAM site inside of the TP. ~~The~~Both simulations ~~at both resolutions~~ can capture this gradient. The simulation ~~at 4 km~~

~~resolution~~with complex topography produces higher AOD than does the one ~~at 20 km resolution~~with smooth topography at both sites. The modeling biases (normalized mean bias, NMB) reduce from -~~28% (20 km resolution~~46% (smooth topography) to ~~11% (4 km resolution~~9% (complex topography) at the QOMS site and from -~~58% (20 km resolution~~26% (smooth topography) to -10% (~~4 km resolution~~complex topography) at the NAM site. Although the correlation coefficient between the simulations and observation increases from 0.37 (smooth topography) to 0.53 (complex topography) at the QOMS site, it is similar (~0.2) between the two simulations at the NAM site. The correlation coefficient is higher at the QOMS site near the source region than the NAM site farther away, which may indicate the model processes affecting the transport over the TP still need examination with more observations. The NAM site over the eastern TP may also be affected by other sources that are not counted in this study. The modeling of temporal variations of pollutants over the TP deserves further investigation with more observations.

~~Figure 8 shows the spatial distribution of surface BC concentration and surface wind field within the inner domain from the simulations at 4 km and 20 km resolutions. The difference between the simulations at two resolutions is also shown. Over the TP, the surface BC concentration near the Himalayas from the simulation at 4 km resolution is higher than that at 20 km resolution, but the difference between the two simulations is relatively small compared to the column BC mass (Fig. 5). The difference also exhibits heterogeneous distribution with evidently higher BC concentration at 4 km resolution than at 20 km resolution near the valleys, which reflects the impact of topography on transport (see the discussion in Section 3.2). Compared with the winds at 500 hPa (Fig. 5), surface winds show stronger southerlies reflecting local circulations, and this enhancement of southerlies is larger at 4 km resolution than at 20 km resolution.~~ There is one in-situ observational ~~site~~station (QOMS) near the Mt. Everest (black dot shown in Fig. ~~8~~1) to collect the surface BC concentration. The observed surface BC concentration at this ~~site~~station is compared with the corresponding simulations for this period as shown in Figure ~~9~~8. Without local emission source, the surface BC concentration at QOMS is primarily contributed by the transport. The temporal variation of observed surface BC concentration ~~correlated~~correlates highly with the biomass burning emissions as shown in Fig. 4, with the peak ~~BC concentration~~value on April 11 reaching ~3~~.5~~ ug/m^3. ~~This~~ One sensitivity experiment without biomass burning emissions shows that the simulated BC concentration at QOMS will be significantly reduced without the peak (not shown), which further proves that the BC concentration over the ~~TP~~ northern Himalayas can be largely influenced by the pollution episode near the southern Himalayas. ~~The~~ It is noteworthy that both simulations at both resolutions can reproduce the episode in time and magnitude. It is interesting to note that the , and the difference at this station is small. The spatial distribution of difference in surface BC concentrations at this siteconcentration between the two simulations at 4 km and 20 km resolutions(Fig. S2) is small. This may be due tomore heterogeneous than that of column BC mass (Fig. 5), reflecting the site is besides Mt. Everest and does not well reflect the difference between the simulations at 4 km and 20 km resolutions, which is shown primarily associated with the valleyimpact of topography on transport (see the discussion in Section 3.2).

3.2 Transport flux into the TP

To further understand the difference in BC surface concentration and column mass loading over the TP between the two simulations at resolutions of 4 km and 20 kmwith different topography, Figure 109 shows the longitude-height cross section of BC transport flux along the cross line (shown as the black dash line in Fig. 3) from the two simulations at local time (LT) 03:00 and 15:00 averaged for April 51-20 to represent nighttime and daytime transport, respectively. The PBL height along the cross line is also shown as the black dash line. The transport flux is calculated by projecting the wind fieldsfield perpendicularly to the cross line and then multiplying the BC mass concentration along the cross line. More specifically, the transport flux is calculated as following:

$$TF = C * (u * \sin\alpha + v * \sin\beta) \quad (1)$$

Where α is the angle between east-west wind component and the cross line, β is the angle between south-north wind component and the cross line, and C is the BC mass concentration at the grid along the cross line. The flux is estimated at each model level. Positive value denotes the northward transport across the Himalayas, and negative value denotes the southward values represent the transport. towards the TP, while negative values represent the transport away from the TP. It is evident that BC is imported into the TP during the day and night inon the west toof ~85°E, although the transport flux is much larger during the daytime than nighttime. InOn the east toof ~85°E, BC is imported into the TP during the day but exported slightly from the TP during the night. The difference of transport flux between on the west and east toof ~85°E is primarily due to the influence of large-scale westerlieswesterly that is relatively weak inon the east toof ~85°E compared with the west (Fig. 5 and 8). If removing the background westerlies, i.e., transport flux anomalies by removing the mean flux averaged during the simulation period, the transport flux dominated by the local circulation reversesanomalies show evident diurnal variation between the day and night (Fig. ~~S2~~S3 in the supporting material). This suggests that on average, the large-scale ~~westerlies are~~westerly is one of the ~~dominant mechanism~~key mechanisms transporting BC across the Himalayas into the TP~~. The local~~, while the circulation ~~strengthens~~anomalies strengthen the prevailing import transport during the daytime and ~~weakens~~weaken the import during the night, particularly in the west ~~to~~of ~85°E. ~~In addition,~~The strong transport is primarily within the PBL during the daytime, and the deeper PBL during the daytime allows BC over the source region mixed to higher altitude, which also leads to stronger import transport during the day than the night.

~~In general, the characteristics of transport flux across the Himalayas discussed above are consistent between the simulations at 4 km and 20 km resolutions. However, the~~ The difference between the simulations with two ~~resolutions~~different topography is ~~also~~ evident. ~~First of all, the~~The mountain ridges are much higher and valleys are much deeper ~~at 4 km than at 20 km resolution. Overall, the topography is more smoothing at 20 km than at 4 km resolution.~~with the complex topography than with the smooth topography. The simulation with smooth topography produces overwhelming crossing-Himalayas transport towards the TP within the PBL, in particular during the daytime. Although, in the simulation with complex topography, the mountain ridges resolved weaken the crossing-Himalayas transport compared to the simulation with smooth topography, the overall positive values near the surface indicate that the transport can overcome most mountain ridges along the Himalayas. The transport fluxes near the surface from the simulation with complex topography become close-to-zero only at a few mountain ridges that are 6.5 km or higher. To better demonstrate the transport pathway ~~through valleys and~~ across mountain ridges, ~~the valley~~one cross-section ~~and~~across the mountain ~~cross-section~~ ridge as shown as ~~the two~~one black ~~lines~~solid line in Fig. 3 ~~are selected to show the~~ is taken as one example. Figure 10 shows the latitude-height cross section of BC mass concentration and transport ~~mechanisms in Figure 11 and 12, respectively,~~flux across one mountain ridge from the simulations ~~at 20 km and 4 km resolutions at~~ with complex and smooth topography at local time (LT) 03:00 and 15:00 averaged for April ~~5~~1-20, 2016. Near the southern part of ~~both valley and~~ mountain, the elevated ~~concentrations~~concentration of BC mass ~~accumulate~~accumulates and can mix up reaching as high as 5 km~~. The spatial distributions of BC mass concentration between day and night are similar. Through the valley, the PBL is deeper during the daytime than nighttime. At both resolutions, uphill BC transport is evident in the day and night. The transport is primarily within the PBL during the daytime and is much stronger than that during the night. The transport flux anomalies by removing the mean flux averaged during the period show that the local circulation strengthens the uphill~~ with the much stronger transport during the daytime~~ but weakens the uphill transport during the night (~~. It is obvious that the mountain ridge in the simulation with smooth topography is quite low. With the high mountain ridge resolved by the complex topography, the simulated BC transport flux can still cross the mountain. Analysis of transport ~~Fig. S3 in the supporting material). The transport~~ flux ~~is much stronger at 4 km than at 20 km resolution for both daytime and nighttime. Although mountain ridges can hinder the crossing Himalayas transport, Figure 12 shows evident transport fluxes from the southern foothill of Himalayas to the TP at both resolutions. The simulation at 20 km resolution produces~~ across a few more mountain ridges indicates similar results ~~as that along the valley due to its smoothing topography. The simulation at 4 km resolution with the high mountain ridge can still produce efficient transport across the mountain ridge, although the flux is weaker than that through the valley. Similar as the transport through the valley, the local circulation strengthens (weakens) the uphill transport during the daytime (night) (Fig. S4 in the supporting material).~~(not shown). The results above ~~suggest that the BC accumulated near the southern~~ indicate that the transport of pollutants can cross a majority of mountain ridges of Himalayas~~ can be transported across the Himalayas no matter of through valleys or across mountain ridges~~, which is consistent with the observation-based estimate by Gong et al. (2019) that also found pollutants ~~can~~could overcome the blocking effect of mountain ridges of Himalayas as a transport pathway. –On the other hand, the resolved deeper valleys in the simulation with complex topography enhance the transport flux compared to the one with the smooth topography. Similarly, Figure 11 shows one example of latitude-height cross section of BC mass concentration and transport flux across one valley from the simulations with complex and smooth topography at local time (LT) 03:00 and 15:00 averaged for April 1-20, 2016. The transport is much stronger and deeper along the valley from the simulation with complex topography than the one with smooth topography. Again, analysis of transport flux across a few more valleys does not show different results (not shown).

~~The~~ In order to further demonstrate the overall inflow flux across the Himalayas, the vertically integrated BC mass ~~fluxes distributed~~ flux along the longitudinal cross section (as shown in Fig. ~~10~~9) from the simulations ~~at 20 km and 4 km resolutions are~~with different topography is shown in Figure ~~13~~12. The terrain heights from the two simulations along the cross section are also shown as black lines. ~~Again, it shows that the topography at 4 km resolution is more complex than that at 20 km resolution with more mountain ridges and valleys. The positive import~~The total mass flux is calculated by integrating the right-hand term of equation (1) as following:

$$ITF = \int_{z=z_{sfc}}^{z=z_{top}} \delta z * C * (u * \sin\alpha + v * \sin\beta) \qquad (2)$$

Where δz is the thickness of each vertical model level. Similarly, positive values represent the transport towards the TP, while negative values represent the transport away from the TP. More evidently, the positive BC ~~fluxes~~inflows towards the TP occur not only through the valleys but also across the mountain ridges ~~at both resolutions. At 4 km resolution, although~~with both topography. The negative values only exist to the east of 88°E. With complex topography, higher mountain ridges can reduce the transport flux to some extent compared to the ~~relatively smoothing terrain at 20 km resolution, they cannot block the transport. On the other hand, the deeper valleys at 4 km resolution~~ smooth topography. The complex topography results in significantly ~~enhance~~larger BC inflow towards the ~~transport~~TP compared to the ~~20 km resolution. All the enhancement of transport flux at 4 km resolution corresponds well~~smooth topography, particularly corresponding to the ~~deeper~~deep valleys, such as the Karnali River Valley around 82°E and the Kali Gandaki Valley around 84°E.

One reason for the enhanced transport across the Himalayas with the complex topography is the resolved deeper valleys that lead to the increased valley wind. The wind across the valleys can be significantly larger with the complex topography than the smooth one (Fig. S4). The enhanced valley wind across the Himalayas has also been found by previous studies with observations and numerical simulations (Egger et al., 2000; Zängl et al., 2001; Carrera et al., 2009; Karki et al., 2017; Lin et al., 2018). The second impact of resolved complex topography on the BC transport is that more BC masses can be transported with the deeper valley channels (Fig. S5a, b). With deeper valley, the column of high-concentration BC is deeper. Even with similar wind velocity, the transport flux can be larger. The third impact is through changing the small-scale circulation around the Himalayas due to the increase of topography complexity of Himalayas. The simulation with complex topography produces more near-surface winds following the direction towards the TP compared to the one with smooth topography (Fig. S6), which favors the BC transport across the Himalayas. Lastly, the simulated PBL heights from the two experiments are a little different (Fig. 9), which may also contribute partly to the different transport flux. The sensitivity of PBL height and structure to topography complexity that can result in different surface heat has been studied before (e.g., Wagner et al., 2014).

This turns out that the overall ~~transport at 4 km resolution~~BC inflow with the complex topography is much stronger than that ~~at 20 km resolution.~~with the smooth topography. Figure ~~14~~13 shows the accumulated integrated total transport flux of BC across the Himalayas estimated from the simulations ~~at 20 km~~with complex and ~~4 km resolutions~~smooth topography for April 1-20, 2016. The accumulated import flux of BC increases during the period ~~at~~in both ~~resolutions~~experiments, and the difference between the two ~~resolutions~~experiments gradually increases with the time. At the end of period, the simulation ~~at 4 km resolution~~with complex topography estimates a total import flux of BC of ~1.5×10^4 Ton that is ~50% higher than ~1.0×10^4 Ton estimated based on the simulation ~~at 20 km resolution.~~with smooth topography. The sensitivity analysis by moving the cross line (cross-section of the analysis in Fig. 9, 12, 13) towards or away from the TP within a certain distance and re-calculating the flux indicates that the impacts of topography on the simulated results do not change significantly.

~~To confirm that the different modeling results between the two resolutions is due to their different complexity of topography of Himalayas, a sensitivity experiment is conducted in the same way as the control experiment except that the inner domain at 4 km resolution applies the topography distribution exactly following that at 20 km resolution. It is interesting that the sensitivity experiment simulates very similar transport flux of BC along the longitude cross section (Fig. 13 and 14). This indicates that the difference between the simulations at the two resolutions is primarily determined by their difference of topography, which highlights the significant impact of the complexity of topography on BC transport across the Himalayas. The simulation at 4 km resolution resolves more valleys and thus produces much stronger transport fluxes, which indicates that although the transport of South Asian BC across the Himalayas can overcome the mountain ridges, the valley transport is much more efficient and this enhancement cannot be ignored.~~All the analysis above focuses on investigating the BC transport flux across the Himalayas. Although the inflow can reflect the impact of transport on the BC mass over the TP to some extent, the change of BC mass concentration is eventually determined by the convergence of transport. Therefore, the contribution of each model process (transport, dry-deposition, emission, PBL mixing, and wet deposition) to the increase of BC column mass averaged over the TP (with elevation > 4 km) during this episode is analyzed for both simulations following the methodology introduced by Du et al. (2020). The results show that the two main processes affecting the BC column mass over the TP during the period are transport and dry deposition. The transport is the dominant process that increases the BC column mass over the TP, while the dry deposition reduces it. The contribution of transport to the increase of BC column mass over the TP during the episode from the simulation with complex topography is significantly larger than that with the smooth topography, which is consistent with the results shown by analyzing the transport flux across the Himalayas.

3.3 Radiative forcing of BC over the TP

The BC transported over the TP could significantly influence the regional climate and water resources over Asia through heating the atmosphere and accelerating the melting of snow and glacier (e.g., Qian et al., 2011, 2015; Lau et al., ~~2016,~~ 2017). Therefore, the impact of the complex topography on estimating the BC radiative heating profile in the atmosphere and radiative forcing in surface snow deserves investigation. Figure ~~15~~14 shows the vertical ~~profile~~profiles of BC induced radiative heating rate in the atmosphere averaged over the TP (with elevation > 4 km) within the inner domain shown in Fig.~~-~~1 for April ~~5~~1-20, 2016 from the simulations ~~at 20 km~~with complex and ~~4 km resolutions. The result from the sensitivity experiment at 4 km but with the smoothing 20km~~ smooth topography~~ is also shown. The~~. Both simulations~~ at both resolutions~~ generate higher BC heating rate near the surface and the rate gradually decreases with altitude, which is consistent with the vertical profiles of BC mass concentration averaged over the TP (Fig. ~~S5~~S7 in the supporting material). The BC heating rate over the TP from the simulation ~~at 4 km resolution~~ with complex topography is ~0.17 K/day near the surface and reduces to ~0.08 K/day at 8 km, which ~~are ~20~~is ~50% and ~~~50~~30%, respectively, higher than that from the simulation ~~at 20 km resolution~~with smooth topography at the corresponding altitudes. The higher BC heating rate over the TP estimated by the simulation ~~at 4 km resolution~~with complex topography is consistent with its higher BC column mass (Fig. 5) and concentration profile (Fig. ~~S5). The sensitivity experiment at 4 km resolution with the smoothing 20km topography simulates more similar BC heating profile as that from the experiment at 20 km resolution, which is consistent with the vertical profiles of BC mass concentration (Fig. S5). However, it is noteworthy that with the same topography, the sensitivity experiment at 4 km resolution produces significantly lower BC mass concentration and heating rate near the surface than the one at 20 km resolution. The process analysis indicates that this is mainly due to that the sensitivity experiment simulates smaller net transported BC concentration near the surface of TP compared to the experiment at 20 km resolution (not shown~~S7).

The BC radiative forcing in surface snow is controlled by both the distributions of BC mass concentration and snow coverage (e.g., Zhao et al., 2014). Figure ~~16~~15 shows the spatial distributions of snow water equivalent (SWE) averaged for April ~~5~~1-20, 2016 from the simulations ~~at 20 km and 4 km resolutions. The sensitivity experiment at 4 km resolution but~~ with ~~the smoothing 20km~~ two topography~~-~~. The difference between the two is also shown. It shows that the simulation ~~at 4 km resolution~~ with complex topography generates more areas with higher SWE compared to that ~~at 20 km resolution. In particular, the~~ with the smooth topography over the TP. Along the Himalayas, the simulated SWE is higher over the mountain ridges along the Himalayas and over the TP at 4 km than at 20 km resolution. The sensitivity experiment at 4 km resolution but with the smoothing 20km-topography still produces larger SWE alongwith the complex topography, particularly for the East Himalayas but similar SWE, while the smooth topography leads to broader snow coverage over the TP compared to the simulation at 20 km resolution. This is mainly induced by theWest Himalayas. The difference in SWE between the two simulations is highly correlated with their difference in precipitation between the two resolutions (Fig. S6S8 in the supporting material). Along the Himalayas, the simulated precipitation fromwith the simulation at 4 km resolutioncomplex topography is larger than that at 20 km resolution regardless ofwith the complexity ofsmooth topography. However, over at the mountain ridges and smaller at the valleys. Over the TP, largerthe overall precipitation is producedlarger with morethe complex topography at 4 km resolution than that at 20 km resolutionwith the smooth topography (Fig. S6). S8). Previous studies have found that the topography could significantly affect the precipitation over the Himalayas region (e.g., Bookhagen and Burbank, 2010; Wulf et al., 2016; Cannon et al., 2017; Karki et al., 2017).

Figure 1716 shows the spatial distributions of BC radiative forcing in the surface snow over the TP averaged for April 51-20, 2016 from the simulations at 20 km and 4 km resolutions. The sensitivity experiment at 4 km resolution but with the smoothing 20km-two topography, and the difference between the two is also shown. The BC radiative forcing in surface snow is largely coincident with the spatial distributions of SWE as shown in Fig. 1615, mainly due to the heterogeneous distributions of snow cover over the TP. The BC radiative forcing in surface snow over the TP from the simulation at 4 km resolution with complex topography reaches 65 W/m^2 where the snow exists, much larger than that at 20 km resolution.with the smooth topography. Along the Himalayas, the simulation at 4 km with complex topography produces higher BC snow forcing over mountains almost along the entiremountain ridges, particularly over the eastern Himalayas, while the one at 20 km resolution only haswith the considerablesmooth topography simulates higher BC snow forcing over the most areas of western Himalayas, which follows the distributions of due to its broader snow coverage along the Himalayas (Fig. 16). Over the western Himalayas, the simulation at 20 km resolution generates higher BC forcing in snow to some extent. With the smoothing 20km-topography at the 4 km resolution, the simulated BC forcing in snow covers more areas along the Himalayas than that from the 20 km resolution and is similar as that at the simulation at 4 km resolution. However, with the smoothing 20km-topography, the BC forcing in snow from the simulation at 4 km resolution is higher over the western Himalayas.there. Overall, the complex topography at 4 km leads to higher BC forcing in snow over the TP and the eastern Himalayas and reduces thelower BC forcing in snow over the western Himalayas, and therefore results in athe different distribution of BC forcing in snow over the TP and Himalayas, compared to that at 20 km resolutionwith the smooth topography.

4. Summary and discussion

In this study, the model experiments atwith different resolutionstopography are conducted to illustrate the impacts of complexity of topography of Himalayas on BC transport from South Asia to the TP. The observed pollution episode at the QOMS station besides the Mt. Everest during the pre-monsoon season is simulated. The observed surface BC concentrations showconcentration shows a peak of ~3.5 ug/m^3 much larger than the background value of < 0.54 ug/m^3 over the TP. The observed temporal variation of surface BC concentrations correlates highly with that of biomass burning emissions near the southern Himalayas, indicating the significant impacts of biomass burning on the pollutants over the TP. The simulations can reproduce the episode in time and magnitude, and are used to investigate the BC transport mechanisms and the impacts of topography.

The high BC mass loading during the simulation period accumulates near the southern Himalayas driven by the large-scale circulation, which is also observed by satellites. The modeling results demonstrate that the westerlies favorwesterly favors the accumulation of pollutants near the southern Himalayas and can carry the pollutants to the TP during the day and night, which is consistent with previous modeling studies (e.g., Kopacz et al., 2011). The transport is stronger across the West Himalayas than that across the East. The local circulation strengthens the prevailing import transport during the daytime and weakens the import during the night. In addition,The deeper PBL during the daytime allows BC over the source region mixed to higher altitude, which also leads to stronger import transport during the day than the night. It is also noteworthy that the BC accumulated near the southern Himalayas can be transported across the Himalayas no matter of through valleys or acrossovercoming a majority of mountain ridges, which is consistent with the observation-based estimate by Gong et al. (2019) that also found pollutants cancould overcome the blocking effect of the mountain ridges of Himalayas as the efficient transport pathway. However, the transport through the valleys is found much stronger and more efficient than across the mountain ridges and the enhancement effect cannot be ignored. The complex topography results in 50% higher overall transport flux across the Himalayas during the simulation period than that with the smooth topography, primarily due to the enhanced valley wind, deeper valley channels, and induced small-scale favorable circulation. This turns out that the simulation with complex topography produces 30-50% higher BC radiative heating rate in the atmosphere up to 10 km averaged over the TP than does the simulation with smooth topography.

~~The~~ Previous studies also found the induced change of circulation and transport due to the complex topography at convection-permitting scales with the focus on the meteorological fields (e.g., Karki et al., 2017; Lin et al., 2018). However, most of them conducted the sub-10 km simulations over a much smaller region (e.g., 101×96 grids at 5 km in Karki et al., 2017, and 181×121 grids at 2 km in Lin et al., 2018) compared to this study (400×300 grids at 4 km). Karki et al. (2017) found that the complex topography resolving more valleys and mountain ridges ~~are much higher and valleys are much deeper at 4 km~~yielded more realistic strong and narrower winds and also small-scale mountain-valley circulations over the Himalayas region compared to the smoother topography. Lin et al. (2018) analyzed the simulations over the region situated in the central Himalayas (87°E-89°E) with very complex terrain including several high mountains and low valleys, e.g., Mt. Everest, Mt. Kanchenjunga, and the Yadong Valley. Although Lin et al. (2018) simulated enhanced moisture flux along the valley, the overall moisture transported was lower with the complex topography (10 km resolution~~ than at 20~~) compared to that with the smooth topography (30 km resolution~~.~~). The difference between their study and this study can be due to several factors. First, Lin et al. (2018) focused on a relatively small region of Himalayas (87°E-89°E) compared to that in this study (75°E-92°E). The ~~transport strength through the valleys and across the mountains are similar from the simulation at 20 km resolution due to its smoothing topography. At 4 km resolution, the deeper valleys result in much stronger~~lower-lever transport flux ~~than that at 20 km resolution, which highlights the significant impact of the complexity of topography on BC~~simulated in this study also exhibits weaker wind with complex topography between 87°E and 89°E (Fig. 9 and 12), maybe due to several very high mountains such as Mt. Everest and Mt. Kanchenjunga over this area. Second, the spatial (horizontal and vertical) distributions between air pollutants and moisture are also different and may contribute partly to the different impacts of topography on the overall transport ~~across the Himalayas. The complex topography resolved by the 4 km resolution leads to 50% higher overall transport fluxes of BC across the Himalayas compared to that from the simulation at 20 km resolution during the simulation period. This turns out that the simulation at 4 km resolution produces 20-50% higher BC radiative heating rate in the~~

~~atmosphere averaged over the TP than does the simulation at 20 km resolution.~~ flux across the Himalayas.

For the BC radiative forcing in surface snow, the simulation ~~at 4 km resolution~~with complex topography produces stronger forcing over the TP than that ~~at 20 km resolution.~~with the smooth one. The complex topography makes the distribution of BC forcing in surface snow quite different ~~between~~from the ~~simulations at the two resolutions~~simulation with smooth topography, partly due to ~~their~~its different ~~distributions~~distribution of surface snow. The simulated BC radiative forcing in snow ~~are~~is distributed more heterogeneously than those in previous studies using global models at relatively coarse resolutions (e.g., Qian et al., 2011). He et al. (2014) used a global chemical transport model to simulate the BC forcing in snow at the horizontal resolution of ~0.2° and obtained the similar distribution as the simulation with smooth topography in this study with the high values over the western Himalayas. However, their simulated values near the Himalayas are higher than the simulated results ~~at 20 km resolution~~ of this study~~ and are close to the results at 4 km resolution~~, which may be due to their estimation are averaged for November-April.

This study highlights the importance of resolving complex topography of the Himalayas in modeling the aerosol ~~radiative impact over the TP. Climate models at coarser horizontal resolutions than 20 km~~transport across the Himalayas and radiative impact over the TP. Although this study focuses on the impacts of topography on the simulated results, the additional analysis (Fig. S9-11 in the supporting material) of the outer domain simulation at 20 km resolution and the inner domain simulation at 4 km with different topography indicates that the resolution-dependent difference between 20 km and 4 km is largely contributed by their different representations of topography over the Himalayas region, consistent with previous studies (e.g., Karki et al., 2017; Lin et al., 2018). Climate models at coarser horizontal resolutions than 20 km and thus with relatively smooth topography may underestimate the aerosol transport from South Asia to the TP during the pre-monsoon season and represent inappropriately the aerosol radiative forcing in the atmosphere and surface snow over the TP. ~~In addition~~Since this study only demonstrates the potential impacts for a relatively short period, a longer-term study should be conducted to examine the impacts of topography on aerosol climatic effect over the TP. In addition, the active convection during the monsoon season may also play an important role on pollutant transport across the Himalayas, which deserves further investigation. Furthermore, aerosol impact on cloud and precipitation, particularly during the monsoon season, and thus on the latent heat in the atmosphere and the associated responses may also depend on the complex topography. Previous studies based on observations found that the rain frequency and intensity reached the highest and the cloud thickness reached the deepest at the foothill of Himalayas and decreased as the elevation increased up to the TP (e.g., Chen et al., 2017; Fu et al., 2018; Zhang et al., 2018), which was explained by Fu et al. (2018) due to the blocking of the air flow by the steep slope of southern Himalayas. However, the large amount of transported aerosol along the slope from the foothill up to the TP may also play a role. These potential impacts of aerosols on regional hydro-climate around the TP and over Asia using high-resolution model that can resolve the complex topography of Himalayas and TP deserve further investigation.

Data availability

The released version of WRF-Chem can be downloaded from http://www2.mmm.ucar.edu/wrf/users/download/get_source.html. The updated USTC version of WRF-Chem can be downloaded from http://aemol.ustc.edu.cn/product/list/ or contact chunzhao@ustc.edu.cn. Also, the code modifications will be incorporated the release version of WRF-Chem in future.

Author contributions

Meixin Zhang and Chun Zhao designed the experiments, conducted and analyzed the simulations. All authors contributed to the discussion and final version of the paper.

Acknowledgements

This research was supported by the National Key Research and Development Program of China (2016YFA0602001), the National Natural Science Foundation of China NSFC (Grant No. 91837310), the second Tibetan Plateau Scientific Expedition and Research Program (STEP) (2019QZKK0605), and the Fundamental Research Funds for the Central Universities. The study used computing resources from the High-Performance Computing Center of University of Science and Technology of China (USTC) and the TH-2 of National Supercomputer Center in Guangzhou (NSCC-GZ).

Reference

Bansal, O., Singh, A., and Singh, D.: Characteristics of Black Carbon aerosols over Patiala Northwestern part of the IGP: Source apportionment using cluster and CWT analysis, Atmospheric Pollution Research, 10, 244–256, doi:10.1016/j.apr.2018.08.001, 2019.

Barnard, J. C., Fast, J. D., Paredes-Miranda, G., Arnott, W. P., and Laskin, A.: Technical Note: Evaluation of the WRF-Chem "Aerosol Chemical to Aerosol Optical Properties" Module using data from the MILAGRO campaign, Atmos. Chem. Phys., 10, 7325–7340, doi: 10.5194/acp-10-7325-2010, 2010.

Barnett, T. P., Adam, J. C., and Lettenmaier, D. P.: Potential impacts of a warming climate on water availability in snow-dominated regions, Nature, 438, 303–309, doi:10.1038/nature04141, 2005.
~~doi: 10.1038/nature04141, 2005.~~

Binkowski, F. S. and Shankar, U.: The Regional Particulate Matter Model: 1. Model description and preliminary results, J. Geophys. Res., 100, 26191, doi:10.1029/95JD02093, 1995.

Bookhagen, B. and Burbank, D. W.: Toward a complete Himalayan hydrological budget: Spatiotemporal distribution of snowmelt and rainfall and their impact on river discharge, J. Geophys. Res., 115, 39, doi:10.1029/2009JF001426, 2010.

Boos, W. R. and Kuang, Z.: Sensitivity of the South Asian monsoon to elevated and non-elevated heating, Scientific reports, 3, 1192, doi:10.1038/srep01192, 2013.

~~Brun, J., Shrestha, P., and Barros, A. P.: Mapping aerosol intrusion in Himalayan valleys using the Moderate Resolution Imaging Spectroradiometer (MODIS) and Cloud–Aerosol Lidar and Infrared Pathfinder Satellite Observation (CALIPSO), Atmospheric Environment, 45, 6382–6392, doi: 10.1016/j.atmosenv.2011.08.026, 2011.~~

Cannon, F., Carvalho, L. M. V., Jones, C., Norris, J., Bookhagen, B., and Kiladis, G. N.: Effects of topographic smoothing on the simulation of winter precipitation in High Mountain Asia, J. Geophys. Res. Atmos., 122, 1456–1474, doi:10.1002/2016JD026038, 2017.

Cao, J., Tie, X., Xu, B., Zhao, Z., Zhu, C., Li, G., and Liu, S.: Measuring and modeling black carbon (BC) contamination in the SE Tibetan Plateau, Journal of Atmospheric Chemistry, 67, 45-60, doi:10.1007/s10874-011-9202-5, 2010.

Carrera, M. L., Gyakum, J. R., and Lin, C. A.: Observational Study of Wind Channeling within the St. Lawrence River Valley, J. Appl. Meteor. Climatol., 48, 2341–2361, doi:10.1175/2009JAMC2061.1, 2009.

Chapman, E. G., Gustafson, W. I., Easter, R. C., Barnard, J. C., Ghan, S. J., Pekour, M. S., and Fast, J. D.: Coupling aerosol-cloud-radiative processes in the WRF-Chem model: Investigating the radiative impact of elevated point sources, Atmos. Chem. Phys., 9, 945–964, doi:10.5194/acp-9-945-2009, 2009.

Chen, J. and Bordoni, S.: Orographic Effects of the Tibetan Plateau on the East Asian Summer Monsoon: An Energetic Perspective, J. Climate, 27, 3052–3072, doi:10.1175/JCLI-D-13-00479.1, 2014.

Chen, X., Kang, S., Cong, Z., Yang, J., and Ma, Y.: Concentration, temporal variation, and sources of black carbon in the Mt. Everest region retrieved by real-time observation and simulation, Atmos. Chem. Phys., ~~doi: 10.1175/JCLI-D-13-00479.1, 2014.~~

~~Chen, P., Li, C.,~~ 18, 12859–12875, doi:10.5194/acp-18-12859-2018, 2018.

~~Kang, S., Rupakheti, M., Panday, A. K., Yan, F., Li, Q., Zhang, Q., Guo, J., Ji, Z., Rupakheti, D., and Luo, W.: Characteristics of Particulate-Phase Polycyclic Aromatic Hydrocarbons (PAHs) in the Atmosphere over the Central Himalayas, Aerosol Air Qual. Res., 17, 2942–2954, doi: 10.4209/aaqr.2016.09.0385, 2017.~~

Chen, X., Kang, S., Cong, Z., Yang, J., and Ma, Y.: Concentration, temporal variation, and sources of black carbon in the Mt. Everest region retrieved by real-time observation and simulation, Atmos. Chem. Phys., 18, 12859–12875, doi:10.5194/acp-18-12859-2018, 2018.

Chen, Y.~~L.~~, Fu, Y.~~F.~~, Xian, T., and Pan, X.~~, 2017.~~.: Characteristics of cloud cluster over the steep southern slopes of the Himalayas observed by CloudSat~~.~~, Int. J. Climatol~~.~~., 37, 4043–4052, doi:10.1002/joc.4992, 2017.

Cong, Z., Kang, S., and Qin, D.: Seasonal features of aerosol particles recorded in snow from Mt. Qomolangma (Everest) and their environmental implications, Journal of environmental sciences (China), 21, 914–919, doi:10.1016/S1001-0742(08)62361-X, 2009.

~~Cong, Z., Kang, S., Gao, S., Zhang, Y., Li, Q., and Kawamura, K.: Historical Trends of Atmospheric Black Carbon on Tibetan Plateau As Reconstructed from a 150-Year Lake Sediment Record, Environ. Sci. Technol., 47, 2579–2586,doi: 10.1021/es3048202, 2013.~~

Cong, Z., Kang, S., Kawamura, K., Liu, B., Wan, X., Wang, Z., Gao, S., and Fu, P.: Carbonaceous aerosols on the south edge of the Tibetan Plateau: concentrations, seasonality and sources, Atmos. Chem. Phys., 15, 1573–1584, doi:10.5194/acp-15-1573-2015, ~~2015(a).~~2015a.

Cong, Z., Kawamura, K., Kang, S., and Fu, P.: Penetration of biomass-burning emissions from South Asia through the Himalayas: new insights from atmospheric organic acids, Scientific reports, 5, 9580, doi:10.1038/srep09580, ~~2015(b).~~2015b.

Dentener, F., Kinne, S., Bond, T., Boucher, O., Cofala, J., Generoso, S., Ginoux, P., Gong, S., Hoelzemann, J. J., Ito, A., Marelli, L., Penner, J. E., Putaud, J.~~–~~. P., Textor, C., Schulz, M., van der Werf, G. R., and Wilson, J.: Emissions of primary aerosol and precursor gases in the years 2000 and 1750, prescribed data-sets for AeroCom, Atmos. Chem. Phys~~–~~., 6, 4321–4344, doi:10.5194/acp-6-4321-2006,~~Discuss., 6, 2703–2763, doi: 10.5194/acpd-6-2703-2006,~~ 2006.

~~Dhungel, S., Kathayat, B., Mahata, K., and Panday, A.: Transport of regional pollutants through a remote trans-Himalayan valley in Nepal, Atmos. Chem. Phys. Discuss., 1–23, doi: 10.5194/acp-2016-824, 2016.~~

Ding, Y., Sun, Y., Wang, Z., Zhu, Y., and Song, Y.: Inter-decadal variation of the summer precipitation in China and its association with decreasing Asian summer monsoon Part II: Possible causes, Int. J. Climatol., 29, 1926–1944, doi:-10.1002/joc.1759, 2009.

Du, Q., Zhao, C., Zhang, M., Dong, X., Chen, Y., Liu, Z., Hu, Z., Zhang, Q., Li, Y., Yuan, R., and Miao, S.: Modelling diurnal variation of surface PM2.5 concentration over East China with WRF-Chem: Impacts from boundary layer mixing and anthropogenic emission, Atmos. Chem. Phys. Discuss., https://doi.org/10.5194/acp-2019-739, in review, 2020.

Duan, A. M. and Wu, G. X.: Role of the Tibetan Plateau thermal forcing in the summer climate patterns over subtropical Asia, Climate Dynamics, 24, 793–807, doi:-10.1007/s00382-004-0488-8, 2005.

Dubovik, O. and King, M. D.: A flexible inversion algorithm for retrieval of aerosol optical properties from Sun and sky radiance measurements, J. Geophys. Res., 105, 20673–20696, doi:10.1029/2000JD900282, 2000.

Dubovik, O., Holben, B., Eck, T. F., Smirnov, A., Kaufman, Y. J., King, M. D., Tanré, D., and Slutsker, I.: Variability of Absorption and Optical Properties of Key Aerosol Types Observed in Worldwide Locations, J. Atmos. Sci., 59, 590–608, doi:10.1175/1520-0469(2002)059<0590:VOAAOP>2.0.CO;2, 2002.

Dumka, U. C., Moorthy, K. K., Kumar, R., Hegde, P., Sagar, R., Pant, P., Singh, N., and Babu, S. S.: Characteristics of aerosol black carbon mass concentration over a high altitude location in the Central Himalayas from multi-year measurements, Atmospheric Research, 96, 510–521, doi:-10.1016/j.atmosres.2009.12.010, 2010.

~~Dubovik, O., and King, M. D.: A flexible inversion algorithm for retrieval of aerosol optical properties from sun and sky radiance measurements, J. Geophys. Res., 105, 20673–20696, 2000.~~

Dubovik, O., Holben, B., Eck, T. F., Smirnov, A., Kaufman, Y.J., King, M.D., Tanre, D., and Slutsker, I.: Variability of absorption and optical properties of key aerosol types observed in worldwide locations, J. Atmos. Sci., 59, 590-608, 2002.

Easter, R. C., Ghan, S. J., Zhang, Y., Saylor, R. D., Chapman, E. G., Laulainen, N. S., Abdul-Razzak, H., Leung, L. R., Bian, X., and Zaveri, R. A.: MIRAGE: Model Description and Evaluation of Aerosols and Trace Gases, J. Geophys. Res., 109, D20210, doi:10.1029/2004JD004571, 2004.

Egger, J., Bajracharya, S., Egger, U., Heinrich, R., Reuder, J., Shakya, P., Wendt, H., and Wirth, V.: Diurnal winds in the Himalayan Kali Gandaki Valley. Part I: Observations, Mon. Weather Rev., 128, 1106–1122, 2000.

Engling, G. and Gelencser, A.: Atmospheric Brown Clouds: From Local Air Pollution to Climate Change, Elements, 6, 223–228, doi:-10.2113/gselements.6.4.223, 2010.

Fan, J., Rosenfeld, D., Yang, Y., Zhao, C., Leung, L. R., and Li, Z.: Substantial contribution of anthropogenic air pollution to catastrophic floods in Southwest China, Geophys. Res. Lett., 42, 6066–6075, doi:10.1002/2015GL064479, 2015.

Fast, J. D., Gustafson Jr, W. I., Easter, R. C., Zaveri, R. A., Barnard, J. C., Chapman, E. G., Grell, G. A., and Peckham, S. E.: Evolution of ozone, particulates, and aerosol direct radiative forcing in the vicinity of Houston using a fully coupled meteorology - chemistry - aerosol model, J. Geophys. Res., 111, D21305, doi:-10.1029/2005JD006721, 2006.

Feng, Y., Kotamarthi, V. R., Coulter, R., Zhao, C., and Cadeddu, M.: Radiative and thermodynamic responses to aerosol extinction profiles during the pre-monsoon month over South Asia, Atmos. Chem. Phys., 16, 247–264, doi:10.5194/acp-16-247-2016, 2016.

Flanner, M. G. and Zender, C. S.: Snowpack radiative heating: Influence on Tibetan Plateau climate, Geophys. Res. Lett., 32, L06501, doi:-10.1029/2004GL022076, 2005.

Fu, Y., Pan, X., Xian, T., Liu, G., Zhong, L., Liu, Q., Li, R., Wang, Y., 2018.and Ma, M.: Precipitation characteristics over the steep slope of the Himalayas in rainy season observed by TRMM PR and VIRS. Clim. Dyn. http://dx., Climate dynamics, 51, 1971-1989, doi.org/10.1007/s00382-017-3992-3: 10.1007/s00382-017-3992-3, 2018.

Gautam,Gao, Y., Zhao, C., Liu, X., Zhang, M., and Leung, L. R.: WRF-Chem simulations of aerosols and anthropogenic aerosol radiative forcing in East Asia, Atmospheric Environment, 92, 250–266, doi:10.1016/j.atmosenv.2014.04.038, 2014.

R.,Hsu, N. C., Tsay, S. C., Lau, K.-M., Holben, B., Bell, S.,Smirnov, A., Li, C.,Hansell, R., Ji, Q., Payra, S., Aryal, D., Kayastha, R., and Kim, K. M.: Accumulation of aerosols over

~~the Indo-Gangetic plains and southern slopes of the Himalayas: distribution, properties and radiative effects during the 2009 pre-monsoon Season, Atmos. Chem. Phys. Discuss., 11, 15697–15743, doi: 10.5194/acpd-11-15697-2011, 2011.~~

Ginoux, P., Chin, M., Tegen, I., Prospero, J. M., Holben, B., Dubovik, O., and Lin, S.-J.: Sources and distributions of dust aerosols simulated with the GOCART model, J. Geophys. Res., 106, 20255–20273, doi:10.1029/2000JD000053, 2001.

Gong, P., Wang, X.~~-p~~., Pokhrel, B., Wang, H., Liu, X., Liu, X., and Wania, F.: Trans-Himalayan ~~transport~~Transport of ~~organochlorine compounds: three-year observations~~Organochlorine Compounds: Three-Year Observations and ~~model-based flux estimation~~Model-Based Flux Estimation, Environ. Sci. Technol., 53, 6773–6783, doi: 10.1021/acs.est.9b01223, 2019.

Gong, S. L.: A parameterization of sea-salt aerosol source function for sub- and super-micron particles, Global Biogeochem. Cycles, 17, n/a-n/a, doi:10.1029/2003GB002079, 2003.

Grell, G. A., Peckham, S. E., Schmitz, R., McKeen, S. A., Frost, G., Skamarock, W. C., and Eder, B.: Fully coupled “online” chemistry within the WRF model, Atmospheric Environment, 39, 6957–6975, doi:10.1016/j.atmosenv.2005.04.027, 2005.

Gustafson, W. I., E. G. Chapman, S. J. Ghan, R. C. Easter, and J. D. Fast: Impact on modeled cloud characteristics due to simplified treatment of uniform cloud condensation nuclei during NEAQS 2004, Geophys. Res. Lett., 34, L19809, doi:10.1029/2007GL030021, 2007.

Hansen, J. and Nazarenko, L.: Soot climate forcing via snow and ice albedos, Proceedings of the National Academy of Sciences, 101, 423–428, doi:10.1073/pnas.2237157100, 2004.

He, C., Li, Q., Liou, K. N., Takano, Y., Gu, Y., Qi, L., Mao, Y., and Leung, L. R.: Black carbon radiative forcing over the Tibetan Plateau, Geophys. Res. Lett., 41, 7806–7813, doi: 10.1002/2014GL062191, 2014.

He, C., Wang, Z., Zhou, T., and Li, T.: Enhanced Latent Heating over the Tibetan Plateau as a Key to the Enhanced East Asian Summer Monsoon Circulation under a Warming Climate, J. Climate, 32, 3373–3388, doi:10.1175/JCLI-D-18-0427.1, 2019.

Hess, M., Koepke, P., and Schult, I.: Optical Properties of Aerosols and Clouds: The Software Package OPAC, Bull. Amer. Meteor. Soc., 79, 831–844, doi:10.1175/1520-0477(1998)079<0831:OPOAAC>2.0.CO;2, 1998.

Hindman, E. E. and Upadhyay, B. P.: Air pollution transport in the Himalayas of Nepal and Tibet during the 1995–1996 dry season, Atmospheric Environment, 36, 727–739, doi: 10.1016/S1352-2310(01)00495-2, 2002.

Holben, B. N., Eck, T. F., Slutsker, I., Tanr~~' e~~é, D., Buis, J. P., ~~Stezer~~Setzer, A., Vermote, E., Reagan, ~~Y~~J. A., Kaufman, ~~U~~Y. J., Nakajima, T., Lavenu, F., Jankowiak, I., and Smirnov, A.: AERONET~~ A federated instrument network~~ – A Federated Instrument Network and ~~data archive~~Data Archive for ~~aerosol characterization, Rem. Sens. Environ.,~~Aerosol Characterization, Remote Sensing of Environment, 66, 1–16, doi:10.1016/S0034-4257(98)00031-5, 1998.

Holben, B. N., Tanre, D., Smirnov, A., ECK T. F., Slutsker, I., Abuhassan, N., Newcomb, W., Schafer, J., Chatenet, B., Lavenu, F., Kaufman, Y., Vande Castle, J., Setzer, A., Markham, B., Clark, D., Frouin, R., Halthore, R., Karneli, A., O'Neill, N., Pietras, C., Pinker, R., Voss, K., and Zibordi, G.: An emerging ground-based aerosol climatology: Aerosol optical depth from AERONET, J. Geophys. Res., 106, 12067-12097, doi:10.1029/2001JD900014, 2001.

~~Leung, L. R., Qian, Y., Yu, H., Huang, L., and Kalashnikova, O. V.: Trans-pacific transport and evolution of aerosols: Evaluation of quasi global WRF-Chem simulation with multiple observations, Geosci. Model Dev. Discuss., 1–65, doi: 10.5194/gmd-2015-248, 2016.~~

Hu, Z., Huang, J., Zhao, C., Bi, J., Jin, Q., Qian, Y., Leung, L. R., Feng, T., Chen, S., and Ma, J.: Modeling the contributions of Northern Hemisphere dust sources to dust outflow from East Asia, Atmospheric Environment, 202, 234–243, doi:~~-~~10.1016/j.atmosenv.2019.01.022, 2019.

Hu, Z., Huang, J., Zhao, C., Jin, Q., Ma, Y., and Yang, B.: Modeling dust sources, transport, and radiative effects at different altitudes over the Tibetan Plateau, Atmos. Chem. Phys. Discuss., https://doi.org/10.5194/acp-2019-431, in press, 2020.

Hu, Z., Zhao, C., Huang, J., Leung, L. R., Qian, Y., Yu, H., Huang, L., and Kalashnikova, O.V.: Trans-pacific transport and evolution of aerosols: Evaluation of quasi global WRF-Chem simulation with multiple observations, Geosci. Model Dev. Discuss., 1–65, doi:10.5194/gmd-2015-248, 2016.

Huang, X., Song, Y., Zhao, C., Cai, X., Zhang, H., and Zhu, T.: Direct Radiative Effect by Multicomponent Aerosol over China, J. Climate, 28, 3472–3495, doi:10.1175/JCLI-D-14-00365.1, 2015.

Iacono, M. J., Mlawer, E. J., Clough, S. A., and Morcrette, J.~~-~~ J.: Impact of an improved longwave radiation model, RRTM, on the energy budget and thermodynamic properties of the NCAR community climate model, CCM3, J. Geophys. Res., 105, 14873–14890, doi:10.1029/2000JD900091, 2000.

Immerzeel~~ WW~~, W. W., van Beek~~ LPH~~, L. P. H., and Bierkens~~ MFP.~~, M. F. P.: Climate change will affect the Asian water towers~~.~~, Science ~~2010;~~(New York, N.Y.), 328~~:~~, 1382–~~5~~1385, doi:10.1126/science.1183188, 2010.

Jaeglé, L., Quinn, P. K., Bates, T. S., Alexander, B., and Lin, J~~.~~. T.: Global distribution of sea salt aerosols: new constraints from in situ and remote sensing observations, Atmos. Chem. Phys., 11, 3137–3157, doi:~~ ~~10.5194/acp-11-3137-2011, 2011.

Janssens-Maenhout, G., Crippa, M., Guizzardi, D., Dentener, F., Muntean, M., Pouliot, G., Keating, T., Zhang, Q., Kurokawa, J., Wankmüller, R., van der Denier Gon, H., Kuenen, J. J. P., Klimont, Z., Frost, G., Darras, S., Koffi, B., and Li, M.: HTAP_v2.2: a mosaic of regional and global emission grid maps for 2008 and 2010 to study hemispheric transport of air pollution, Atmos. Chem. Phys., 15, 11411–11432, doi:~~ ~~10.5194/acp-15-11411-2015, 2015.

Ji, Z. M.: Modeling black carbon and its potential radiative effects over the Tibetan Plateau, Advances in Climate Change Research, 7, 139–144, doi:10.1016/j.accre.2016.10.002, 2016.

Ji, Z., Kang, S., Cong, Z., Zhang, Q., and Yao, T.: Simulation of carbonaceous aerosols over the Third Pole and adjacent regions: distribution, transportation, deposition, and climatic effects, Clim Dyn, 45, 2831–2846, doi:~~ ~~10.1007/s00382-015-2509-1, 2015.

~~Ji, Z. M.: Modeling black carbon and its potential radiative effects over the Tibetan Plateau, Advances in Climate Change Research, 7, 139–144, doi: 10.1016/j.accre.2016.10.002, 2016.~~

Kain, J. S.: The Kain–Fritsch ~~convective parameterization~~Convective Parameterization: An ~~update~~Update, J. Appl. ~~Meteorol~~Meteor., 43, 170–181, doi:10.1175/1520-0450(2004~~.~~

~~Kang, S., Xu, Y., You, Q., Flügel, W. A., Pepin, N., and Yao, T.: Review of climate and cryospheric change in the Tibetan Plateau, Environ. Res. Lett., 5, 15101, doi: 10.1088/1748-9326/5/1/015101, 2010.~~

~~Kang, S.: Atmospheric Aerosol Elements over the Inland Tibetan Plateau: Concentration, Seasonality, and Transport, Aerosol Air Qual. ~~)043<0170:TKCPAU>2.0.CO;2, 2004~~Res., doi: 10.4209/aaqr.2015.02.0307, 2015~~.

Kang, S., Q. Zhang, Y. Qian, Z. Ji, C. Li, Z. Cong, Y. Zhang, J. Guo, W. Du, J. Huang, Q. You, A. K. Panday, M. Rupakheti, D. Chen, O. Gustafsson, M. H. Thiemens, and D. Qin: Linking atmospheric pollution to cryospheric change in the Third Pole region: current progress and future prospects, National Science Review, 6, 796–809, doi:~~ ~~10.1093/nsr/nwz031, 2019.

Kang, S.: Atmospheric Aerosol Elements over the Inland Tibetan Plateau: Concentration, Seasonality, and Transport, Aerosol Air Qual. Res., doi:10.4209/aaqr.2015.02.0307, 2015.

Kant, Y., Shaik, D. S., Mitra, D., Chandola, H. C., Babu, S. S., and Chauhan, P.: Black carbon aerosol quantification over north-west Himalayas: Seasonal heterogeneity, source apportionment and radiative forcing, Environmental pollution (Barking, Essex 1987), 113446, doi:10.1016/j.envpol.2019.113446, 2019.

Karki, R., ul Hasson, S., Gerlitz, L., Schickhoff, U., Scholten, T., and Böhner, J.: Quantifying the added value of convection-permitting climate simulations in complex terrain: a systematic evaluation of WRF over the Himalayas, Earth Syst. Dynam., 8, 507–528, doi:10.5194/esd-8-507-2017, 2017.

Kok, J. F.: A scaling theory for the size distribution of emitted dust aerosols suggests climate models underestimate the size of the global dust cycle, Proceedings of the National Academy of Sciences of the United States of America, 108, 1016–1021, doi: 10.1073/pnas.1014798108, 2011.

Kopacz, M., Mauzerall, D. L., Wang, J., Leibensperger, E. M., Henze, D. K., and Singh, K.: Origin and radiative forcing of black carbon transported to the Himalayas and Tibetan Plateau, Atmos. Chem. Phys., 11, 2837–2852, doi:~~-~~10.5194/acp-11-2837-2011, 2011.

Kuhlmann, J. and Quaas, J.: How can aerosols affect the Asian summer monsoon? Assessment during three consecutive pre-monsoon seasons from CALIPSO satellite data, Atmos. Chem. Phys~~. Discuss~~., 10, ~~4887–4926~~4673–4688, doi:~~-~~10.5194/~~acpd~~acp-10-~~4887~~4673-2010, 2010.

Lau, K. M. and Kim, K. M.: Observational relationships between aerosol and Asian monsoon rainfall, and circulation, Geophys. Res. Lett., 33, D22101, doi: 10.1029/2006GL027546, 2006b.

Lau, K. M., Kim, M. K., and Kim, K. M.: Asian summer monsoon anomalies induced by aerosol direct forcing: the role of the Tibetan Plateau, Clim Dyn, 26, 855–864, doi: 10.1007/s00382-006-0114-z, ~~2006(a).~~2006a.

Lau, W. K. and Kim, K. M.:~~Lau, K. M. and Kim, K. M.: Observational relationships between aerosol and Asian monsoon rainfall, and circulation, Geophys. Res. Lett., 33, D22101, doi: 10.1029/2006GL027546, 2006(b).~~

~~Lau, W. K. M., Kim, M. K., Kim, K. M., and Lee, W. S.: Enhanced surface warming and accelerated snow melt in the Himalayas and Tibetan Plateau induced by absorbing aerosols, Environ. Res. Lett., 5, 25204, doi: 10.1088/1748-9326/5/2/025204, 2010.~~

~~Lau, W. K. M. and Kim, K. M.: Impacts of aerosols on the Asian Monsoon – An interim assessment, Climate Change: Multidecadal and Beyond, 361–376, doi: 10.1142/9789814579933_0023, 2016.~~

Lau, W. K. M., Kim, K. M., Shi, J. J., Matsui, T., Chin, M., Tan, Q., Peters-Lidard, C., and Tao, W. K.: Impacts of aerosol monsoon interaction on rainfall and circulation over Northern India and the Himalaya Foothills, Clim Dyn, 49, 1945–1960, doi: 10.1007/s00382-016-3430-y, 2017.

Lau, W.K.M.; Kim, K. M. Impact of Snow Darkening by Deposition of Light-Absorbing Aerosols on Snow Cover in the Himalayas–Tibetan Plateau and Influence on the Asian Summer Monsoon: A Possible Mechanism for the Blanford Hypothesis., Atmosphere, 9, 438, doi: 10.3390/atmos9110438,10.3390/atmos9110438, 2018.

Lau, W. K. M., Kim, K. M., Lee, W. Shi, J. S., Bhawar, R. L., Kim, M. J., Matsui, T., Chin, M., Tan, Q., Peters-Lidard, C., and Tao, W. K.: Impacts of aerosol–monsoon interaction on rainfall and circulation over Northern India and the Himalaya Foothills, Clim Dyn, 49, 1945–1960, doi:10.1007/s00382-016-3430-y, 2017.

Lau, W. K. M., Kim, M. K., Kim, K. M., and Lee, W. S.: Enhanced surface warming and accelerated snow melt in the Himalayas and Tibetan Plateau induced by absorbing aerosols, Environ. Res. Lett., 5, 25204, doi:10.1088/1748-9326/5/2/025204, 2010.

Lee, W. S., Bhawar, R. L., Kim, M. K., and Sang, J.: Study of aerosol effect on accelerated snow melting over the Tibetan Plateau during boreal spring, Atmospheric Environment, 75, 113–122, doi:-10.1016/j.atmosenv.2013.04.004, 2013.

Li, C., Bosch, C., Kang, S., Andersson, A., Chen, P., Zhang, Q., Cong, Z., Chen, B., Qin, D., and Gustafsson, Ö.: Sources of black carbon to the Himalayan–Tibetan Plateau glaciers, Nat Commun, 7, 4825, doi:-10.1038/ncomms12574, 2016.

Li, M., Zhang, Q., Kurokawa, J.-. i., Woo, J.-. H., He, K., Lu, Z., Ohara, T., Song, Y., Streets, D. G., Carmichael, G. R., Cheng, Y., Hong, C., Huo, H., Jiang, X., Kang, S., Liu, F., Su, H., and Zheng, B.: MIX: a mosaic Asian anthropogenic emission inventory under the international collaboration framework of the MICS-Asia and HTAP, Atmos. Chem. Phys., 17, 935–963, doi:-10.5194/acp-17-935-2017, 2017.

Li, R.,., and Q. L. Min, 2010:Q. L.: Impacts of mineral dust on the vertical structure of precipitation, J. Geophys. Res., 115, D0920311337, doi:10.1029/2009JD011925, 2010.

Li, R., X. Dong, J.X., Guo, Y.J., Fu, Y.., Zhao, C., Wang, Q.Y., and Min, 2017:Q.: The implications of dust ice nuclei effect on cloud top temperature in a complex mesoscale convective system, Scientific Reports, Sci Rep, 7: 13826, , 291, doi:10.1038/s41598-017-12681-0, 2017.

Li, R., ~~W. ~~Shao, ~~J.~~W., Guo, ~~Y.~~J., Fu, ~~G. Liu, ~~Y.~~.~~., Wang, ~~W.~~Y., Liu, G., Zhou, R., and Li, ~~2019:~~W.: A Simplified Algorithm to Estimate Latent Heating Rate Using Vertical Rainfall Profiles ~~over~~Over the Tibetan Plateau, J. Geophys. Res. Atmos., 124,~~DOI: https://~~ 942–963, doi~~.org/~~:10.1029/2018JD029297, 2019.

Lin, C., Chen, D., Yang, K., and Ou, T.: Impact of model resolution on simulating the water vapor transport through the central Himalayas: implication for models' wet bias over the Tibetan Plateau, Clim Dyn, 51, 3195–3207, doi:10.1007/s00382-018-4074-x, 2018.

Liu, P., Tsimpidi, A. P., Hu, Y., Stone, B., Russell, A. G., and Nenes, A.: Differences between downscaling with spectral and grid nudging using WRF, Atmos. Chem. Phys., 12, 3601–3610, doi:~~-~~10.5194/acp-12-3601-2012, 2012.

Liu, Y., Sato, Y., Jia, R., Xie, Y., Huang, J., and Nakajima, T.: Modeling study on the transport of summer dust and anthropogenic aerosols over the Tibetan Plateau, Atmos. Chem. Phys~~. Discuss~~., 15, ~~15005–15037~~12581–12594, doi:~~—~~10.5194/~~acpd~~acp-15-~~15005~~12581-2015, 2015.

Liu, Z., Ming, Y., Zhao, C., Lau, N. C., Guo, J., Bollasina, M., and Yim, S. H. L.: Contribution of local and remote anthropogenic aerosols to a record-breaking torrential rainfall event in Guangdong Province, China, Atmos. Chem. Phys., 20, 223–241, doi:10.5194/acp-20-223-2020, 2020.

Lu, Z., Streets, D. G., Zhang, Q., and Wang, S.: A novel back-trajectory analysis of the origin of black carbon transported to the Himalayas and Tibetan Plateau during 1996-2010, Geophys. Res. Lett., 39, n/a-n/a, doi:~~-~~10.1029/2011GL049903, 2012.

Lüthi, Z. L., Škerlak, B., Kim, S~~.~~. W., Lauer, A., Mues, A., Rupakheti, M., and Kang, S.: Atmospheric brown clouds reach the Tibetan Plateau by crossing the Himalayas, Atmos. Chem. Phys., 15, 6007–6021, doi:~~-~~10.5194/acp-15-6007-2015, 2015.

Lutz, A. F., Immerzeel, W. W., Shrestha, A. B., and Bierkens, M. F. P.: Consistent increase in High Asia's runoff due to increasing glacier melt and precipitation, Nature Clim Change, 4, 587–592, doi:~~-~~10.1038/nclimate2237, 2014.

Marinoni, A., Cristofanelli, P., Laj, P., Duchi, R., Calzolari, F., Decesari, S., Sellegri, K., Vuillermoz, E., Verza, G. P., and Villani, P.: Aerosol mass and black carbon concentrations, a two year record at NCO-P (5079 m, Southern Himalayas), Atmos. Chem. Phys., 10, 8551–8562, doi:~~-~~10.5194/acp-10-8551-2010, 2010.

Menon, S., Koch, D., Beig, G., Sahu, S., Fasullo, J., and Orlikowski, D.: Black carbon aerosols and the third polar ice cap, Atmos. Chem. Phys., 10, 4559–4571, doi:~~-~~10.5194/acp-10-4559-2010, 2010.

Ming, J., Cachier, H., Xiao, C., Qin, D., Kang, S., Hou, S., and Xu, J.: Black carbon record based on a shallow Himalayan ice core and its climatic implications, Atmos. Chem. Phys., 8, 1343–1352, 2008.

Ming, J., Xiao, C., Cachier, H., Qin, D., Qin, X., Li, Z., and Pu, J.: Black Carbon (BC) in the snow of glaciers in west China and its potential effects on albedos, Atmospheric Research, 92, 114–123, doi:-10.1016/j.atmosres.2008.09.007, 2009.

Mlawer, E. J., Taubman, S. J., Brown, P. D., Iacono, M. J., and Clough, S. A.: Radiative transfer for inhomogeneous atmospheres: RRTM, a validated correlated - k model for the longwave, J. Geophys. Res., 102, 16663–16682, doi:10.1029/97JD00237, 1997.

Morrison, H., Thompson, G., and Tatarskii, V.: Impact of Cloud Microphysics on the Development of Trailing Stratiform Precipitation in a Simulated Squall Line: Comparison of One- and TwoMomentTwo-Moment Schemes, Mon. WeatherWea. Rev., 137, 991–1007, doi:10.1175/2008MWR2556.1, 2009.

Nakanishi, M. and Niino, H.: An Improved Mellor–Yamada Level-3 Model: Its Numerical Stability and Application to a Regional Prediction of Advection Fog, Boundary-Layer Meteorol, 119, 397–407, doi:10.1007/s10546-005-9030-8, 2006.

Oleson, K. W., Lawrence, D. M., Bonan, G. B., Flanner, M. G., Kluzek, E., Lawrence, P. J., Levis, S., Swenson, S. C., Thornton, P. E., Dai, A., Decker, M., Dickinson, R., Feddema, J., Heald, C. L., Hoffman, F., Lamarque, J.-. F., Mahowald, N., Niu, G.-. Y., Qian, T., Randerson, J., Running, S., Sakaguchi, K., Slater, A., Sto ̈ckliStockli, R., Wang, A., Yang, Z.-. L., Zeng, X., and Zeng, X.: Tech- nicalTechnical Description of version 4.0 of the Community Land Model (CLM), Tech. Rep. NCAR/TN-478 + +STR, National Center for Atmospheric Research, Boulder, Colorado, USA, 2010.

Prasad, A. K. and Singh, R. P.: Comparison of MISR-MODIS aerosol optical depth over the Indo-Gangetic basin during the winter and summer seasons (2000–2005), Remote Sensing of Environment, 107, 109–119, doi:-10.1016/j.rse.2006.09.026, 2007.

Qian, Y., Flanner, M. G., Leung, L. R., and Wang, W.: Sensitivity studies on the impacts of Tibetan Plateau snowpack pollution on the Asian hydrological cycle and monsoon climate, Atmos. Chem. Phys., 11, 1929–1948, doi:-10.5194/acp-11-1929-2011, 2011.

Qian, Y., Yasunari, T. J., Doherty, S. J., Flanner, M. G., Lau, W. K. M., Ming, J., Wang, H., Wang, M., Warren, S. G., and Zhang, R.: Light-absorbing particles in snow and ice: Measurement and modeling of climatic and hydrological impact, Adv. Atmos. Sci., 32, 64–91, doi:-10.1007/s00376-014-0010-0, 2015.

Qiu, J.: China: The third pole, Nature, 454, 393–396, doi:~~-~~10.1038/454393a, 2008.

Ramanathan, V. and Carmichael, G.: Global and regional climate changes due to black carbon, Nature Geosci, 1, 221–227, doi:10.1038/ngeo156, 2008.

Ramanathan, V., Ramana, M. V., Roberts, G., Kim, D., Corrigan, C., Chung, C., and Winker, D.: Warming trends in Asia amplified by brown cloud solar absorption, Nature, 448, 575–578, doi:~~-~~10.1038/nature06019, 2007.

Sarangi, C., Qian, Y., Rittger, K., Bormann, K. J., Liu, Y., Wang, H., Lin, G., and Painter, T. H.: Impact of light-absorbing particles on snow albedo darkening and associated radiative forcing over high-mountain Asia: high-resolution WRF-Chem modeling and new satellite observations. Atmos. Chem. Phys., 19, 7105–7128, doi:10.5194/acp-19-7105-2019, 2019.

~~Ramanathan, V. and Carmichael, G.: Global and regional climate changes due to black carbon, Nature Geosci, 1, 221–227, doi: 10.1038/ngeo156, 2008.~~

Seaman, N. L., Stauffer, D. R., and Lario-Gibbs, A. M.: A Multiscale Four-Dimensional Data Assimilation System Applied in the San Joaquin Valley during SARMAP. Part I: Modeling Design and Basic Performance Characteristics, J. Appl. Meteor., 34, 1739–1761, doi: 10.1175/1520-0450(1995)034<1739:AMFDDA>2.0.CO;2, 1995.

Shi, X., Wang, Y., and Xu, X.: Effect of mesoscale topography over the Tibetan Plateau on summer precipitation in China: A regional model study, Geophys. Res. Lett., 35, 255, doi:10.1029/2008GL034740, 2008.

Singh, P. and Bengtsson, L.: Hydrological sensitivity of a large Himalayan basin to climate change, Hydrol. Process., 18, 2363–2385, doi:~~-~~10.1002/hyp.1468, 2004.

Skamarock, W. C., Klemp, J. B., Dudhia, J., Gill, D. O., Barker, D. M., Duda, M.~~ G~~., Huang, X. Y., Wang, W., and Powers, J. G.: A ~~description~~Description of the ~~advanced research~~Advanced Research WRF ~~version~~Version 3, NCAR ~~Tech.~~Technical Note, NCAR/TN-~~475~~468+STR~~, Natl. Cent. for Atmos. ,Res., Boulder, CO, USA, 8 pp.~~ available ~~online~~ at: http://~~www.mmm.ucar.edu/~~wrf~~/users~~-model.org/wrfadmin/docs/arw ~~v3~~v2.pdf, 2008.

Stauffer, D. R. and Seaman, N. L.: Use of Four-Dimensional Data Assimilation in a Limited-Area Mesoscale Model. Part I: Experiments with Synoptic-Scale Data, Mon. Wea. Rev., 118, 1250–1277, doi:~~-~~10.1175/1520-0493(1990)118<1250:UOFDDA>2.0.CO;2, 1990.

Wagner, J. S., ~~Vernekar, K. G., Sinha, S., Sadani, L. K., Sivaramakrishnan, S., Parasnis, S. S., Mohan, B., Dharmaraj, S., Patil, M. N., Pillai, J. S., and Murthy, B. S.: An overview of the land surface processes experiment (LASPEX) over a semi-arid region of India, Boundary-layer meteorology, 106, 561–572, 2003.~~

Gohm, A., and Rotach, M. W.: The Impact of Horizontal Model Grid Resolution on the Boundary Layer Structure over an Idealized Valley, Mon. Wea. Rev., 142, 3446–3465, doi:10.1175/MWR-D-14-00002.1, 2014.

Wang, X., Gong, P., Sheng, J., Joswiak, D. R., and Yao, T.: Long-range atmospheric transport of particulate Polycyclic Aromatic Hydrocarbons and the incursion of aerosols to the southeast Tibetan Plateau, Atmospheric Environment, 115, 124–131, doi: 10.1016/j.atmosenv.2015.04.050, 2015.

Wiedinmyer, C., Akagi, S. K., Yokelson, R. J., Emmons, L. K., Al-Saadi, J. A., Orlando, J. J., and Soja, A. J.: The Fire INventory from NCAR (FINN): a high resolution global model to estimate the emissions from open burning, Geosci. Model Dev., 4, 625–641, doi: 10.5194/gmd-4-625-2011, 2011.

Wu, G. X., Liu, Y. M., Liu, X., Duan, A. M., and Liang, X. Y.: How the heating over the Tibetan Plateau affects the Asian climate in summer, Chinese J. Atmos. Sci, 29, 47–56, 2005.

Wu, G., Liu, Y., Dong, B., Liang, X., Duan, A., Bao, Q., and Yu, J.: Revisiting Asian monsoon formation and change associated with Tibetan Plateau forcing: I. Formation, Clim Dyn, 39, 1169–1181, doi:-10.1007/s00382-012-1334-z, 2012.

Wu, G., Duan, A., and Liu, Y.: Atmospheric Heating Source Over the Tibetan Plateau and Its Regional Climate Impact, Oxford Research Encyclopedia of Climate Science, doi: 10.1093/acrefore/9780190228620.013.588, 2019.

Xia, X., Zong, X., Wu, G., Liu, Y., He, B., Bao, Q., Duan, A., and Jin, F.-F.: Thermal controls on the Asian summer monsoon, Scientific reports, 2, 404, doi:10.1038/srep00404, 2012.

Wu, G., Liu, Y., Zhang, Q., Duan, A., Wang, T., Wan, R., Liu, X., Li, W., Wang, Z., and Liang, X.: The Influence of Mechanical and Thermal Forcing by the Tibetan Plateau on Asian Climate, J. Hydrometeor., 8, 770–789, doi:10.1175/JHM609.1, 2007.

Wu, L., Su, H., and Jiang, J. H.: Regional simulation of aerosol impacts on precipitation during the East Asian summer monsoon, J. Geophys. Res. Atmos., 118, 6454–6467, doi:10.1002/jgrd.50527, 2013.

Wulf, H., Bookhagen, B., and Scherler, D.: Differentiating between rain, snow, and glacier contributions to river discharge in the western Himalaya using remote-sensing data and distributed hydrological modeling, Advances in Water Resources, 88, 152–169, doi:10.1016/j.advwatres.2015.12.004, 2016.

Cong, Z., Chen, H., Kang, S., and Wang, P.: Baseline continental aerosol over the central Tibetan plateau and a case study of aerosol transport from South Asia, Atmospheric Environment, 45, 7370–7378, doi: 10.1016/j.atmosenv.2011.07.067, 2011.

Xu, B., Cao, J., Hansen, J., Yao, T., Joswia, D. R., Wang, N., Wu, G., Wang, M., Zhao, H., Yang, W., Liu, X., and He, J.: Black soot and the survival of Tibetan glaciers, PNAS, 106, 22114–22118, doi: 10.1073/pnas.0910444106, 2009.

Yang, J., Kang, S., Ji, Z., and Chen, D.: Modeling the Origin of Anthropogenic Black Carbon and Its Climatic Effect Over the Tibetan Plateau and Surrounding Regions, J. Geophys. Res. Atmos., 123, 671–692, doi:-10.1002/2017JD027282, 2018.

Yasunari, T. J., Bonasoni, P., Laj, P., Fujita, K., Vuillermoz, E., Marinoni, A., Cristofanelli, P., Duchi, R., Tartari, G., and Lau, K.-M.: Estimated impact of black carbon deposition during pre-monsoon season from Nepal Climate Observatory – Pyramid data and snow albedo changes over Himalayan glaciers, Atmos. Chem. Phys., 10, 6603–6615, doi:-10.5194/acp-10-6603-2010, 2010.

Ye, D.-. Z. and Wu, G.-. X.: The role of the heat source of the Tibetan Plateau in the general circulation, Meteorl. Atmos. Phys., 67, 181–198, doi:-10.1007/BF01277509, 1998.

Zängl, G., Egger, J., and Wirth, V.: Diurnal Winds in the Himalayan Kali Gandaki Valley. Part II: Modeling, Mon. Wea. Rev., 129, 1062–1080, doi:10.1175/1520-0493(2001)129<1062:DWITHK>2.0.CO;2, 2001.

Zaveri, R. A. and Peters, L. K.: A new lumped structure photochemical mechanism for large-scale applications, J. Geophys. Res., 104, 30387–30415, doi:-10.1029/1999JD900876, 1999.

Zaveri, R. A., Easter, R. C., Fast, J. D., and Peters, L. K.: Model for simulating aerosol interactionsSimulating Aerosol Interactions and chemistryChemistry (MOSAIC), J. Geophys. Res. Atmos., 113, 1591, doi:10.1029/2007JD008782, 2008.

Zhang, Aoqi, YunfeiA., Fu, YilunY., Chen, GuoshengY., Liu, G., and Xiangdong Zhang:, X.: Impact of the surface wind flow on precipitation characteristics over the southern Himalayas: GPM observations, Atmospheric Research, 202, (10), (2018).10–22, doi:10.1016/j.atmosres.2017.11.001, 2018.

Zhang, R., Wang, H., Qian, Y., Rasch, P. J., Easter, R. C., Ma, P.-. L., Singh, B., Huang, J., and Fu, Q.: Quantifying sources, transport, deposition, and radiative forcing of black carbon over the Himalayas and Tibetan Plateau, Atmos. Chem. Phys., 15, 6205–6223, doi: 10.5194/acp-15-6205-2015, 2015.

Zhang, R., Wang, Y., He, Q., Chen, L., Zhang, Y., Qu, H., Smeltzer, C., Li, J., Alvarado, L. M. A., Vrekoussis, M., Richter, A., Wittrock, F., and Burrows, J. P.: Enhanced trans-Himalaya pollution transport to the Tibetan Plateau by cut-off low systems, Atmos. Chem. Phys., 17, 3083–3095, doi:-10.5194/acp-17-3083-2017, 2017.

Zhang, Y., Kang, S., Cong, Z., Schmale, J., Sprenger, M., Li, C., Yang, W., Gao, T., Sillanpää, M., Li, X., Liu, Y., Chen, P., and Zhang, X.: Light-absorbing impurities enhance glacier albedo reduction in the southeastern Tibetan plateau, J. Geophys. Res. Atmos., 122, 6915–6933, doi:10.1002/2016JD026397, 2017.

Zhang, Y., Kang, S., Sprenger, M., Cong, Z., Gao, T., Li, C., Tao, S., Li, X., Zhong, X., Xu, M., Meng, W., Neupane, B., Qin, X., and Sillanpää, M.: Black carbon and mineral dust in snow cover on the Tibetan Plateau, The Cryosphere, 12, 413–431, doi:10.5194/tc-12-413-2018, 2018.

~~Zhao, C., Liu, X., Leung, L. R., Johnson, B., McFarlane, S. A., Gustafson, W. I., Fast, J. D., and Easter, R.: The spatial distribution of mineral dust and its shortwave radiative forcing over North Africa: modeling sensitivities to dust emissions and aerosol size treatments, Atmos. Chem. Phys., 10, 8821–8838, doi: 10.5194/acp-10-8821-2010, 2010.~~

~~Zhao, C., Liu, X., Leung, L. R., and Hagos, S.: Radiative impact of mineral dust on monsoon precipitation variability over West Africa, Atmos. Chem. Phys., 11, 1879–1893, doi: 10.5194/acp-11-1879-2011, 2011.~~

~~Zhao, C., Ruby Leung, L., Easter, R., Hand, J., and Avise, J.: Characterization of speciated aerosol direct radiative forcing over California, J. Geophys. Res. Atmos., 118, 2372–2388, doi: 10.1029/2012JD018364, 2013(a).~~

Zhao, C., Chen, S., Leung, L. R., Qian, Y., Kok, J., Zaveri, R., and Huang, J.: Uncertainty in modeling dust mass balance and radiative forcing from size parameterization, Atmos. Chem. Phys., 13, 10733–10753, doi:doi:10.5194/acp-13-10733-2013, ~~2013(b).~~2013b.

Zhao, C., Hu, Z., Qian, Y., Leung, L. R., Huang, J., Huang, M., Jin, J., Flanner, M., Zhang, R., Wang, H., Yan, H., Lu, Z., and Streets, D. G.: Simulating black carbon and dust and their radiative forcing in seasonal snow: a case study over North China with field campaign measurements, Atmos. Chem. Phys., 14, 11475–11491,~~ doi:~~ doi:10.5194/acp-14-11475-2014, 2014.

Zhao, C., Huang, M., Fast, J. D., Berg, L. K., Qian, Y., Guenther, A., Gu, D., Shrivastava, M., Liu, Y., and Walters, S.: Sensitivity of biogenic volatile organic compounds to land surface parameterizations and vegetation distributions in California, Geosci. Model Dev, 9, 1959–1976, doi:10.5194/gmd-9-1959-2016, 2016.

Zhao, C., Liu, X., and Leung, L. R.: Impact of the Desert dust on the summer monsoon system over Southwestern North America, Atmos. Chem. Phys., 12, 3717–3731, doi:10.5194/acp-12-3717-2012, 2012.

Zhao, C., Liu, X., Leung, L. R., and Hagos, S.: Radiative impact of mineral dust on monsoon precipitation variability over West Africa, Atmos. Chem. Phys., 11, 1879–1893, doi:10.5194/acp-11-1879-2011, 2011.

Zhao, C., Liu, X., Leung, L. R., Johnson, B., McFarlane, S. A., Gustafson, W. I., Fast, J. D., and Easter, R.: The spatial distribution of mineral dust and its shortwave radiative forcing over North Africa: modeling sensitivities to dust emissions and aerosol size treatments, Atmos. Chem. Phys., 10, 8821–8838, doi:10.5194/acp-10-8821-2010, 2010.

Zhao, C., Ruby Leung, L., Easter, R., Hand, J., and Avise, J.: Characterization of speciated aerosol direct radiative forcing over California, J. Geophys. Res. Atmos., 118, 2372–2388, doi:10.1029/2012JD018364, 2013a.

Zhao, P., Zhou, X., Chen, J., Liu, G., and Nan, S.: Global climate effects of summer Tibetan Plateau, Science Bulletin, 64, 1–3, doi:10.1016/j.scib.2018.11.019, 2019.

Zhao, Z., Cao, J., Shen, Z., Xu, B., Zhu, C., Chen, L. W. A., Su, X., Liu, S., Han, Y., Wang, G., and Ho, K.: Aerosol particles at a high-altitude site on the Southeast Tibetan Plateau, China: Implications for pollution transport from South Asia, J. Geophys. Res. Atmos., 118, 11,360-11,375, doi:10.1002/jgrd.50599, 2013.

~~Zhang, Y. L., S. Kang, Z. Cong, J. Schmale, M. Sprenger, C. Li, W. Yang, T. Gao, M. Sillanpää, X. Li, Y. Liu, P. Chen, X. Zhang: Light-absorbing impurities enhance glacier albedo reduction in the southeastern Tibetan Plateau. Journal of Geophysical Research – Atmosphere, 122. Doi: 10.1002/2016JD026397, 2017.~~

~~Zhang, Y. L., S. Kang, M. Sprenger, Z. Cong, T. Gao, C. Li, S. Tao, X. Li, X. Zhong, M. Xu, W. Meng, B. Neupane, X. Qin, M. Sillanpää: Black carbon and mineral dust in snow cover on the Tibetan Plateau. The Cryosphere, 12: 413-431. Doi: 10.5194/tc-12-413-2018, 2018.~~

Zhong, S., Qian, Y., Zhao, C., Leung, R., Wang, H., Yang, B., Fan, Ji., Yan, H., Yang, X., and Liu, D.: Urbanization-induced urban heat island and aerosol effects on climate extremes in the Yangtze River Delta region of China, Atmos. Chem. Phys., 17, 5439–5457, doi:10.5194/acp-17-5439-2017, 2017.

Table 1. Summary of model configurations.

Description	Selection	References
Horizontal grid spacing	20 km (D1),4 km (D2)	
Grid dimensions	250×350, 300×400	
Topography	30 arcsec (USGS)	
Vertical layers	54 (roughly 17 layers below 2 km)	
Model top pressure	50 hPa	
Nesting approach	One-way	
Aerosol scheme	MOSAIC 8 bin	Zaveri et al., 2008
Gas-phase chemistry	CBM-Z	Zaveri and Peters, 1999
Long wave Radiation	RRTMG	Iacono et al., 2000; Zhao et al., 2011, 2013a
Short-wave Radiation	RRTMG	
Cloud Microphysics	Morrison 2-moment	Morrison et al., 2009
Cumulus Cloud	Kain-Fritsch	Kain, 2004
Planetary boundary layer	MYNN level 2.5	Nakanishi and Niino, 2006
Land surface	CLM	Oleson et al., 2010
Meteorological Forcing	ERA-Interim, 0.5°×0.66°, 6 hourly	

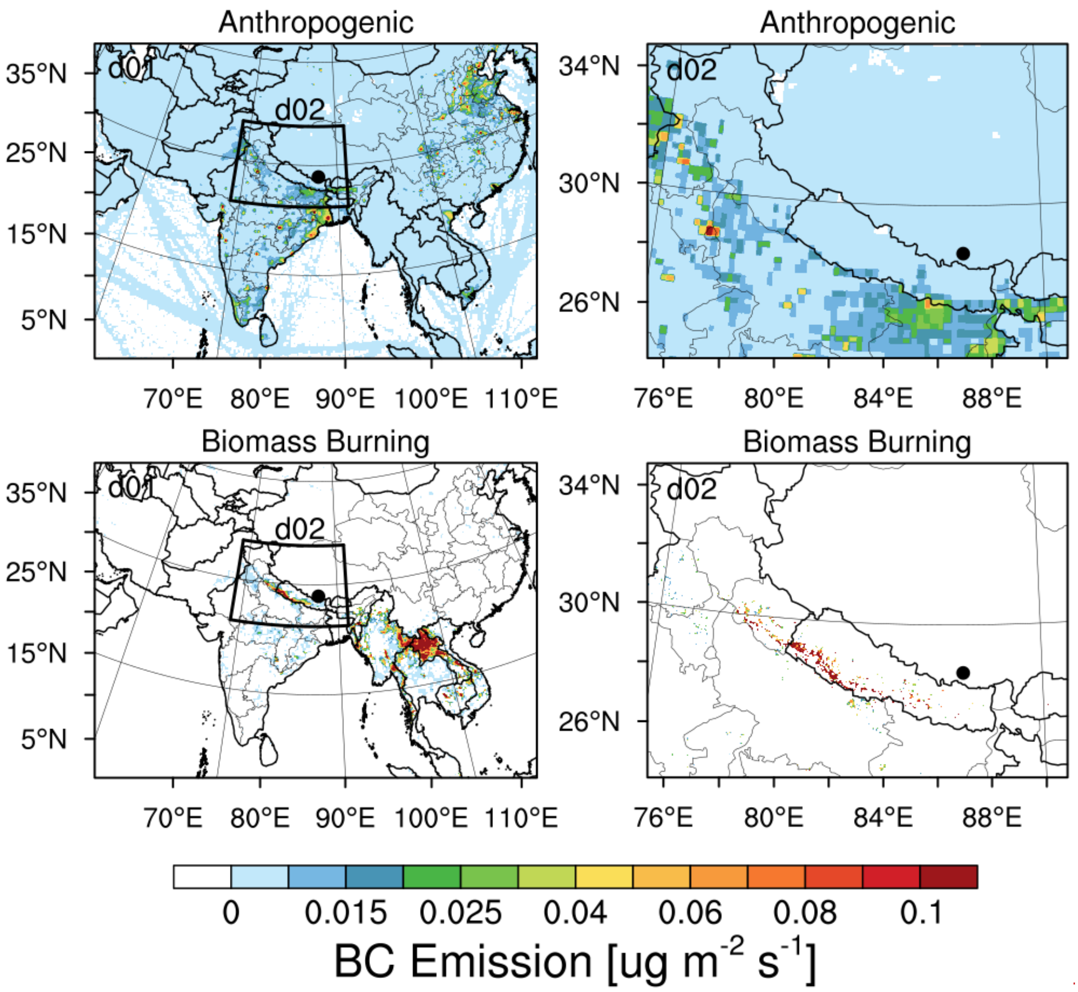
Anthropogenic
Anthropogenic
Biomass Burning
Biomass Burning
d01
d02
d02
d01
d02
d02
35°N
25°N
15°N
5°N
34°N
30°N
26°N
70°E
80°E
90°E
100°E
110°E
76°E
80°E
84°E
88°E
0
0.015
0.025
0.04
0.06
0.08
0.1
BC Emission [ug m-2 s-1]

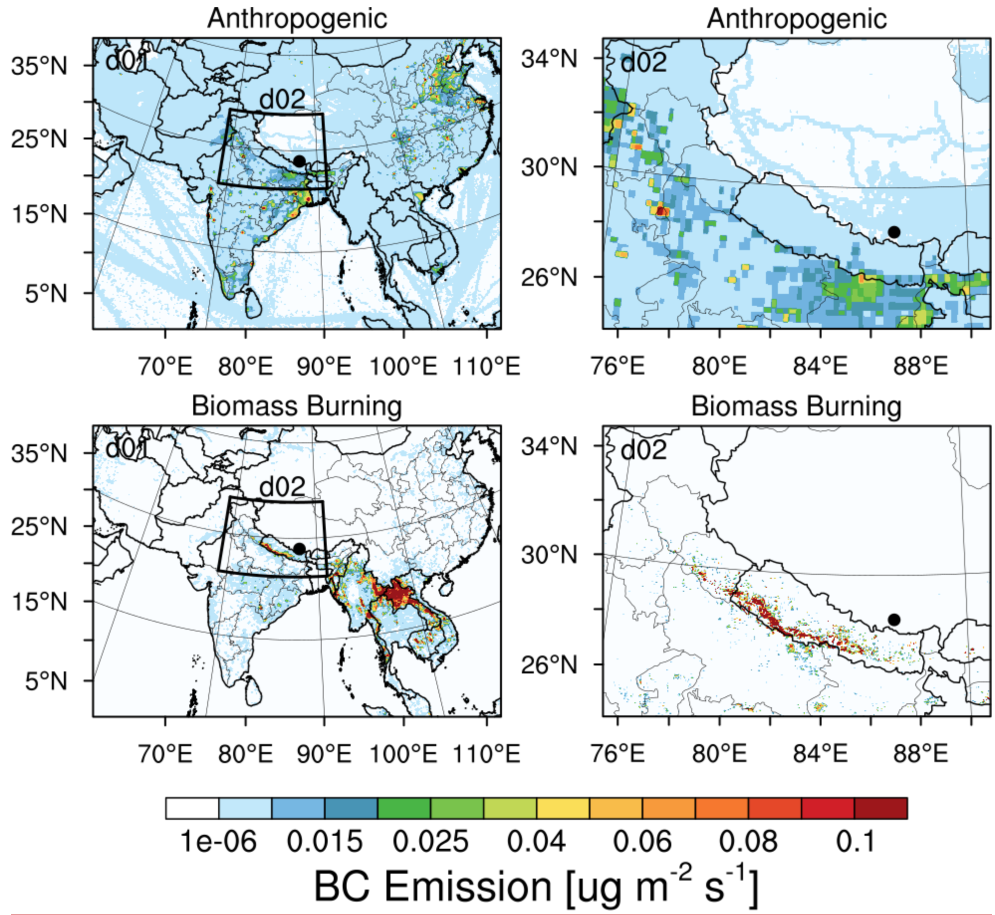

Figure 1. Anthropogenic and fire emissions over the entire simulated regions of 20 km and 4 km resolutions, the black dot represents the ~~Everest Observation Site~~Qomolangma Station (QOMS).

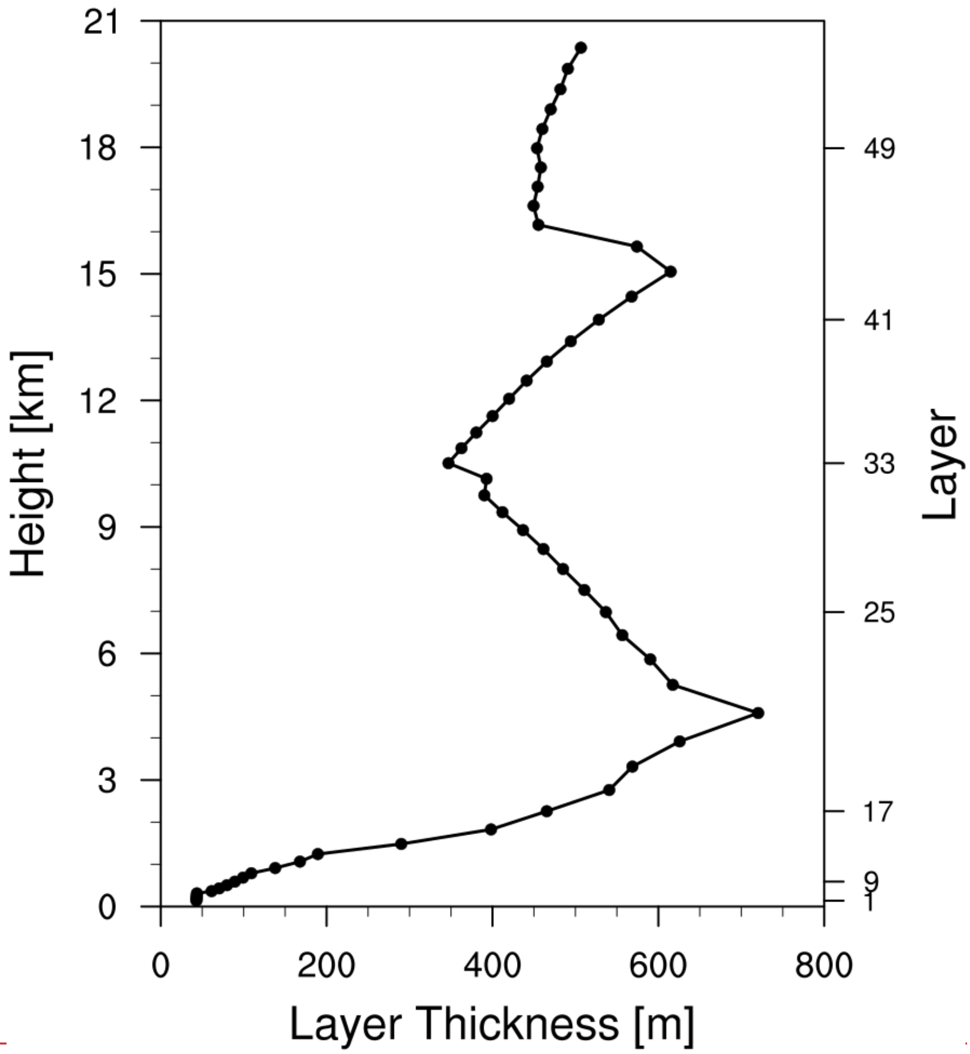

Height [km]
0
3
6
9
12
15
18
21
Layer Thickness [m]
0
200
400
600
800
Layer
1
9
17
25
33
41
49

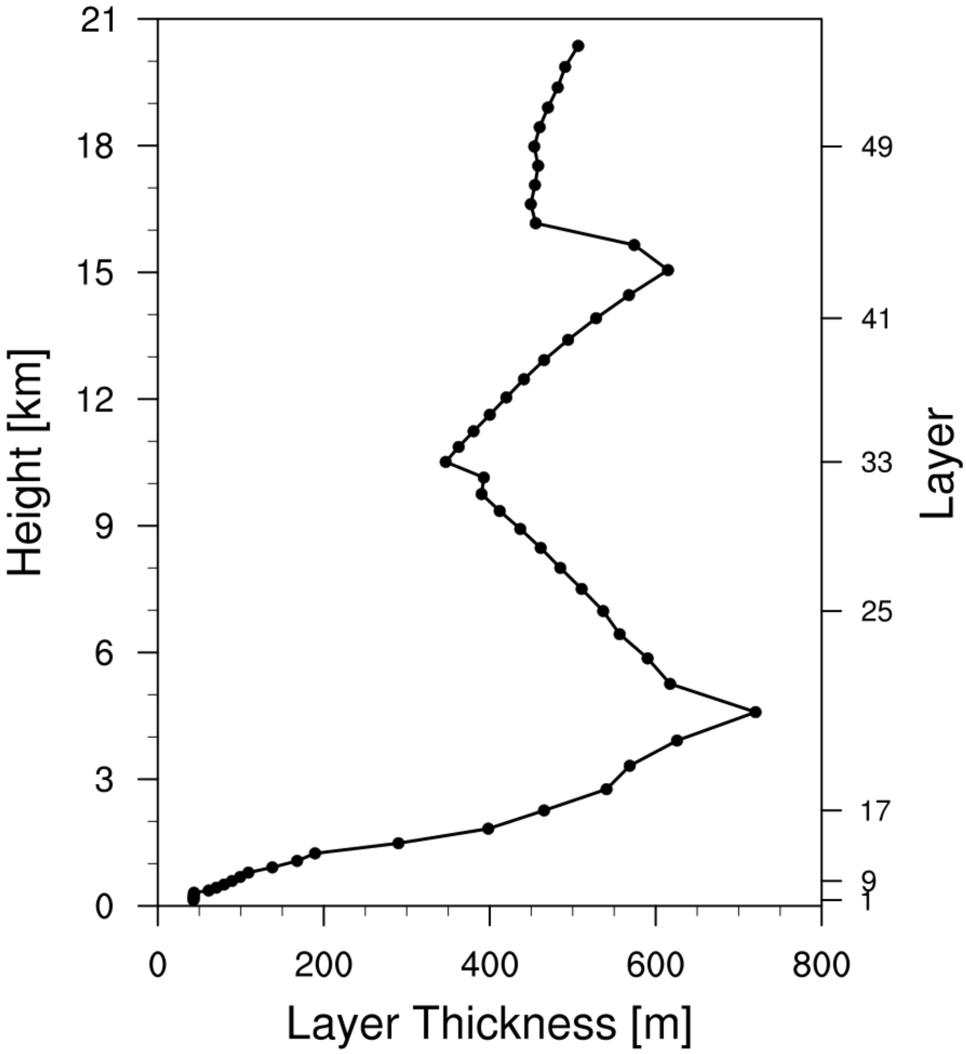

Figure 2. The thickness of each vertical layer in the simulations (54 layers in total).

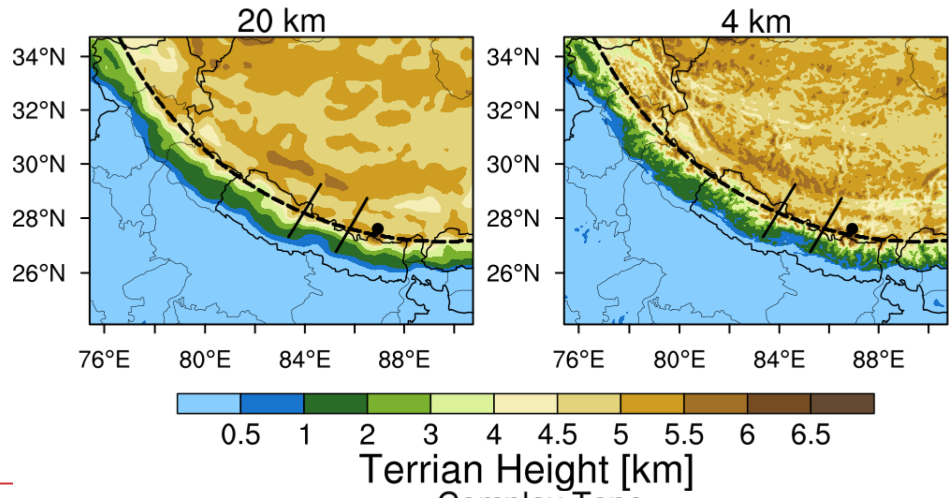

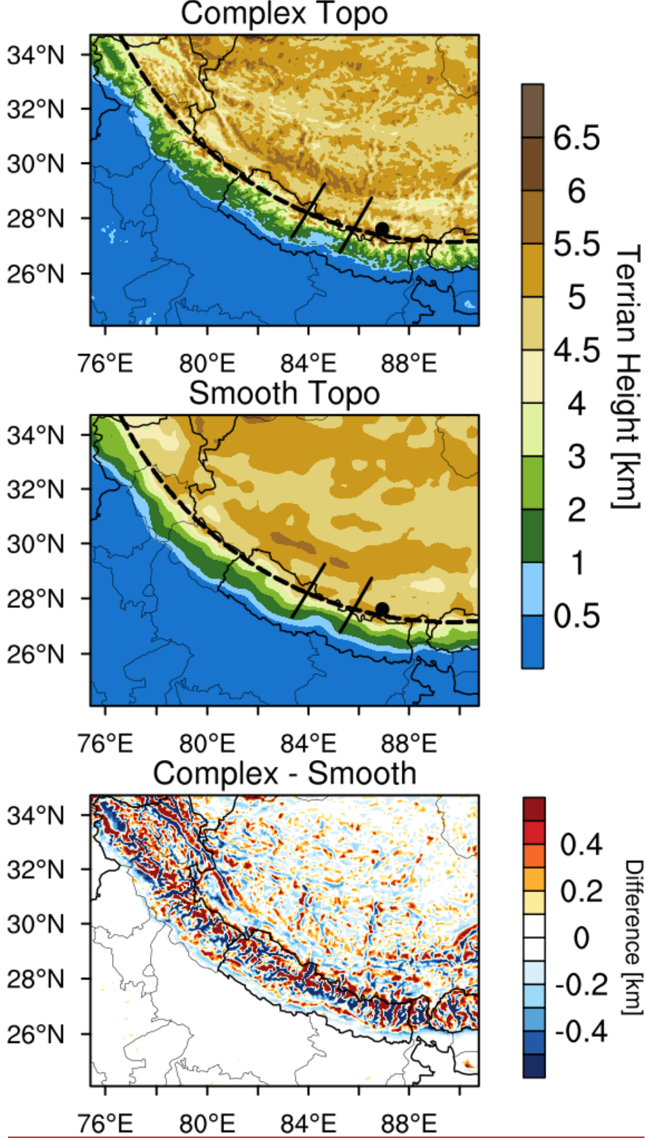

Figure 3. Spatial distributions of terrain height from the ~~simulations~~dataset at 20 km (Smooth Topo) and 4 km (Complex Topo) resolutions. The ~~two black lines and~~ one dash line and two solid lines represent the cross sections for analysis in the following.

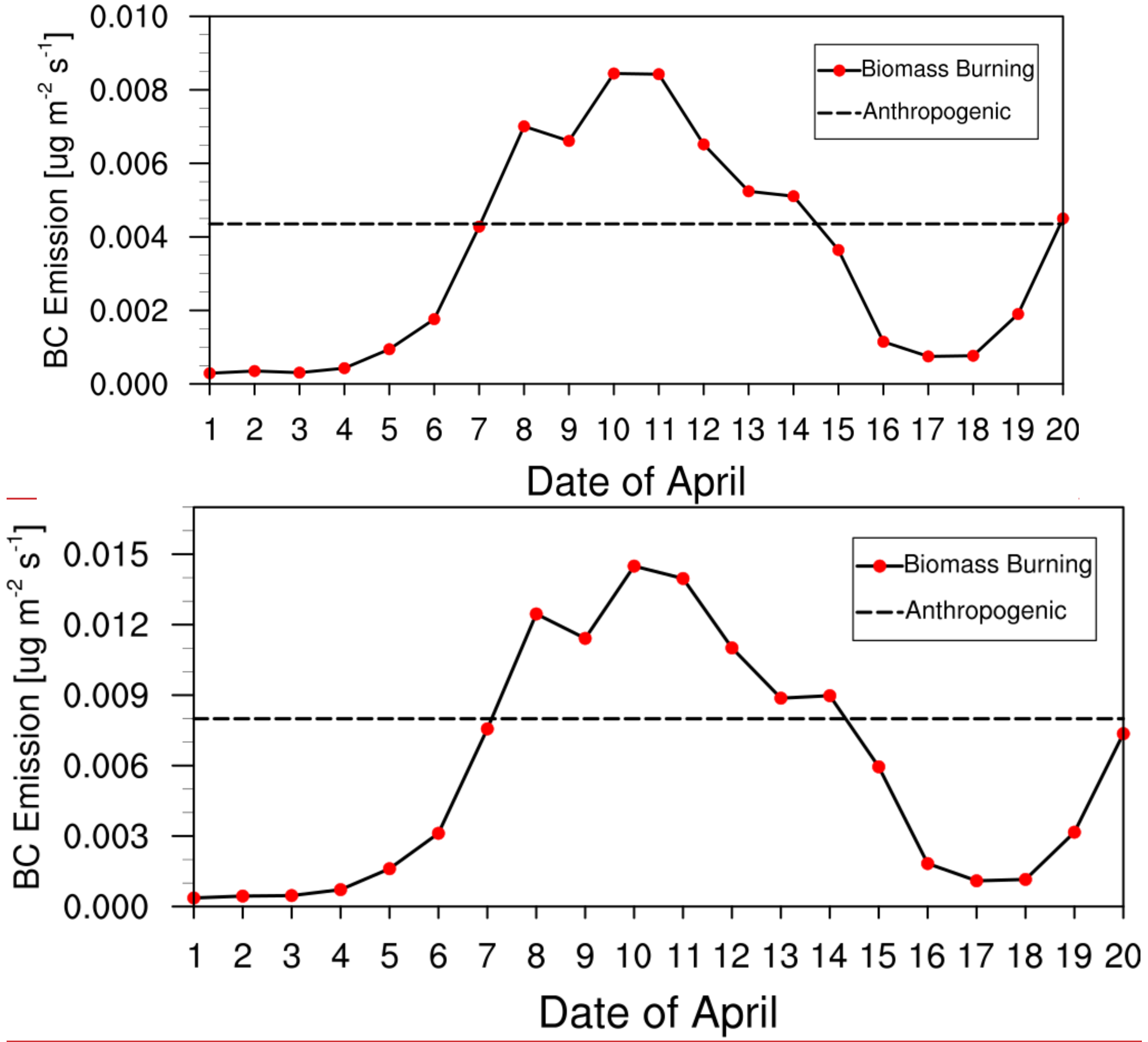

Figure 4. Time series of area-averaged daily fire emissions between 26°N and 29°N over the simulation domain at 4 km resolution (The dash line in the figure represents the anthropogenic ~~emission~~emissions).

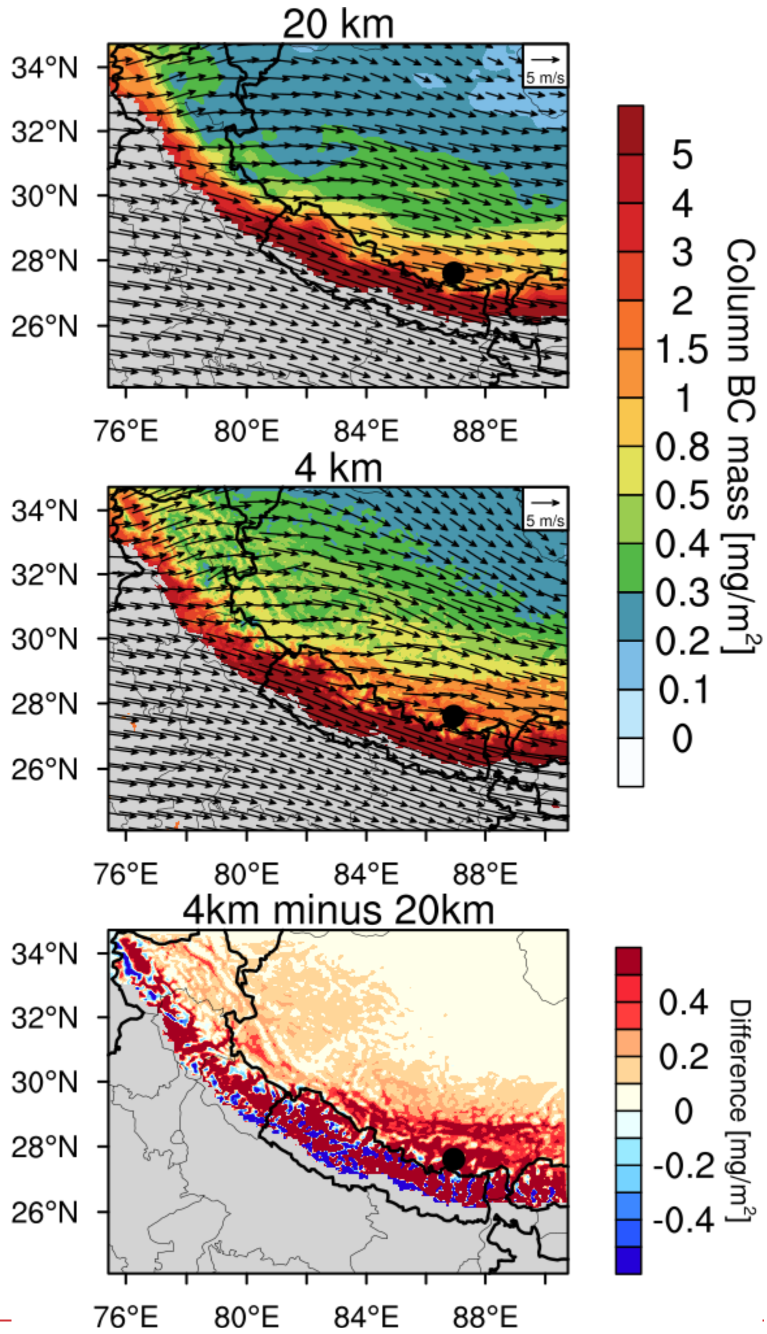
20 km
5 m/s
34°N
32°N
30°N
28°N
26°N
76°E
80°E
84°E
88°E
4 km
5 m/s
4km minus 20km
5
4
3
2
1.5
1
0.8
0.5
0.4
0.3
0.2
0.1
0
Column BC mass [mg/m2]
0.4
0.2
0
-0.2
-0.4
Difference [mg/m2]

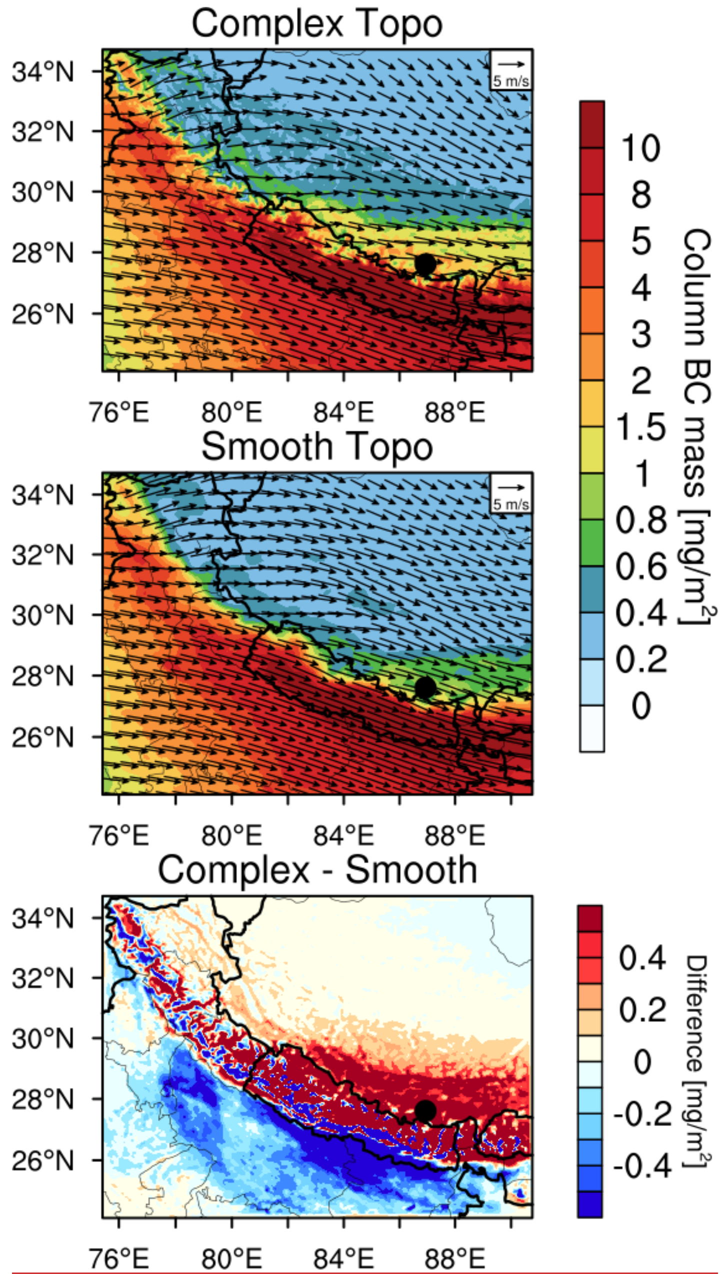

Figure 5. ~~Column~~Spatial distributions of column integrated BC mass ~~in the area with the terrain height larger than 0.5 km~~ and the wind ~~fields~~field at 500 hPa from the simulations ~~at 20 km~~with complex and ~~4 km horizontal resolutions~~smooth topography (Complex Topo and Smooth Topo) averaged for April ~~5~~1-20, 2016. The difference between the ~~simulations at 4 km and 20 km resolutions~~ two is also shown.

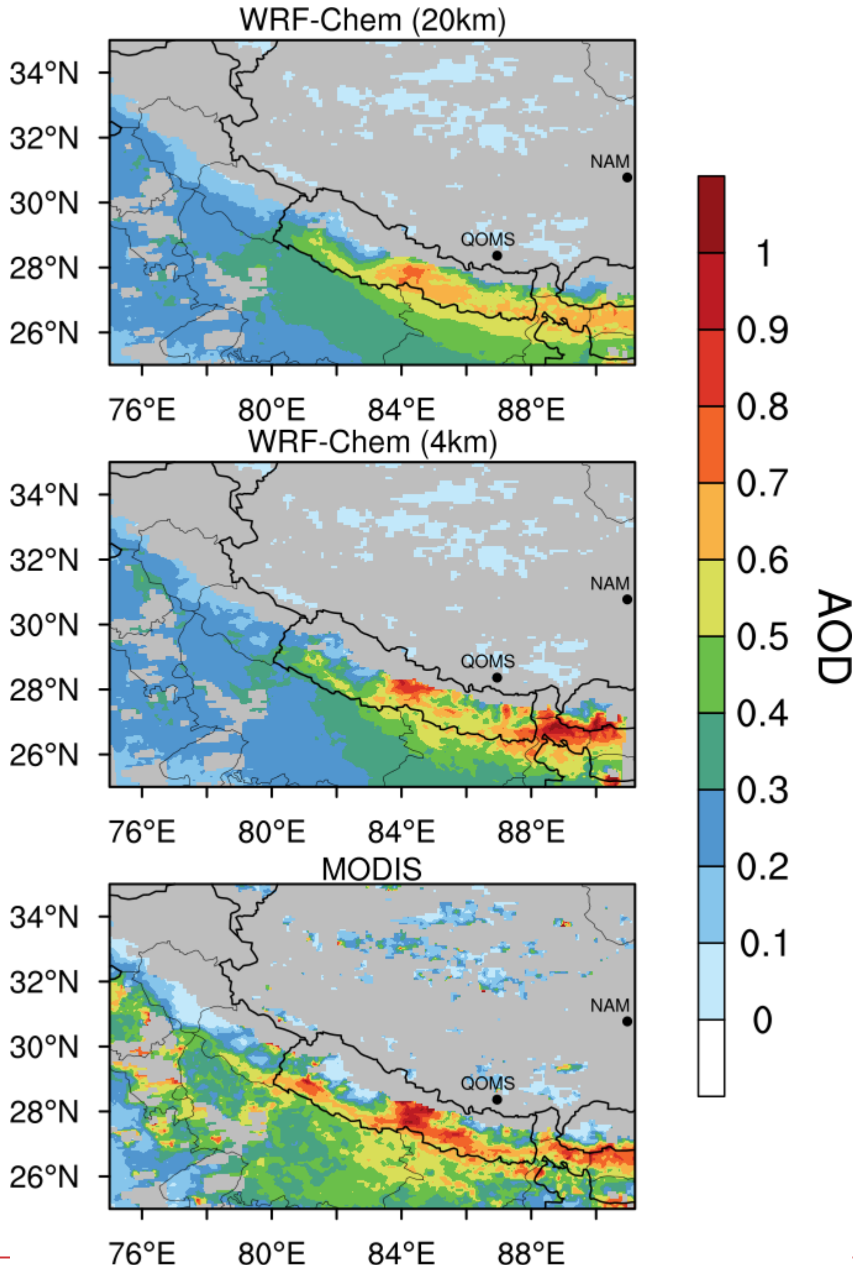
WRF-Chem (20km)
WRF-Chem (4km)
MODIS
34°N
32°N
30°N
28°N
26°N
76°E
80°E
84°E
88°E
NAM
QOMS
AOD
0
0.1
0.2
0.3
0.4
0.5
0.6
0.7
0.8
0.9
1

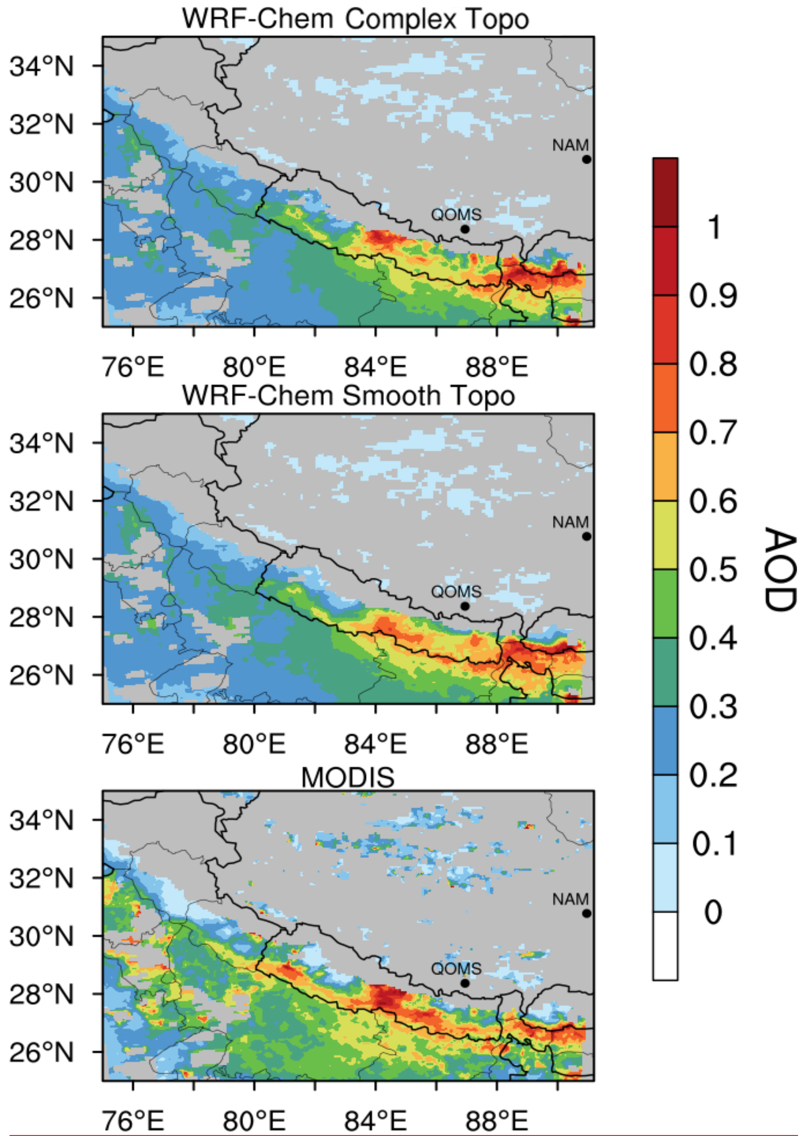

Figure 6. Spatial distributions of AOD from the MODIS retrievals and the simulations ~~at 4 km~~with complex and ~~20 km resolutions~~smooth topography averaged for April ~~5~~1-20, 2016. The two black dots represent the two AERONET sites over the TP (QOMS, 86.~~56~~94°E, 28.~~21~~36°N; NAM, 90.96°E, 30.77°N).

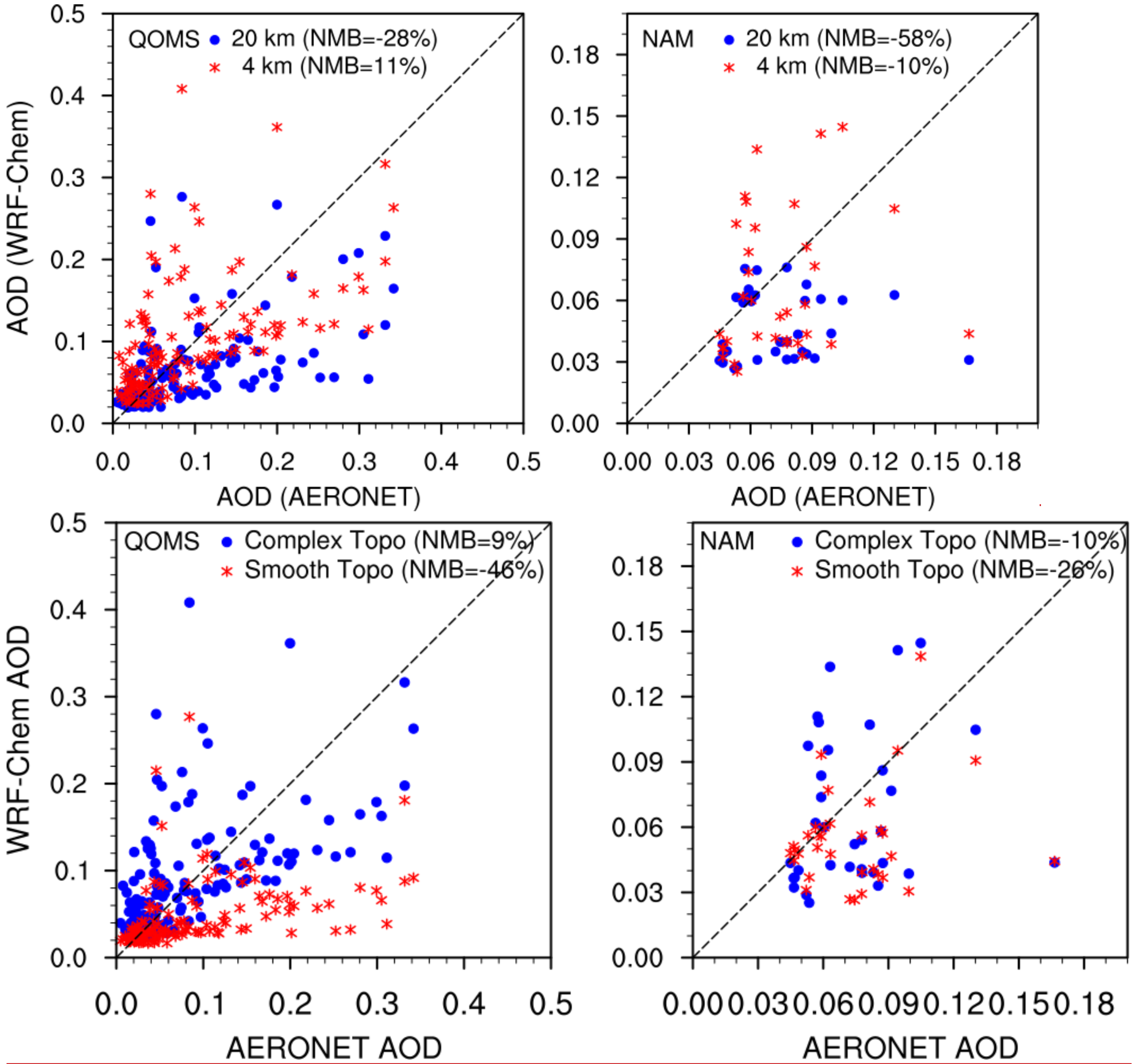

Figure 7. Hourly AOD from the measurements of AERONET and simulations by WRF-Chem at the two sites over the TP (QOMS, 86.~~56~~94°E, 28.~~21~~36°N; NAM, 90.96°E, 30.77°N) for April 1-20, 2016.

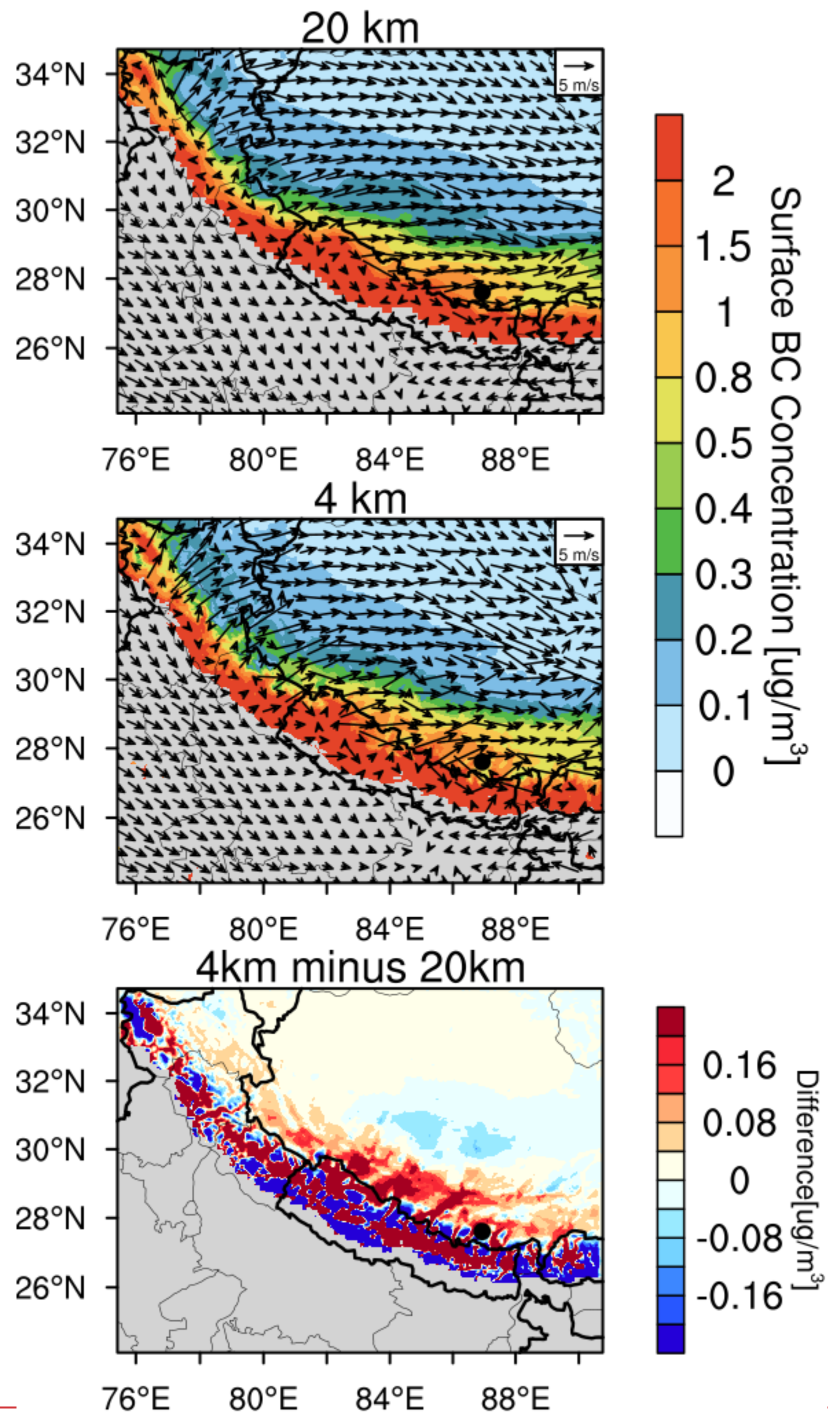

~~**Figure 8.** Spatial distributions of surface BC concentration and surface wind field over the inner domain from the simulations at 4 km and 20 km resolutions. The difference between the simulations at 4 km and 20 km resolutions is also shown.~~

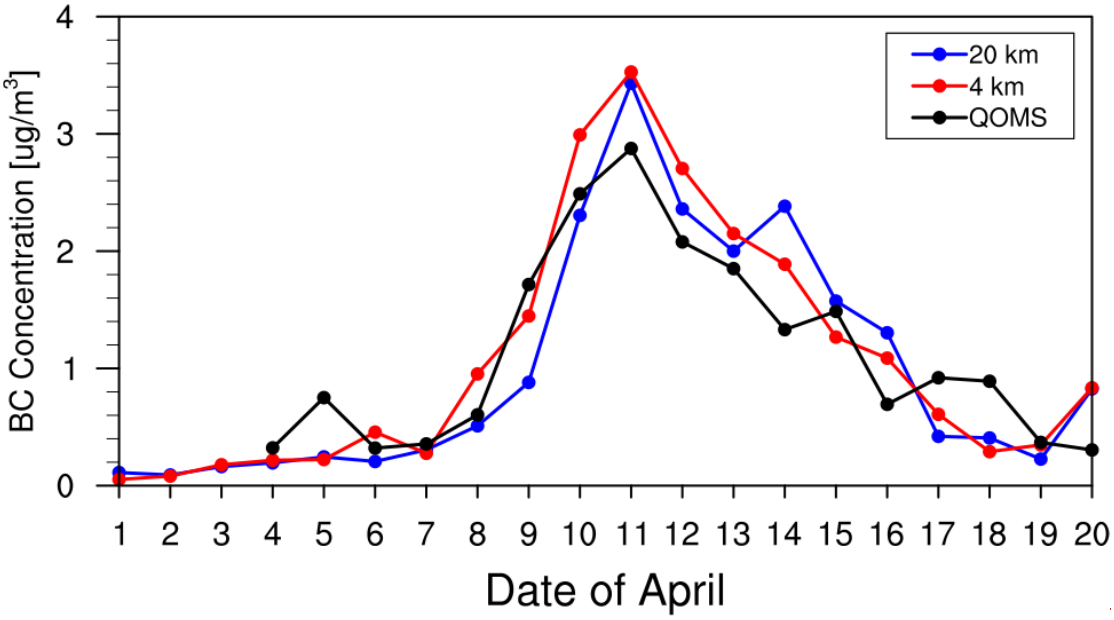

~~**Figure 9.**~~

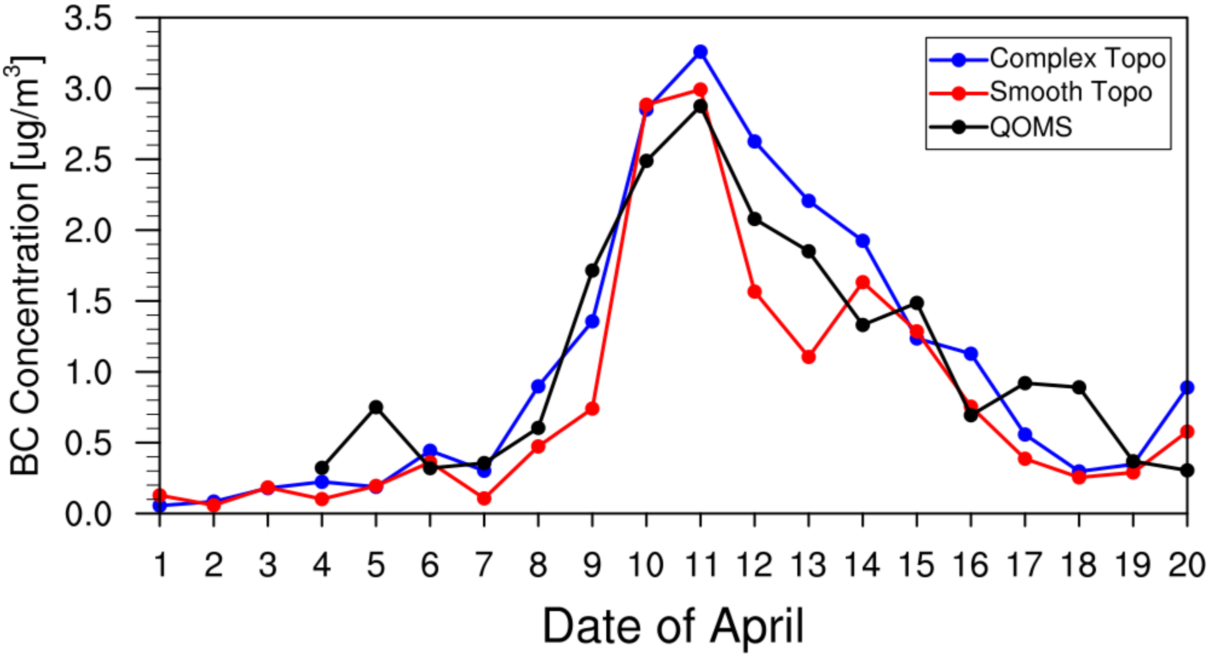

Figure 8. The simulated (colored) and observed (black) temporal variability of surface BC mass concentration at the measurement ~~site~~station during April 1-20 in 2016.

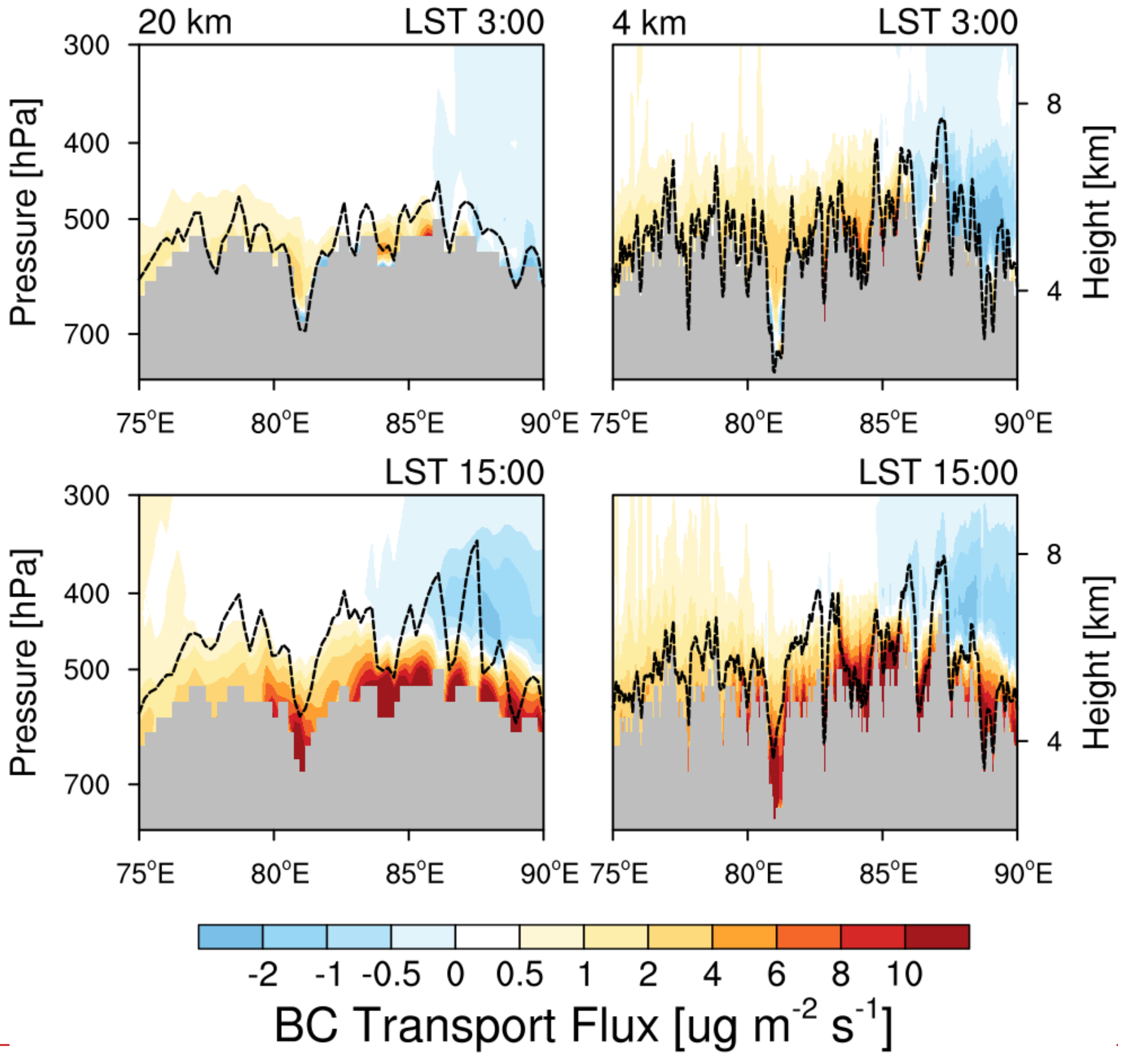
20 km
LST 3:00
4 km
LST 3:00
LST 15:00
LST 15:00
Pressure [hPa]
300
400
500
700
Height [km]
8
4
75°E
80°E
85°E
90°E
-2
-1
-0.5
0
0.5
1
2
4
6
8
10
BC Transport Flux [ug m-2 s-1]

2694

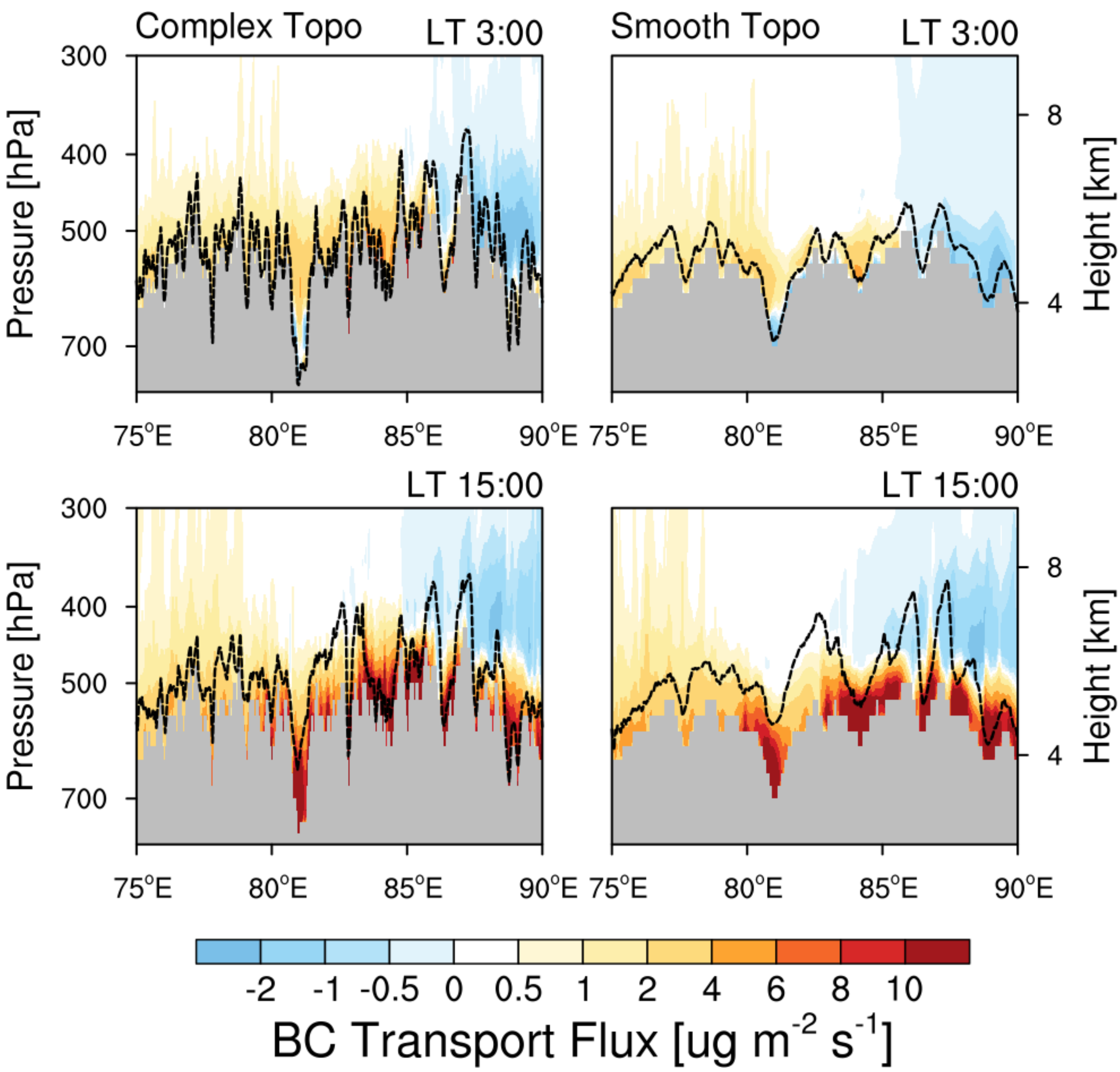

Figure ~~10~~9. Longitude-height cross section of BC transport flux along the cross line (shown as the black dash line in Fig. 3) from the simulations ~~at 20 km~~with complex and ~~4 km resolutions~~smooth topography at local time (LT) 03:00 and 15:00 averaged for April ~~5~~1-20. The PBL height along the cross section is shown here as the black dash line.

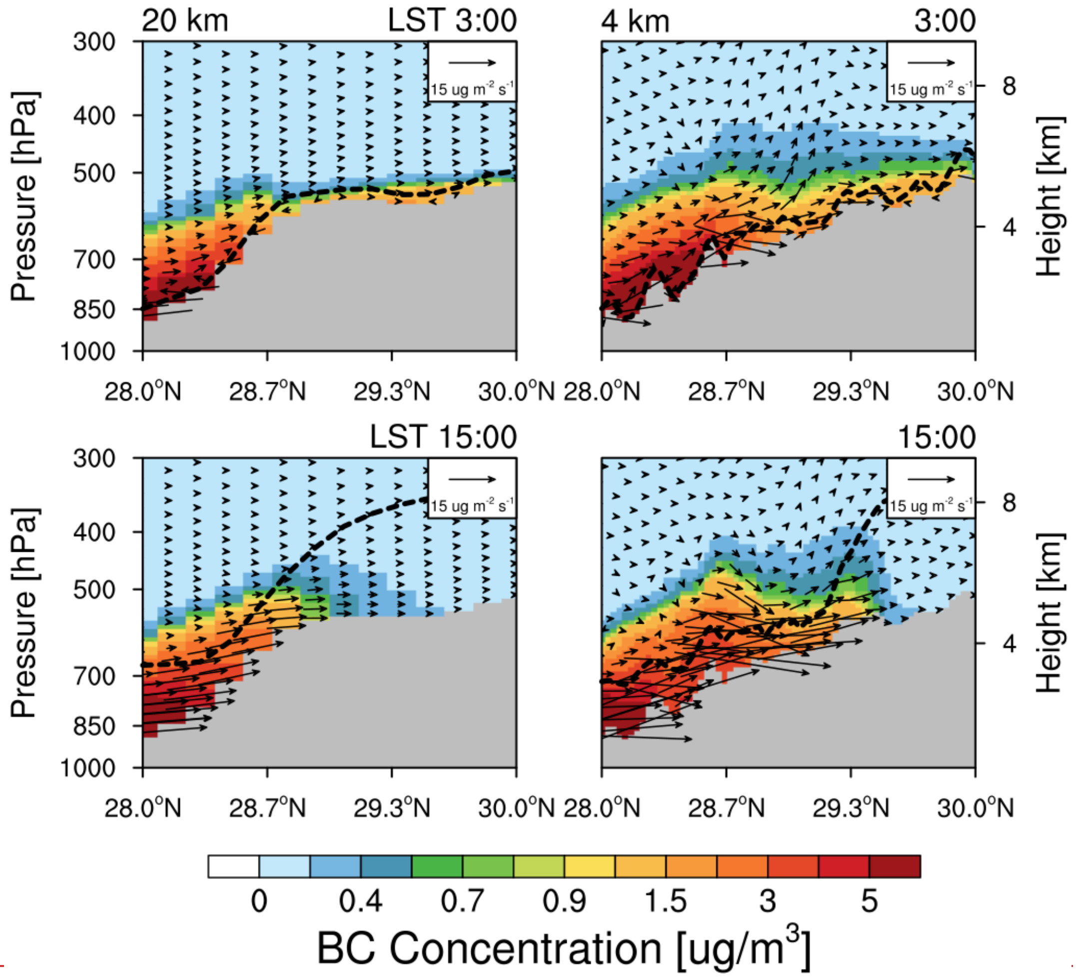

20 km
LST 3:00
4 km
3:00
LST 15:00
15:00
Pressure [hPa]
Height [km]
15 ug m-2 s-1
300
400
500
700
850
1000
8
4
28.0°N
28.7°N
29.3°N
30.0°N
0
0.4
0.7
0.9
1.5
3
5
BC Concentration [ug/m3]

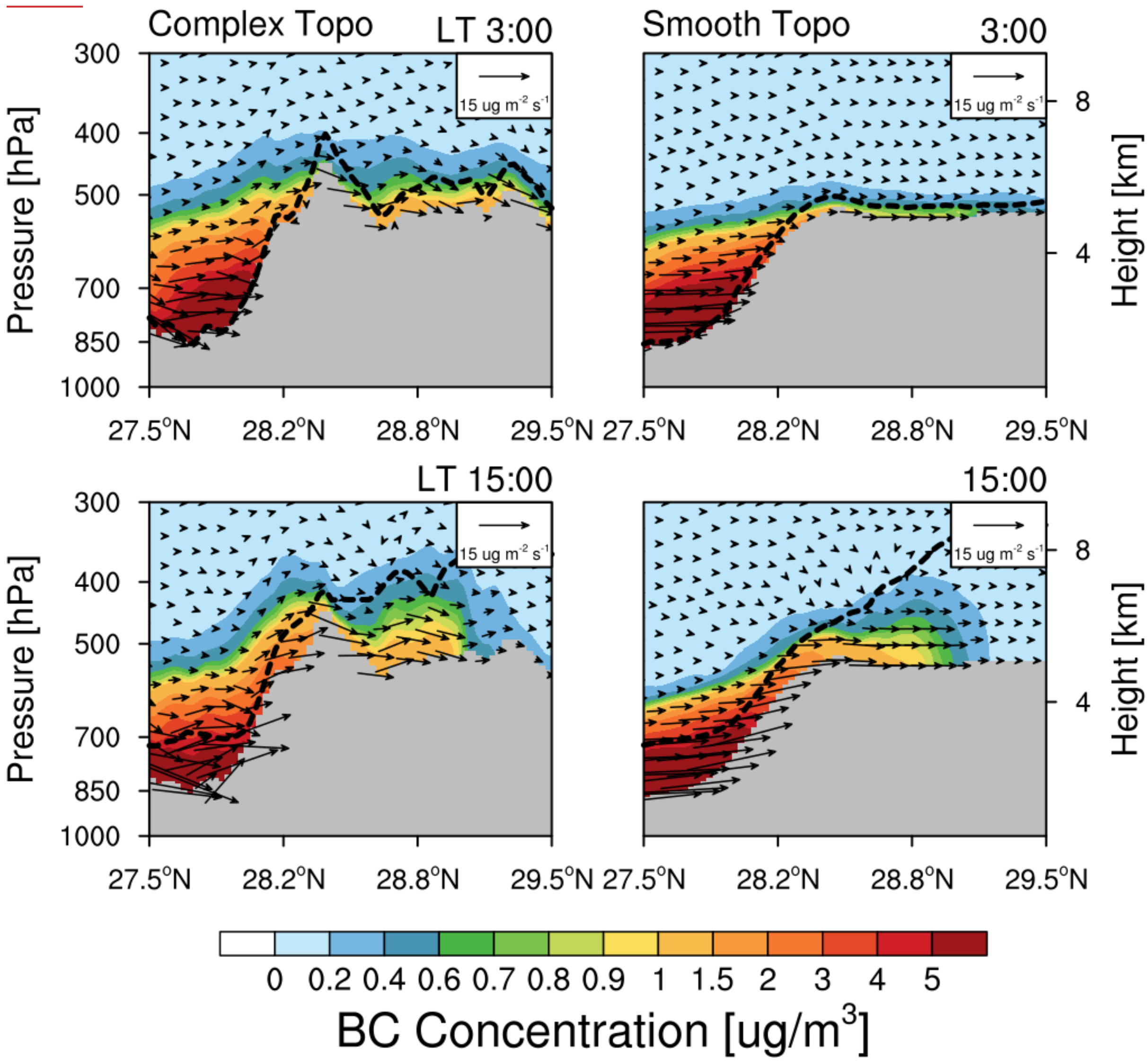

Figure ~~11~~10. Latitude-height cross section of BC flux (vector) ~~along~~across the ~~valley~~mountain (shown as the East black solid line in Fig.~~-~~3) from the simulations ~~at 20 km~~with complex and ~~4 km resolutions~~smooth topography at local time (LT) 03:00 and 15:00 averaged for April ~~5~~1-20, 2016. Contour represents the BC concentration.

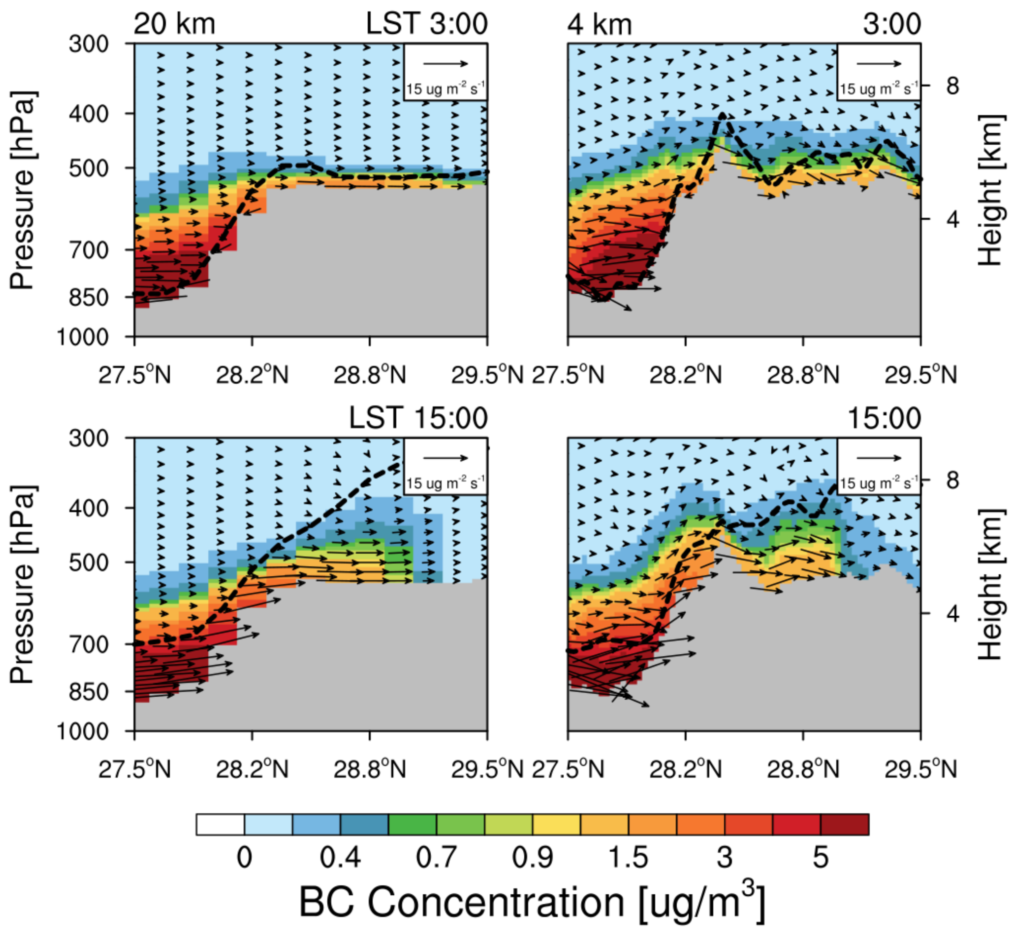
20 km
LST 3:00
4 km
3:00
LST 15:00
15:00
15 ug m-2 s-1
Pressure [hPa]
Height [km]
300
400
500
700
850
1000
8
4
27.5°N
28.2°N
28.8°N
29.5°N
0
0.4
0.7
0.9
1.5
3
5
BC Concentration [ug/m3]

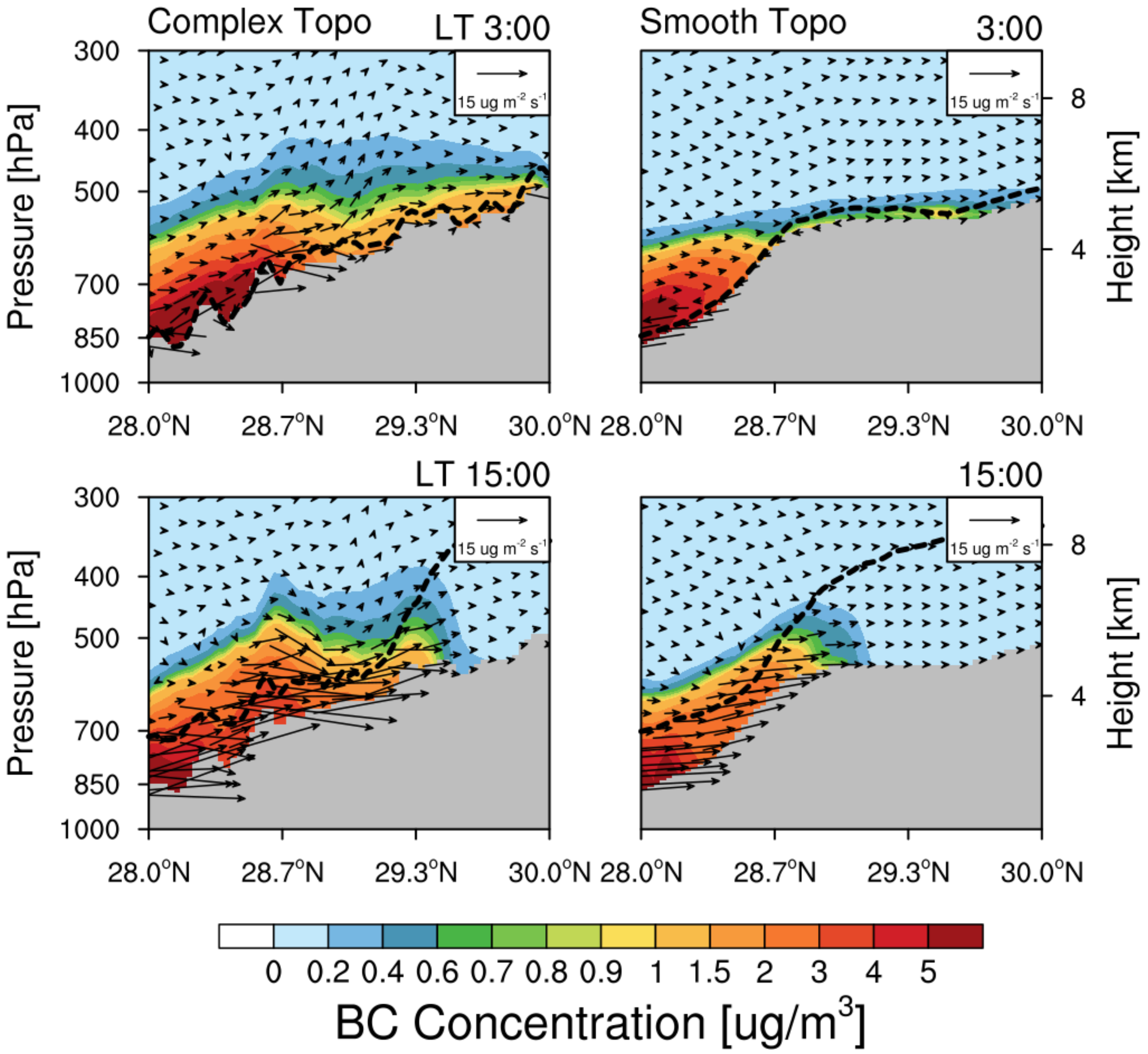

Figure ~~12~~11. Latitude-height cross section of BC flux (vector) ~~across~~along the ~~mountain~~valley (shown as the West black solid line in Fig. 3) from the simulations ~~at 20 km~~with complex and ~~4 km resolutions~~smooth topography at local time (LT) 03:00 and 15:00 averaged for April ~~5~~1-20, 2016. Contour represents the BC concentration.

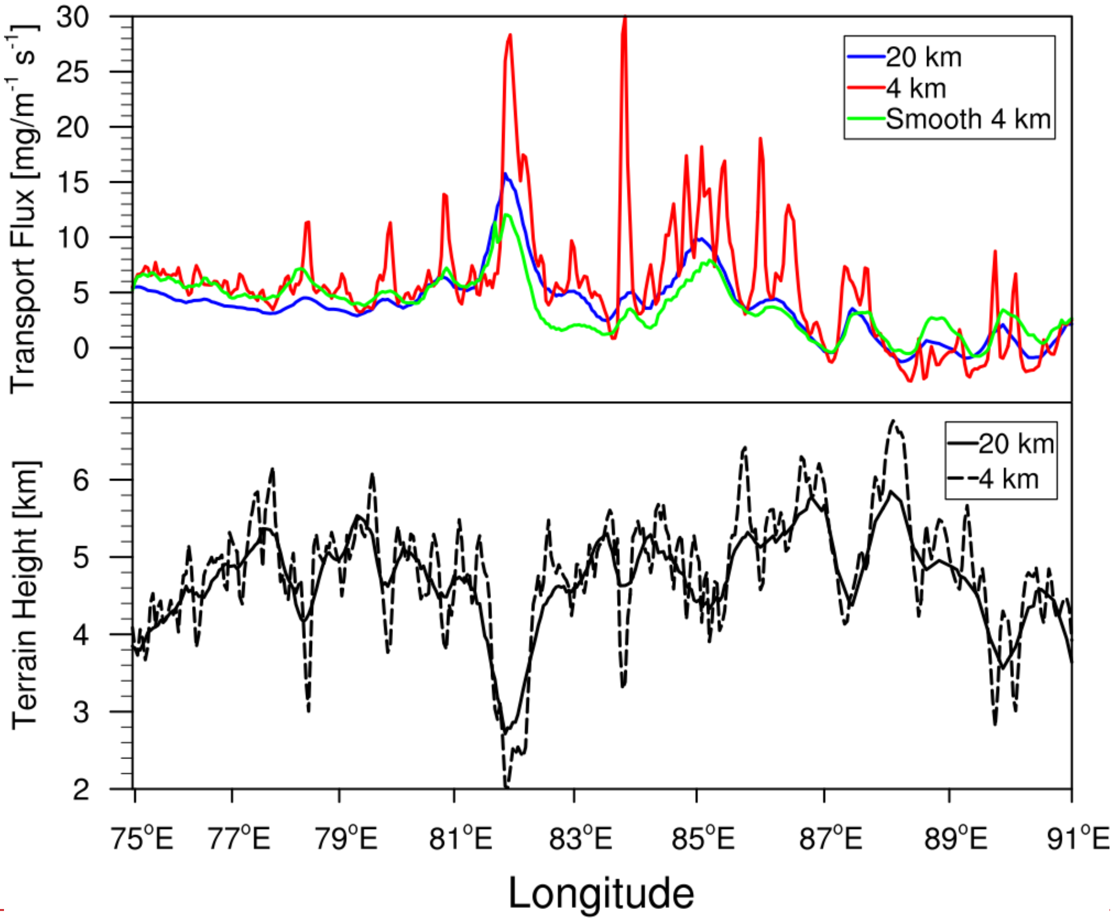
Transport Flux [mg/m-1 s-1]
30
25
20
15
10
5
0
20 km
4 km
Smooth 4 km
Terrain Height [km]
6
5
4
3
2
20 km
4 km
75°E
77°E
79°E
81°E
83°E
85°E
87°E
89°E
91°E
Longitude

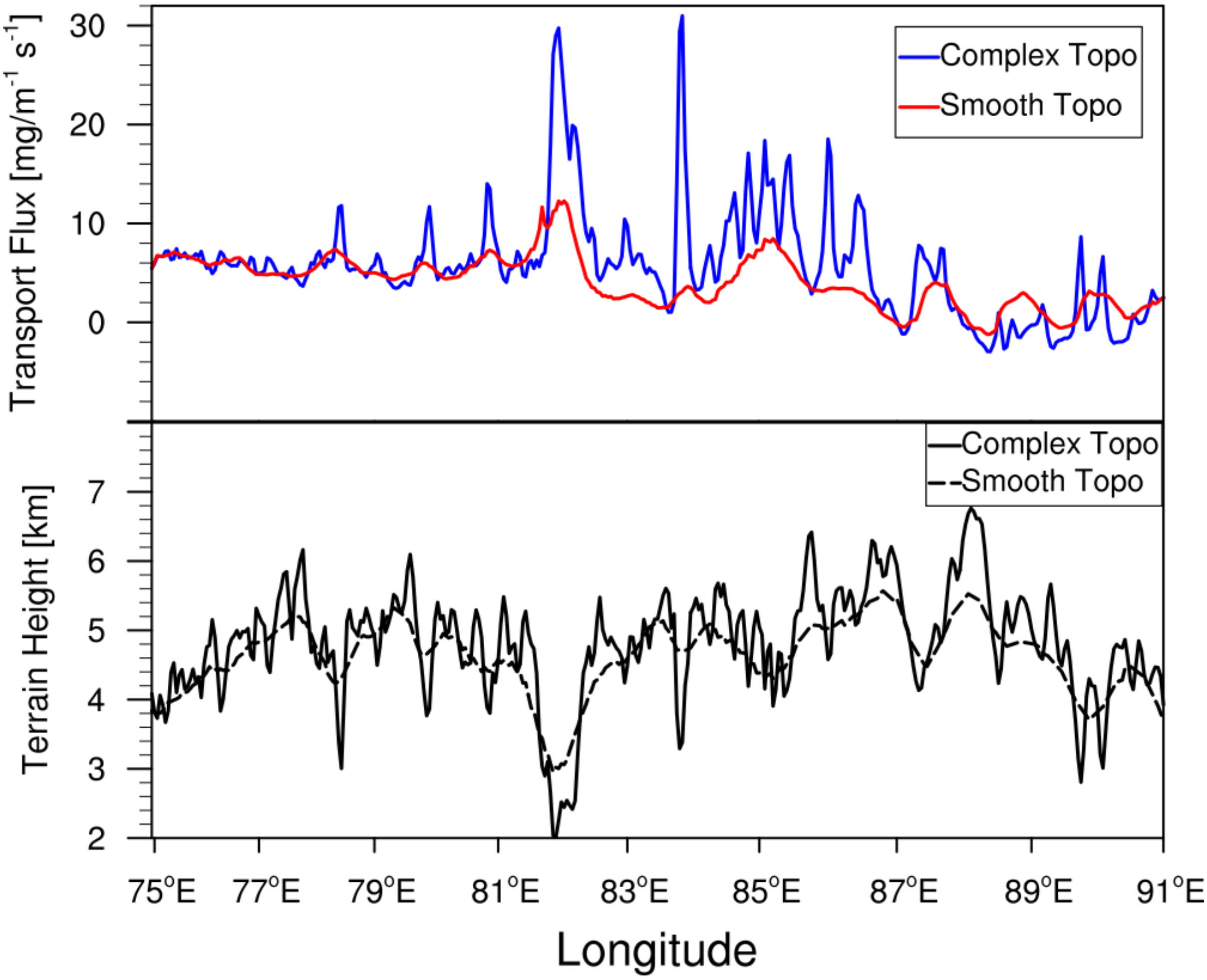

Figure ~~13~~12. Longitudinal distribution of integrated BC mass ~~fluxes~~flux along the cross section in Fig. ~~10~~3 from the simulations ~~at 20 km~~with complex and ~~4 km resolutions. The result (Smooth 4 km) from the sensitivity experiment at 4 km resolution but with the smoothing 20km resolution~~smooth topography~~ is also shown.~~. The black lines represent the terrain heights ~~along the cross section at 20 km and 4 km resolutions~~with different topography.

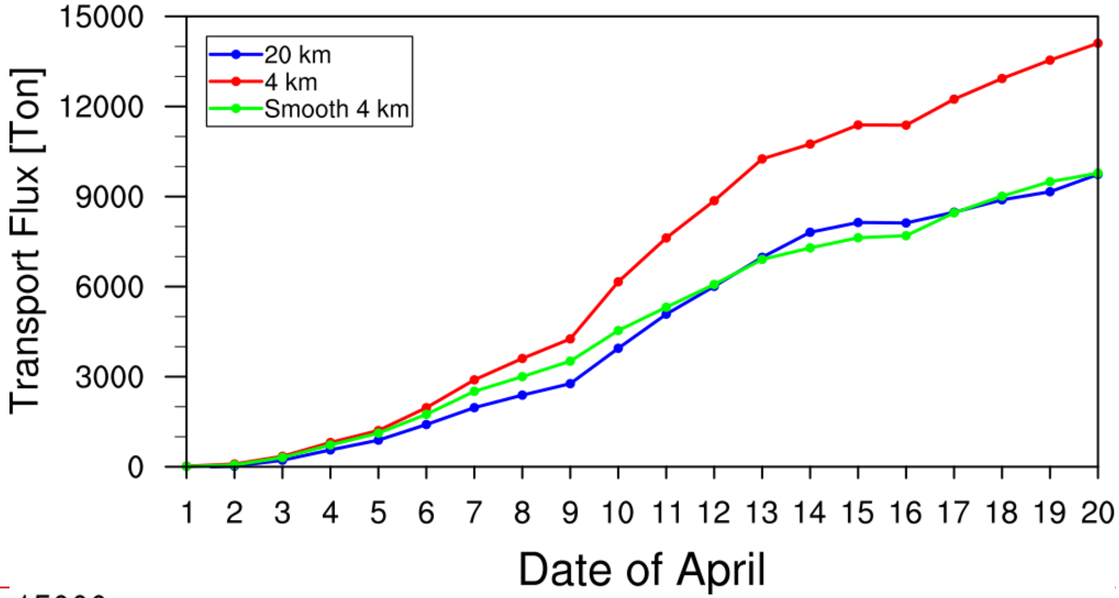

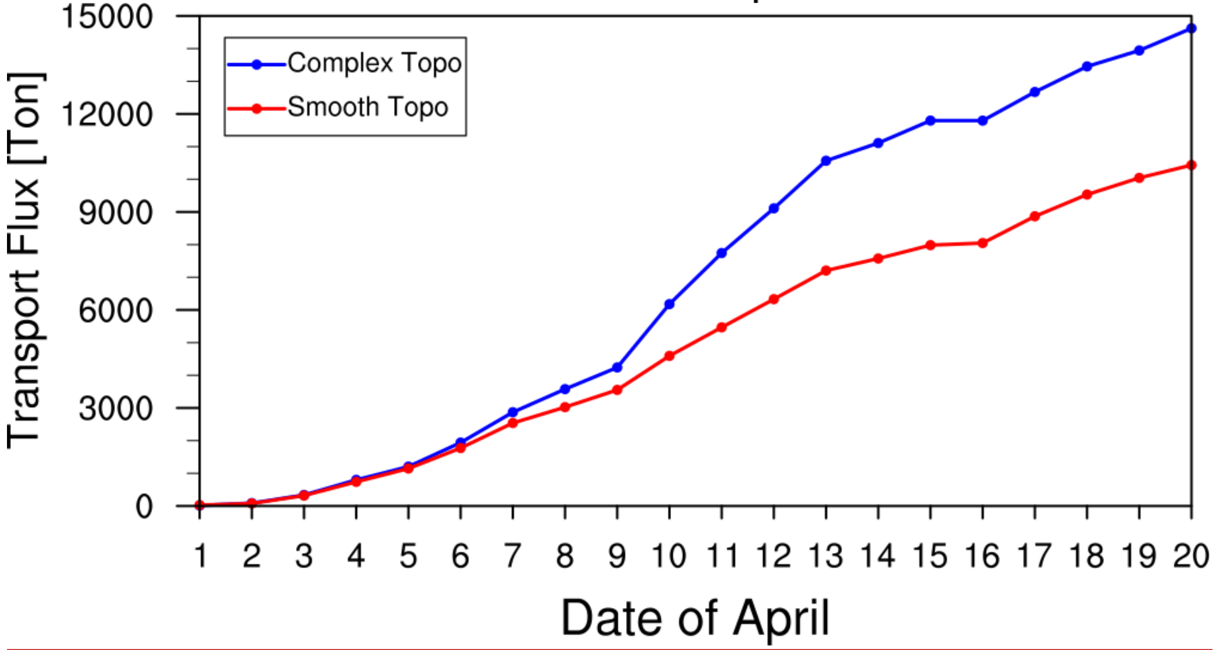

Figure ~~14~~13. Accumulated integrated total transport flux of BC across the Himalayas estimated from the simulations ~~at 20 km~~with complex and ~~4 km resolutions~~ smooth topography during April 1-20, 2016. ~~The sensitivity experiment at 4 km resolution but with the smoothing 20km topography is also shown.~~

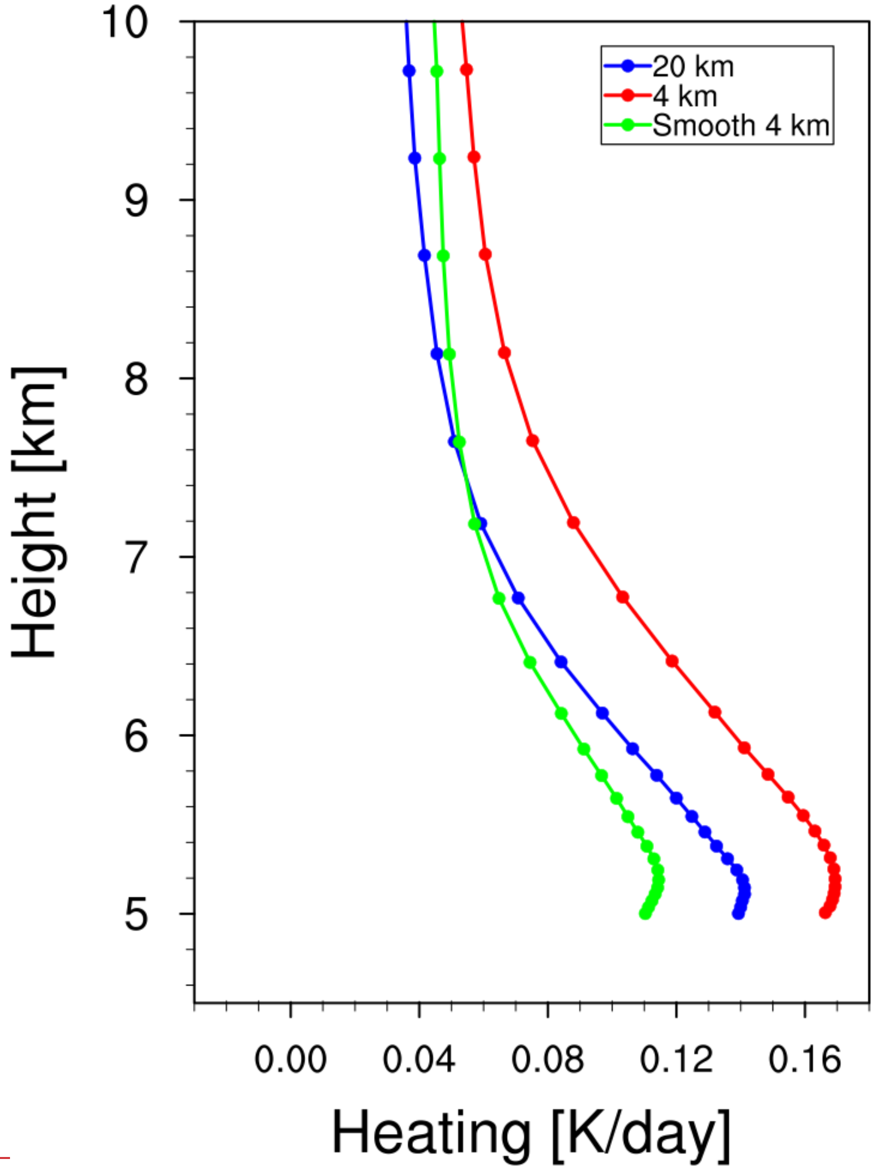
20 km
4 km
Smooth 4 km
10
9
8
7
6
5
Height [km]
0.00
0.04
0.08
0.12
0.16
Heating [K/day]

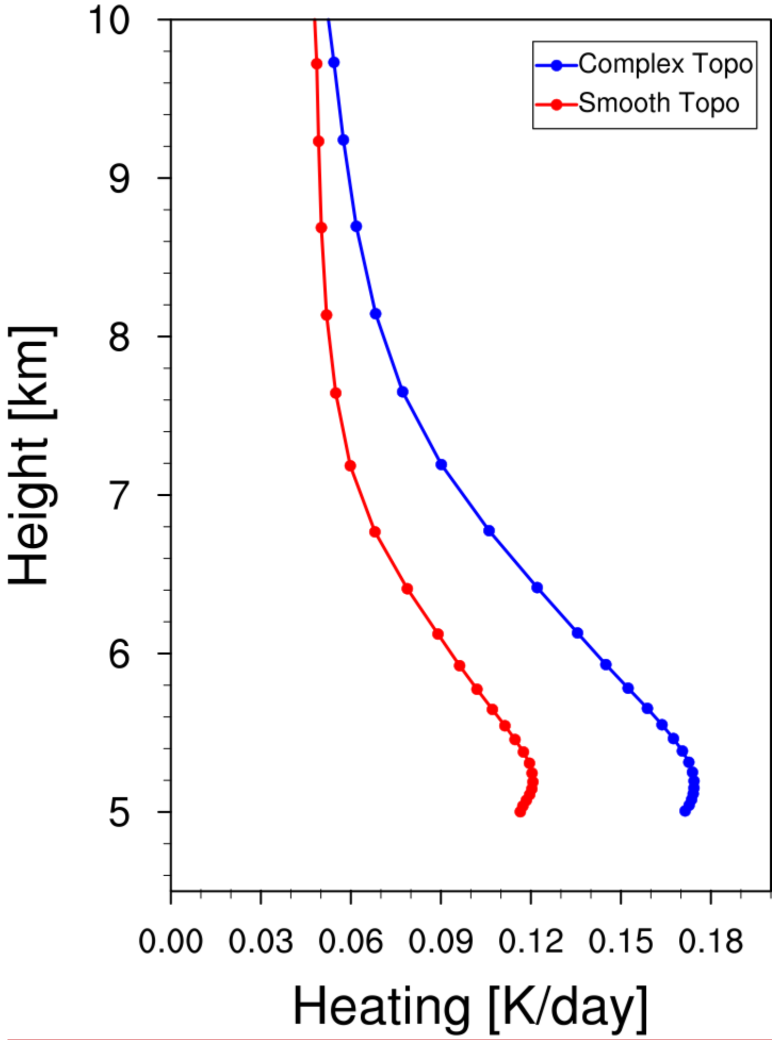

Figure ~~15~~14. Vertical profiles of BC induced radiative heating ~~rates~~rate in the atmosphere averaged over the TP (with elevation > 4 km) ~~within the inner domain shown in Fig. 1~~ from the simulations ~~at 20 km~~with complex and ~~4 km resolutions~~ smooth topography during April ~~5~~1-20, 2016. ~~The sensitivity experiment at 4 km resolution but with the smoothing 20 km topography is also shown.~~

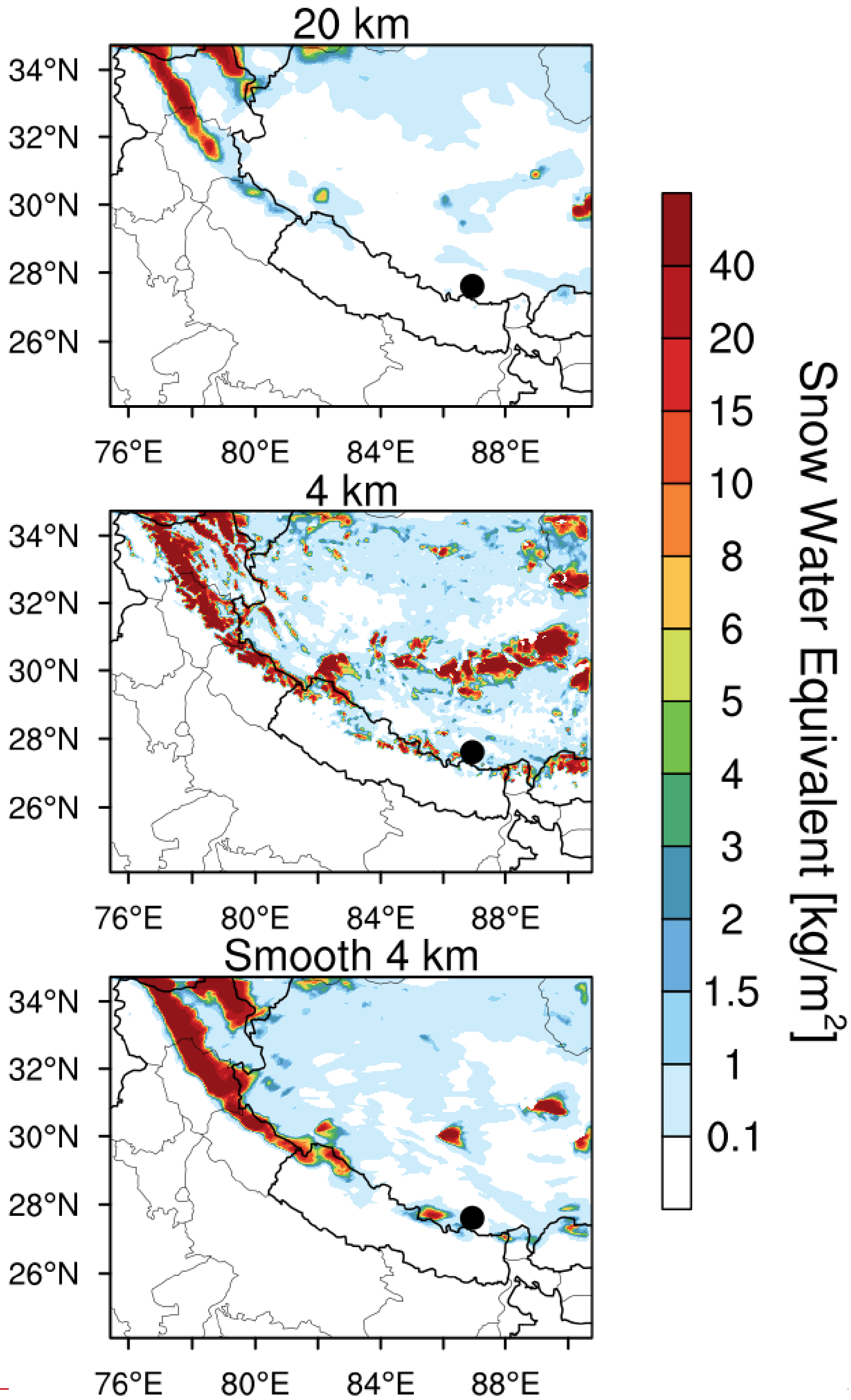
20 km
4 km
Smooth 4 km
34°N
32°N
30°N
28°N
26°N
76°E
80°E
84°E
88°E
Snow Water Equivalent [kg/m2]
40
20
15
10
8
6
5
4
3
2
1.5
1
0.1

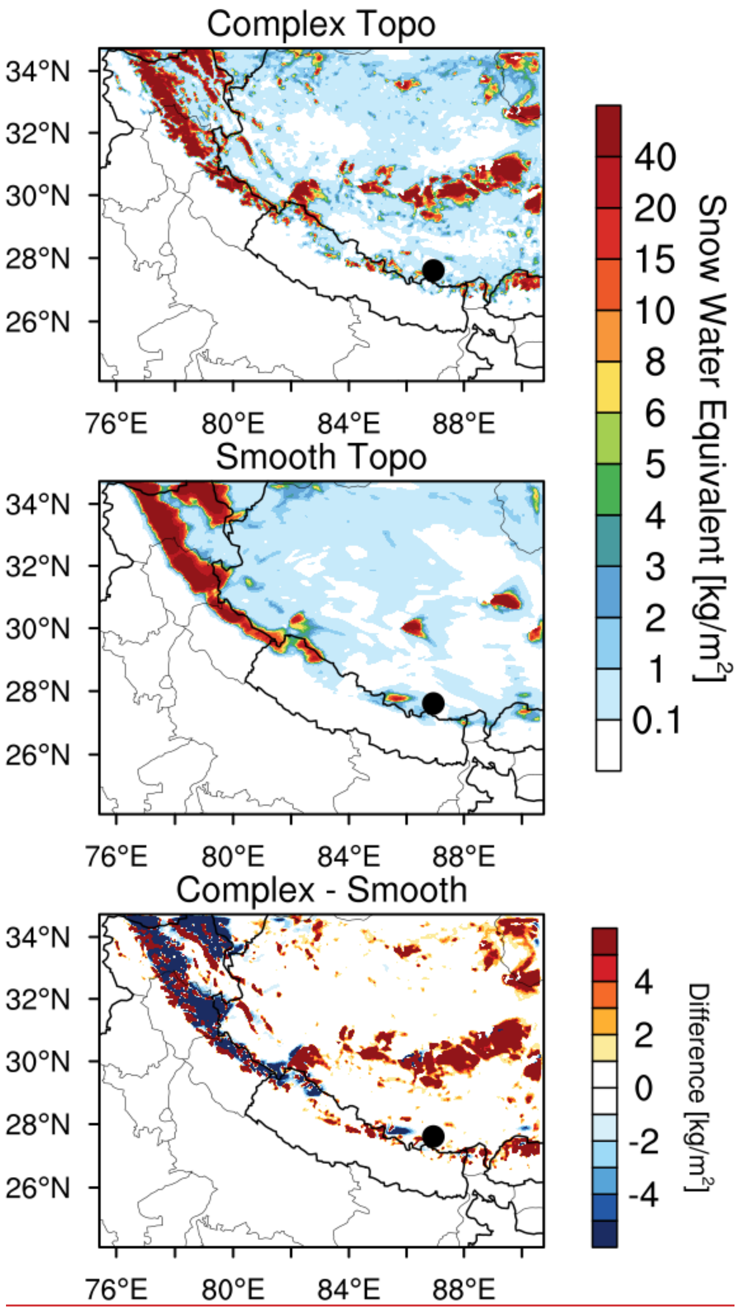

Figure ~~16~~15. Spatial distributions of snow water equivalent averaged for April ~~5~~1-20, 2016 from the simulations ~~at 20 km~~with complex and ~~4 km resolutions. The sensitivity experiment at 4 km resolution but with the smoothing 20km~~ smooth topography. The difference between the two is also shown.

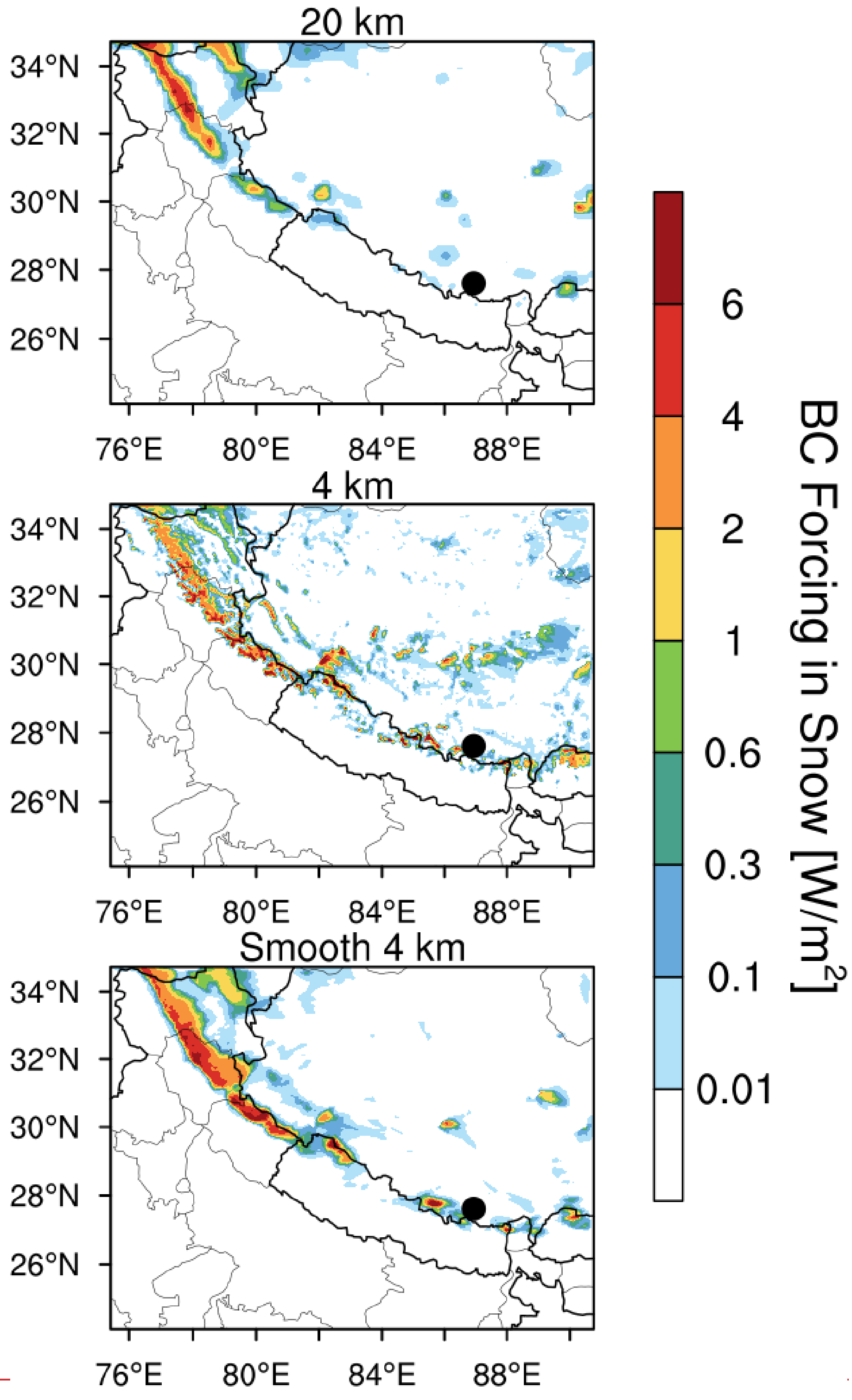
20 km
4 km
Smooth 4 km
34°N
32°N
30°N
28°N
26°N
76°E
80°E
84°E
88°E
BC Forcing in Snow [W/m2]
6
4
2
1
0.6
0.3
0.1
0.01

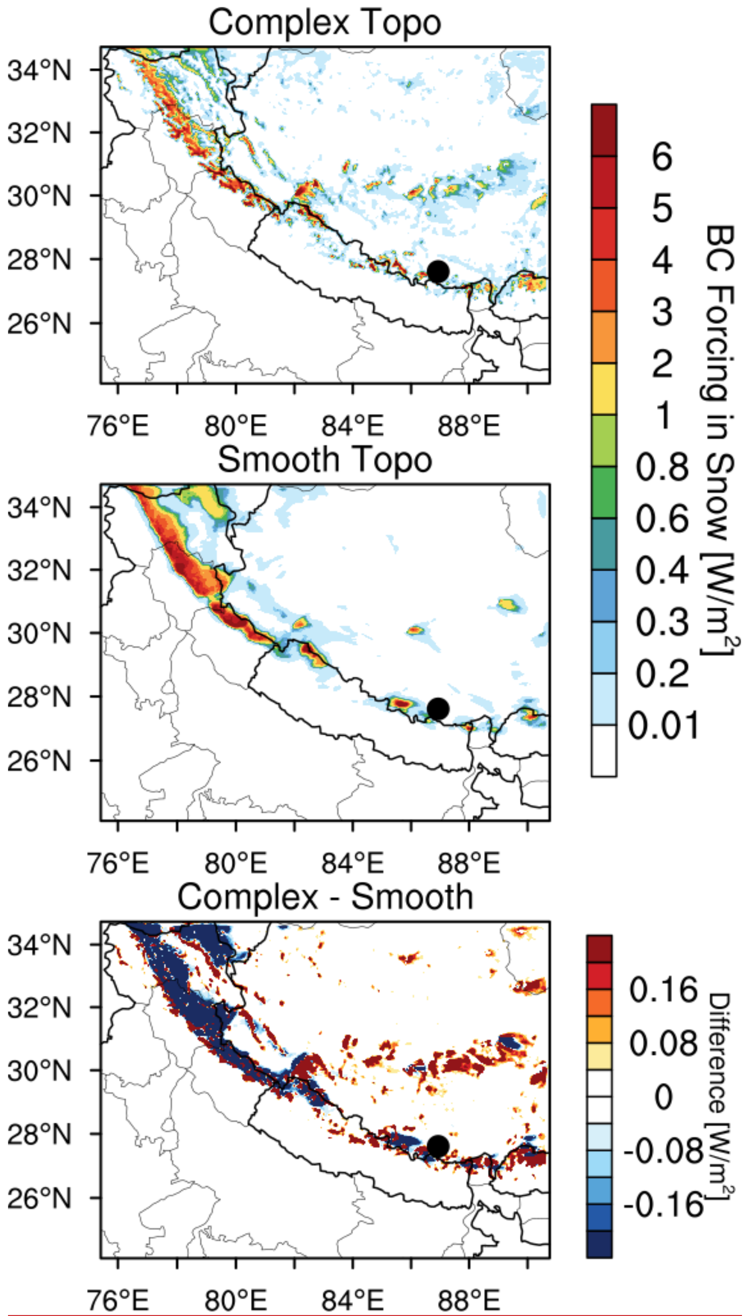

Figure ~~17~~16. Spatial distributions of BC radiative forcing in the surface snow averaged for April ~~5~~1-20, 2016 from the simulations ~~at 20 km~~with complex and ~~4 km resolutions. The sensitivity experiment at 4 km resolution but with the smoothing 20km~~ smooth topography. The difference between the two is also shown.~~–~~